Theory of quantum optomechanics with unconventional nonlinear coupling schemes

Juan Sebastian Restrepo

UNIVERSITÉ PARIS DIDEROT
(PARIS 7) SORBONNE PARIS CITE

ECOLE DOCTORALE: ED 564

DOCTORAT

PHYSIQUE

JUAN SEBASTIÁN RESTREPO

Theory of quantum optomechanics with unconventional nonlinear coupling schemes

Étude théorique de couplages non conventionnels dans des systèmes d'optomécanique quantique

---

Thèse dirigée par Cristiano Ciuti et co-dirigée par Ivan Favero

Soutenue le 3 octobre 2014

JURY

M.	Markus ASPELMEYER	Rapporteur
M.	Fabio PISTOLESI	Rapporteur
M.	Olivier ARCIZET	Examinateur
M.	Serge REYNAUD	Examinateur
M.	Cristiano CIUTI	Directeur de thèse
M.	Ivan FAVERO	Co-directeur de thèse

"When engaged in combat, the vanquishing of thine enemy can be the warrior's only concern. Suppress all human emotion and compassion. Kill whoever stands in thy way, even if that be Lord God, or Buddha himself. This truth lies at the heart of the art of combat."

Hattori Hanzo

Acknowledgements

Revisiting this four years of doctorate I must stare at the fact that I spent most of my time and efforts looking for ways to reach the *quantum ground state*. A simple gaussian state with the minimal amount of fluctuations, in some sense the system's calmest state possible. A state standing at the gates of the quantum world. A gate beyond which nature awaits us with unusual phenomena such as the possibility to have an object occupying two places at the same time. From a more personal point of view, during this four year long conversation with the laws of nature my mind and thoughts were switching permanently between two realms. On the one hand a world of Hamiltonians, master equations, spectral densities of noise, Wigner distributions and multiple mathemagical formulae. On the other hand a more "real", or at least palpable, world of human interactions. The avid reader will find in the remainder of this manuscript the log of my journey through the former. These few pages are the place where I would like to show my appreciation to all the people that accompanied me in the latter.

First of all I would like to thank my advisors Cristiano Ciuti and Ivan Favero. First for entrusting me with this project. Then for their trust, it was a real pleasure to feel free to stir my work according to the winds of my curiosity. Their support was also vital in making it to port safely, thank you for helping me to get out of the conundrums of my endless questions. And your patience, your teachings are tools that will accompany me for the rest of my journey.

I also would like to show my appreciation to the members of my defense jury, Pr. Olivier Arcizet, Pr. Serge Reynaud and the two referees of my manuscript, Pr. Markus Aspelmeyer and Pr. Fabio Pistolesi. Thank you for taking the time to go through this manuscript. Thank you as well for the difficult and interesting questions on the D-day. It was a pleasure and a real honour to discuss with you all the physics that I explored and the boundaries of what I had understood. Thank you above all for brightening the light of curiosity.

Now I would like to ask the english speaking reader some indulgence regarding the language of the rest of these acknowledgments. As a colombian doing science in english from a french university my day to day communication was a salad bowl of english, french, spanish and their combinations, fragnol, franglish, spanglish and some weird cocktail of the three of them.

Un grand merci aux membres du laboratoire MPQ. Merci à la direction et au conseil scientifique du laboratoire pour leur accueil. Les discussions sur le budget, les recrutements, les journées du labo et l'organisation des visionnages des matchs de foot ont été une inoubliable fênetre vers le côté le plus humain de la recherche scientifique. Merci à Anne Servouze. Merci pour tes bonbons, pour le sourire à chaque fois que je montais avec une excuse bidon pour prendre un carambar et pour ta disponibilité quand il s'agissait de problèmes plus sérieux. Merci aussi à Jocelyne Moreau et à Ludovic Vezien. Savoir que je pouvais compter avec votre temps et votre énergie simplifiait grandement l'organisation des voyages et l'achat des bricoles diverses et variées.

Merci à tous les thésards anciens et nouveaux pour leur manque de sérieux. Partager les espaces humains du laboratoire et hors de celui-ci avec vous a été un énorme plaisir. Mention espécial à David Hagenmuller et Simon Pigeon qui auront été les premiers échantillons non représentatifs mais inoubliables du thésard théorique. Merci à la bande des doctorants avec qui on a bien rigolé, discuté, voyagé et trinqué tout au long de cette thèse. Merci à Philippe, mon frère d'armes au conseil et sur la terrasse du labo, nos discussions ont toujours été une source importante pour continuer à aller de l'avant. Grand merci à *Bakchichi* mon moséllien préféré. On a partagé bien de moments, surtout cette fin de thèse qui restera gravée dans ma mémoire sur fond de guerre de boulettes de papier à sarbacane, blagues foireuses et discussions plus ou moins profondes mais toujours intéressantes de physique. Je me demanderais toujours si on n'aurait pas fait des meilleures thèse si on avait partager un bureau dès le début. Ça se trouve ça nous aurait pris plutôt six ans. Merci particulier à Florent Storme, je te dois encore un plein de bière pour avoir ressusciter une partie de mes travaux, merci aussi pour la disponibilité dont t'as fait preuve pour m'aider à améliorer ce manuscrit de thèse. Luc, merci pour la recherche permanente d'un futur différrent et plus geek. Alex, Jonathan, Loic, Constance, Siam, Hélène, Jared, Benjamin, Pierre et autres expérimentateurs et théoriciens, merci d'avoir créé des espaces irremplaçables pour nous échapper du train train de la physique de tous les jours. Bref, à tous et à toutes un grand merci et la meilleure des chances pour les aventures à venir.

Merci aussi au Palais de la Découverte. Merci à la direction du département de physique de m'avoir reçu en son sein pour que je puisse effectuer ma mission complémentaire d'enseignement. Merci aux médiateurs du Palais. À l'équipe permanente pour leurs leçons de science et de présentation devant un public. Merci aussi à toute l' équipe de non-permanents, Stephanie, Maryline, Kevin, Thomas, Pierre, Anne Laure, avec qui j'ai passé des weekends, des nuits des musées et autres évènements extraordinaires dans la meilleure des ambiances. Merci d'avoir

partagé avec moi le plaisir de la vulgarisation scientifique et merci de m'avoir enseigné l'importance de la médiation scientifique.

A la banda. Locombianos de pasaporte y/o de corazón. Gracias por ser una fuente inépuisable de ... otras cosas. Gracias por la excentricidad, por las ansías de hacer las cosas no de la manera más simple pero por lo menos la más divertida posible. Por nuestras diferencias. Por lo que nos acerca. Gracias por estar ahí en las buenas y en las maduras, y en las verdes también. Gracias por las navidades, cumpleaños, trasteos y demás experiencias del diario vivir. Graciar por ser mis piernas, brazos, manos y ojos en la exploración de otros mundos. Gracias por enriquecerme a tantos niveles. Esta tesis, este manuscrito y esta aventura en general les deben más de lo que llegaré a darme cuenta. Mención especial a Nicolás *el Qkey* López por ser mi compañero virtual de investigación. Gracias por convencerme que : "Why ask google if Qkey probably doesn't know the answer but will try and look for it with me anyway". Y gracias por el gigante coup de main con mis slides. Todavía le debo los *acknowledgments* oficiales en un artículo ...

Merci à Estelle. Ton arrivée d'un autre univers est en permanence une bouffée d'air frais et nouveau qui me motive pour continuer cet incroyable voyage. T'es une fenêtre vers un monde immense qui dépasse l'entendement de ce physicien, merci de m'accompagner de la main dans cette nouvelle découverte.

A mi familia. Por lo que soy y seré. Gracias a mis padres, motores de curiosidad y tenacidad para siempre seguir avanzando. Gracias a mi hermana y mi hermano por ser faros de luz guiándome en el día a día. Gracias a todos por aportar piezas esenciales en la construcción y culminación de este trabajo.

Contents

List of Figures

English abstract

This PhD thesis presents the results of our theoretical exploration of unconventional nonlinear coupling schemes in quantum optomechanical systems. Our research was focussed on two main aspects, namely cooling mechanisms and creation of non-classical states for a mechanical oscillator. The first two chapters of this manuscript define the theoretical framework and numerical approaches used to perform the theoretical investigations. The last two chapters present the main original results obtained during the doctorate.

In chapter I we introduce the subject of optomechanics and describe in a gradual and pedagogical way the theoretical framework necessary to treat the corresponding physics. We start by deriving the Hamiltonian of a general optomechanical system, consisting of an optical cavity resonator with a moving mirror, which can oscillate harmonically around an equilibrium position. We introduce microscopic Hamiltonians to take into account the coupling of the system to its radiative and non-radiative environment at finite temperature. Using a quantum Langevin equations approach we describe optomechanical cooling of mechanical motion and by doing so we introduce the main concepts, which were considered throughout this manuscript. We also briefly discuss optomechanical amplification of mechanical motion.
In chapter II we present the numerical algorithms and methods used to study the open system dynamics of an optomechanical cavity coupled both to an electromagnetic vacuum field and to a thermal reservoir for the mechanical resonator. We discuss numerical resolutions of the Lindblad master equation in order to gain insight on the stationary and time-dependent behavior of the system. In particular we introduce the finite-dimension numerical representation of a discrete and infinite Fock Hilbert space we used. We also present a numerical method of resolution of the equations of motion based on the truncated Wigner distribution of the system. We map the Lindblad master equation on the system density matrix onto a partial derivative equation on the corresponding Wigner distribution. By neglecting the higher order terms, and thus neglecting quantum correlations leading to negative values of the Wigner distribution, we obtain a Fokker-Planck equation for the Wigner distribution. The system is then described in terms of an equivalent set of stochastic equations for two scalar $\mathbb{C}$-fields. We present the Monte Carlo algorithm used to solve this set of equations. We discuss the convergence of our numerical resolution and show that it yields the expected results

concerning the noise statistics and mean field behavior of an optomechanical cavity. We also show that the numerical resolution is able to correctly describe cooling of mechanical motion in single-cavity and auxiliary-cavity scenarios. Finally, we show recent results on the synchronization appearing in a mechanically-coupled array of optomechanical cavities.

Chapter III presents our contributions to the theoretical study of optomechanical cooling of mechanical motion. We explore the quantum limits of photothermal cavity cooling. We show that in this case the relevant time scale in the cooling mechanism is the thermal relaxation time after photon absorption. It turns out that photothermal cavity cooling is able to produce cooling close to the ground state even in the "bad cavity" regime, in contrast to what happens with the more standard radiation pressure coupling. We also present our calculations for an optomechanical cavity coupled to an auxiliary cavity. We show that the spectral modification introduced by the coupling to the auxiliary cavity changes the spectral density of noise felt by the mechanical resonator. This modified spectral density of noise is expected to lead to a richer stability diagram for the system as well as cooling of mechanical motion by resonantly pumping the optomechanical cavity.
Finally, chapter IV reports our results on a hybrid system combining cavity/circuit quantum electrodynamics and optomechanics. We analytically diagonalize a Hamiltonian describing Jaynes-Cummings coupling between a cavity photon mode and an artificial two-level atom and radiation pressure coupling between the same cavity mode and a mechanical resonator. We explore the open system dynamics and show that it leads to atom-enhanced resonant cooling (or amplification depending on the pump frequency detuning) and to non-classical states of mechanical motion. We obtain expressions for the stationary state correlations of the system under incoherent pumping. In particular we show that by incoherently pumping the first two excited states of the Jaynes-Cummings ladder of dressed atom-photon modes the system behaves as a single phonon emitter thus displaying truly non-classical behavior.

Our results on the photothermal cavity cooling are published in [1]. They were presented in two international conferences (CLEO Europe 2011, March Meeting 2013) and during a poster session at les Houches summer school on "Quantum Machines: measurement and control of engineered quantum systems" [2]. Our results on the hybrid cQED-optomechanics system are published in [3]. They have been presented in three international conferences and workshops ("frontiers

of nanomechanics" at the ICPT in Trieste in 2013, March Meeting 2014 and the Gordon Research Seminar on "Mechanical systems in the quantum regime" in Ventura CA in 2014). These results were also showcased in a science communication article [4].

Résumé en français

Ce manuscrit de thèse présente les résultats de notre travail théorique sur des couplages non conventionnels dans des systèmes d'optomécanique quantique. Nous nous sommes intéressés à deux problématiques particulières. D'une part l'étude des effets de ces nouvelles formes de couplages sur le mécanisme de refroidissement ayant lieu dans ce type de systèmes. D'autre part nous avons aussi considéré l'apparition d'états non classiques du mouvement d'un résonateur mécanique. Les deux premiers chapitres de ce manuscrit définissent le cadre théorique et les outils numériques utilisés pendant cette thèse. Les deux derniers chapitres présentent les principaux résultats originaux obtenus pendant ce doctorat.

Dans le chapitre I nous introduisons les systèmes optomécaniques et décrivons graduellement et pédagogiquement le cadre théorique nécessaire pour décrire la physique en jeu. Nous commençons en introduisant le Hamiltonien général d'une cavité optomécanique, composée d'un résonateur optique avec un miroir mobile qui oscille sous un potentiel harmonique autour de sa position d'équilibre. Nous introduisons des Hamiltoniens microscopiques pour prendre en compte le couplage du système à des bains radiatives et non radiatives à température finie. Utilisant des équations de Langevin quantiques nous décrivons le refroidissement optomécanique d'un résonateur mécanique, nous en profitons pour introduire les principaux concepts mobilisés tout au long de ce manuscrit. Nous discutons aussi brièvement l'amplification du mouvement mécanique jusqu'à des régimes d'auto-oscillation.
Le chapitre II présente les algorithmes et méthodes numériques utilisés pour mener à bien l'étude de la dynamique d'une cavité optomécanique couplée au vide électromagnétique et à un reservoir thermique pour le résonateur mécanique. Nous discutons la résolution numérique de l'équation maîtresse sous forme de Lindblad afin d'obtenir des informations sur le comportement dynamique et stationnaire du système. En particulier nous introduisons la représentation numérique de taille finie d'un espace de Hilbert infini et discret utilisée pendant cette thèse. Nous présentons aussi une méthode de résolution numérique des équations du mouvement basée sur la distribution de Wigner tronquée du système. L'équation maîtresse sous forme de Lindblad de la matrice densité du système est projetée vers une équation aux dérivées partielles sur la distribution de Wigner associée au problème. En négligeant les termes d'ordre supérieur dans cette équation, et donc en négligeant les corrélations quantiques menant à des valeurs négatives de

la distribution de Wigner, nous obtenons une équation de type Fokker-Planck pour la distribution de quasi-probabilité. Le système peut alors être représenté en termes d'un système d'équations de Langevin sur des variables scalaires complexes. Nous présentons l'algorithme Monte Carlo mis en place pour intégrer ces équations stochastiques. Nous discutons la convergence de l'algorithme et montrons qu'il décrit correctement les statistiques du bruit et le comportement en champ moyen du système. Nous montrons aussi que cette résolution donne une représentation adéquate du refroidissement optique dans des scénarios à une et deux cavités. Finalement, nous présentons des résultats récents sur la synchronisation dans un réseau de cavités optomécaniques couplées mécaniquement.

Le chapitre III présente nos contributions à l'étude théorique du refroidissement optomécanique d'un résonateur optomécanique. Nous explorons la limite quantique du refroidissement photothermique de cavité. Nous montrons que dans ce cas l'échelle de temps en jeu dans le processus de refroidissement est le temps de relaxation thermique après absorption d'un photon. Il en résulte que le refroidissement photothermique en cavité est capable de refroidir le mouvement du résonateur mécanique jusqu'à son état fondamental et ce dans un régime de cavité non résolue ("bad cavity limit") à différence de ce qui se produit dans le cas standard de refroidissement par pression de radiation. Nous présentons aussi nos calculs sur une cavité optomécanique couplée optiquement à une cavité auxiliaire. Nous montrons que la modification spectrale introduite par le couplage à la deuxième cavité change la densité spectrale de bruit optique ressenti par le résonateur mécanique. Cette nouvelle densité spectrale de bruit devrait mener à un diagramme de stabilité plus riche pour le système ainsi qu'à du refroidissement du mouvement mécanique en excitant de manière résonante la cavité optomécanique. Finalement, le chapitre IV expose nos résultats sur un système hybride combinant l'electrodynamique quantique (en cavité ou des circuits supraconducteurs) et l'optomécanique quantique. Nous diagonalisons analytiquement un Hamiltonien décrivant un couplage de type Jaynes-Cummings entre un atome artificiel à deux niveaux et un mode optique et un couplage par pression de radiation entre le même mode optique et un résonateur mécanique. Nous explorons la dynamique en présence d'excitations et pertes et montrons qu'elle mène à un refroidissement rehaussé par l'atome (ou amplification en fonction du désaccord entre la pompe optique et la cavité) et à des états non-classiques du mouvement du résonateur mécanique. Nous obtenons des expressions analytiques pour la statistique stationnaire du système sous excitation incohérente. En particulier nous montrons que lorsque les deux premiers niveaux de l'échelle Jaynes-Cummings sont excités

de manière incohérente le système se comporte comme un émetteur de phonons uniques et donc qu'il présente un comportement non-classique.

Nos résultats sur le refroidissement photothermique sont publiés dans [1]. Ils ont été présentés lors de deux conférences internationales (CLEO Europe 2011, March Meeting 2013) et pendant une session poster de l'école d'été des Houches "Quantum machines : Measurement and control of engineered quantum systems" [2]. Nos résultats sur le système hybride sont publiés dans [3]. Ils ont été présentés lors de trois conférences internationales ("Frontiers of nanomechanics" à l'ICTP à Trieste en 2013, March Meeting 2014 et au Gordon Research Seminar "Mechanical systems in the quantum regime" à Ventura CA en 2014). Ces derniers ont aussi été discutés dans un article de médiation scientifique [4].

General Introduction

" But, in the end, can you see the electrons?
- Well, it depends.
- It depends on what?
- It depends on what you understand by seeing . . . "
Conversation at a science museum.

The sensory act of "seeing" can be objectified in terms of the physical phenomena taking place between the observer and the observed object. The object emits, reflects or diffuses light that travels through some medium (usually air). After a finite time light arrives at the observer's retina. There the photons are absorbed and converted into electrical signals sent to the brain. Finally the brain interprets the electrical signals and the observer "sees" this manuscript. In this sense "seeing" amounts to capturing some signal emitted by the object, analyzing it and obtaining relevant information. By means of an ammeter or an oscilloscope it is possible to detect electrons and obtain quantitative information about them such as the associated current or voltage. Equipped with such apparatuses the observer "sees" and measures the system under consideration. Quantitative data is then available and can be used to infer or test a predictive theoretical model.

This far in the discussion the measurement process completely separates the observer from the observed object. Indeed we just considered some information-conveyor signal joining the latter to the former. The information travels in one direction and the observed object remains unaltered while the observer steadily acquires more and more information. When moving to the realm of quantum physics the observer is placed in a radically new and exciting situation. The observer has to face the intrinsic probabilistic nature of a quantum system. In order to completely determine the state (wave function) of the system a series of measurements on an ensemble of copies is required. Simultaneously the state of the system itself is changed by the measurement. The measurement perturbs the system such that the observer and the observed object interplay in a more intricate way. One

striking example is the Heisenberg microscope *gedanken experiment*. Let us now briefly follow an insightful discussion on this problem which can be found in [5].

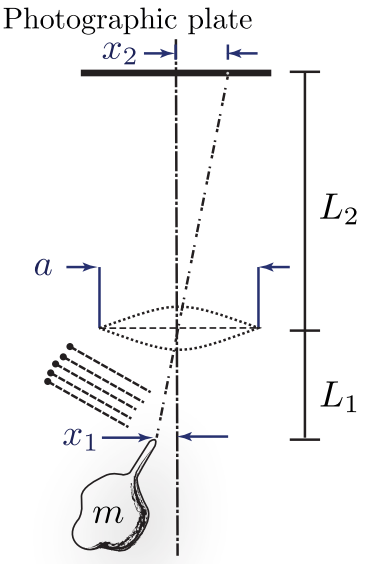

FIGURE 1: The Heisenberg microscope as discussed in [5].

Let us assume that we want to determine the position x_1 of an object of mass m by means of an optical measurement. The information between the object and the observer is carried by the light shone on and diffracted by the mass. In order to perform this measurement one attaches a sub-wavelength (in comparison to the used light field) stick to the mass which will be able to scatter the light field. The scattered photons are sent through a lens of focal length L_1 into a photographic plate where they are collected. Now, let us consider a stream of photons arriving at the mass/stick. An individual photon reaches the stick, is scattered, goes through the lens aperture a and is finally absorbed by the photographic plate thus leaving a mark at the position x_2. By means of a simple Thales relation we obtain that the position of the mass is $x_1 = -x_2 L_1/L_2$. So far we are still performing measurements as in the first paragraph. We obtain information on the system without perturbing it.

The mark left on the photographic plate is not a point but an Airy disk with a finite size. The position x_2 can only be defined within a certain interval. We thus know that the mass position is within an area centered in the previously computed x_1 and of finite width given by

$$\Delta x_{measure} \sim \frac{1}{6}\lambda\frac{L_1}{a}. \tag{1}$$

$\Delta x_{measure}$ is the error in the infered position of the mass. At this point we have only taken into account the fact that due to diffraction there is no perfectly precise optical measurement. We still have to describe the effects of the measurement on the mass.

As was intuited by Kepler in 1619 [7], predicted by Maxwell in 1873 and experimentally measured by Lebedew [8] in 1901 and by Nichols and Hull in 1903 [9] light carries mechanical momentum and can exert pressure. A single photon of frequency ω holds a mechanical momentum $P_{photon} = h\omega/c$ (c being the speed of light) that can be transfered to the mass when the scattering takes place. We know that the photon must have been diffracted by the aperture a, it thus gives to the stick (and thus to the mass) a random momentum along the x axis $\Delta p_{perturb}$. This random momentum kick has unknown sign but, for $a \ll L_1$, it has a magnitude of order

$$\Delta p_{perturb} \gtrsim \frac{h\omega}{c}\frac{a}{2L_1}. \tag{2}$$

Measuring the mass position thus leads to a perturbation of its momentum in a random fashion that ultimately perturbs further measurements of its position. Multiplying these expressions we obtain the following relationship between the imprecision of the measurement and its random recoil on the mass

$$\Delta x_{measure}.\Delta p_{perturb} \geq \frac{h}{2}. \tag{3}$$

Eq.3 is reminiscent of the well known Heisenberg uncertainty principle linking the simultaneous knowledge one can get on the position x and momentum p of a quantum object :

$$\Delta x.\Delta p \geq \frac{h}{2}. \tag{4}$$

Although Eq.3 and Eq.4 are both called "Heisenberg inequalities" they rise from different physical pictures. Eq.4 is a property of any quantum object for which one cannot have simultaneous and infinitely precise information about its position and its momentum. Eq.3 on the other hand results from the properties of the performed measurement, it links the imprecision of the position measurement to the uncertainty on the recoil felt by the system. Both inequalities are nevertheless closely related. If one was to perform a measurement of x_1 with an imprecision given by Eq.1 then the Heisenberg uncertainty principle (Eq.4) implies that the momentum has been perturbed by at least the amount given in Eq.2. Quantum mechanics imposes a fundamental limit on the precision of a position weak measurement, the so-called standard quantum limit [5, 10].

The achievable precision in a position measurement is of central interest in the field of gravitational wave interferometry. In order to detect such astronomical waves, optical interferometers with arms at the scale of the kilometer have been set [11, 12]. Instead of measuring the position of a stick attached to a mass, these interferometers aim at determining the changes in length of the interferometers' arms down to a precision of 10^{-20} meters (we remind the reader that the Bohr radius of an hydrogen atom is approximately 5.10^{-11} meters). Reaching such precisions implies having control and understanding of the different noise sources disturbing the measurement. The standard quantum limit was hence considered as technologically relevant upon the development of these interferometers. In the 1970's Vladimir Borisovich Braginsky et al. published a paper investigating the mechanical effects of light in an interferometric position measurement [13]. At the time these effects associated to photon recoil were considered to be detrimental to the detection of gravitational waves. Nevertheless, further investigation showed that the radiation pressure back action could lead to controllable and useful modification of the deformable interferometer mechanical properties.

In a Michelson interferometer the light intensity depends on the length of the arms. On the other hand, radiation pression on the end mirrors changes this length. The optical modification of the interferometer mechanical properties is a signature of this optomechanical coupling between the light field and mechanical motion. For about ten years now the interest for this coupling has quickly overflown the field of gravitational wave interferometry and has become a whole field of physics itself. The rise of optomechanical systems, where light and mechanical motion are coupled, is supported by a solid community exploring and pushing further the limits of optomechanical coupling [2, 14–17].

Using systems with masses ranging from the gram down to the zeptogram a plethora of research groups are exploring the capabilities of optomechanical systems. It has been shown that the influence of light leads to a modification of the mechanical resonance frequency (optical spring effect [13]), to a modification of the dissipation constant as if light were a viscous medium (optical damping [18]) and even to bistable behavior of mechanical motion for intense enough electromagnetic fields [19]. Changing the mechanical properties of mechanical motion also induces a modification of its response to the different noise sources at play in real life experiments. In the 1950's it was shown that it is possible to reduce the effects of thermal Brownian motion on an electrometer by time-delayed electrical feedback [20]. Following the same principles, in 1998 a theoretical article [21] proposed using radiation pressure external feedback in order to cool mechanical brownian

motion below its equilibrium temperature. Soon after, this proposition was experimentally realized [22] and followed in 2004 by an experimental demonstration of optical self-cooling of a cavity mirror using photothermal forces [23]. Similar cavity self-cooling of a mirror, but with radiation pressure as the optomechanical force, was achieved by four groups over 2006-2007 [24–27] and followed by several others. By cooling the thermal fluctuations on the mirror position the frontier between classical and quantum mechanics for mechanical motion became a reachable goal. 2007-2008 saw the publication of four theoretical papers [28–31] investigating the limits of radiation pressure cooling and showing that it should indeed be possible to reach the quantum ground state of mechanical motion. Mechanical systems in their quantum ground state are now a reality, either by directly using cryogenic techniques to put a 6 GHz microwave resonator in its ground state [32] or by combining cryogenics and radiation pressure cooling in systems in the optical domain [33] or in microwave superconducting circuits [34]. Recent experiments have successfully measured radiation pressure shot noise [35] and measuring the position of a moving mirror at the standard quantum limit seems to be within reach in a not so distant future.

Experiments are now paving the way to quantum optomechanics where both light and mechanical motion have to be described in terms of quantum observables. There have been many theoretical proposals to prepare and measure truly quantum states in optomechanical systems. Early on radiation-pressure coupled deformable interferometers were proposed as a mean to perform quantum non-demolition measurements of the number of photons inside the cavity [36]. The parametric dependance between the cavity resonance frequency and mechanical motion can be understood in terms of an effective Kerr-like non-linearity leading to squeezing of the photon field [37–39]. The radiation pressure coupling should also lead to entanglement between mechanical motion and light [40–43] and even to the creation of an EPR pair of two spatially separated mechanical resonators [44]. Following the technological advances on the fabrication of optomechanical resonators [45], reaching the vacuum "strong" coupling regime where a single photon is able to move the mechanical resonator by an amount comparable to its zero point fluctuations may soon open the way for single photon quantum logic using mechanical elements [46–48]. Finally, optomechanical systems are entering the "zoology of tamed quantum systems" [15] and thus the possibility to study optomechanical phenomena interplaying with other quantum systems has become an important center of interest. The possibility to optomechanically couple the center of mass motion of a cold atom cloud to a light field has been theoretically explored [49, 50] and used experimentally to reach sensitivities near the standard quantum limit [51]. Mechanical motion has already been coupled at the quantum

level to the internal degrees of freedom of an artificial solid state atom [32] and recent theoretical papers are now investigating the possibility to bridge cavity/ circuit quantum electrodynamics to optomechanics [3, 52–55].

This manuscript presents the theoretical work we undertook on the description of quantum optomechanics with non conventional coupling schemes. We start in chapter I by giving a theoretical introduction to quantum optomechanics. Chapter II discusses the different numerical tools used during this PhD. Chapters III and IV comprise our new contributions to the field of quantum optomechanics. In chapter III we discuss the modifications of optomechanical cavity cooling by considering photothermal forces and the coupling to an auxiliary cavity. Finally chapter IV reviews our work and results on a hybrid cavity optomechanics-quantum electrodynamics system. Appendices A and B present useful derivations for the formalisms used during this thesis. These derivations can be found in the literature but we have decided to present them here for the sake of consistency. Appendices C and D present generalizations of some of the original calculations performed in the main body of this manuscript.

Chapter I

Quantum optomechanics

I.1. The model system considered

I.1.1. Description of the system

The most simple example of the family of systems considered in this thesis is a Fabry Perot cavity having one of its two end mirrors fixed in space (mirror 1 in the following) and the other one (mirror 2) prone to move under the mechanical effects of light (radiation pressure, photothermal distortion, ...). When mirror 2 is at its equilibrium position the cavity length is denoted L. For the sake of simplicity let us consider only one cavity mode at frequency ω_c (ω_c is such that there is a given $k \in \mathbb{N}$ such that $\omega_c = k\pi c/L$, c being the speed of light). This one mode is excited by a coherent laser which injects photons at frequency ω_p into the cavity. The light intensity that eventually builds up in the cavity depends on the difference $\omega_c - \omega_p$. A shift in the position of mirror 2 changes the cavity length and thus leads to a modification of ω_c. If the laser frequency remains unchanged, the movement of mirror 2 modifies the intensity of the electromagnetic field inside the cavity. Let us now consider that mirror 2 can move under the effects of an optical force depending on the light intensity. The number of photons inside the cavity depends on mirror 2 position, and the position of the mirror depends on the number of photons in the cavity. This way we obtain a mutual coupling between the electromagnetic field and the position of the moving mirror.

In order to study the quantum dynamics of such a configuration we first have to obtain the Hamiltonian of a coupled mirror-field system.

I.1.2. Closed system Hamiltonian

We follow the main steps of the historic derivation by Law [56] for the Hamiltonian of a coupled field-mirror system in the case of a radiation-pressure-based optical force.

I.1.2.1. Hamiltonian formulation for the deformable Fabry-Perot cavity

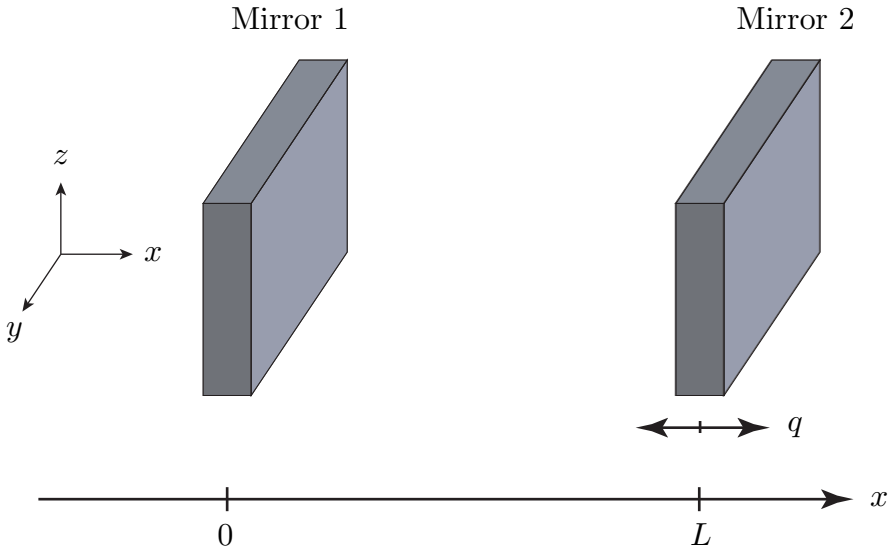

FIGURE I.1: Fabry Perot cavity with a movable mirror. Mirror 2 can move around its equilibrium position ($q = 0$).

As can be seen in Fig.I.1 we now consider a Fabry Perot cavity. The left side mirror (mirror 1) is fixed at the position $x = 0$, the other mirror is prone to move along the x-axis, thus modifying the cavity length. Let q be the position coordinate around mirror 2 equilibrium position $x = L$ (the actual cavity length is thus $L+q$). The dynamical variables of interest in this scenario are the mirror position q along the x-axis and the electromagnetic field between the two mirrors. We assume that the mirror moves in an energy potential $V(q)$ and that the mirrors are perfect conductors. The electromagnetic field and the mirror position are coupled through the radiation pressure exerted by the former.

Let us consider that the dimensions of the mirrors along the y and z-axis are large enough compared to the cavity length L so that the problem can be described as a one-dimensional cavity. We also assume the dynamics of the mirror to be

slow enough so that the system can be described in a non-relativistic way. The electromagnetic field inside the cavity ($0 \leq x \leq L + q(t)$) will be described by its vector potential $A(x,t)$. Setting the speed of light to $c = 1$ one gets the following wave equation for the vector potential,

$$\frac{\partial^2 A(x,t)}{\partial x^2} - \frac{\partial^2 A(x,t)}{\partial t^2} = 0. \tag{I.1}$$

The "perfect conductors" assumption for the mirrors leads to the following boundary conditions

$$\forall t, A(0,t) = A\left(L + q(t), t\right) = 0. \tag{I.2}$$

Finally, the mirror undergoes the forces arising from the potential energy $V(q)$ and from the radiation pressure exerted by the electromagnetic field. The non-relativistic equation of motion for the mirror position is therefore

$$m\ddot{q} = -\frac{\partial V(q)}{\partial q} + \frac{1}{2}\left(\frac{\partial A(x,t)}{\partial x}\right)^2\Bigg|_{x=L+q(t)}. \tag{I.3}$$

The dynamics of the system is fully characterized by Equations I.1,I.2 and I.3. In order to go further with our derivation of the Hamiltonian we now perform an eigenmodes expansion of the cavity field that yields a set of generalized coordinates $\{Q_k\}_{k\in\mathbb{N}}$. Using Equation I.2, the generalized coordinates can be defined by

$$\forall k \in \mathbb{N},\ Q_k(t) = \sqrt{\frac{2}{L+q(t)}} \int_0^{L+q(t)} dx\ A(x,t) \sin\left(\frac{k\pi x}{L+q(t)}\right). \tag{I.4}$$

Given the orthogonality of the mode functions, Eq.I.4 transforms the set of equations I.1 and I.3 into

$$\begin{aligned} \ddot{Q}_k = &-\omega_k Q_k^2 + 2\frac{\dot{q}}{L+q}\sum_j g_{kj}\dot{Q}_j + \frac{\ddot{q}(L+q) - \dot{q}^2}{(L+q)^2}\sum_j g_{kj}Q_j \\ &+ \frac{\dot{q}^2}{(L+q)^2}\sum_{j,l} g_{jk}g_{jl}Q_l \end{aligned} \tag{I.5}$$

$$m\ddot{q} = -\frac{\partial V(q)}{\partial q} + \frac{1}{L+q}\sum_{k,j}(-1)^{k+j}\omega_k\omega_j Q_k Q_j \tag{I.6}$$

where we introduced the position dependent eigen-frequencies $\{\omega_k\}$ and the dimensionless coefficients $\{g_{kj}\}$ defined by

$$\omega_k(q) = \frac{k\pi}{L+q} \tag{I.7}$$

$$g_{kj} = \begin{cases} (-1)^{k+j}\frac{2kj}{j^2-k^2}, & k \neq j \\ 0, & k = j \end{cases} . \tag{I.8}$$

In order to get a quantized Hamiltonian for the system one has to find a way to interpret the set of equations I.5 and I.6 as a set of Euler-Lagrange equations with respect to some Lagrangian L. Law's approach was to derive the following Lagrangian which yields the adequate equations of motion,

$$\begin{aligned} L\left(q,\dot{q},\{Q_k,\dot{Q}_k\}\right) =& \frac{1}{2}\sum_k \dot{Q}_k{}^2 - \omega_k(q)^2 Q_k^2 + \frac{1}{2}m\dot{q}^2 - V(q) \\ & - \frac{\dot{q}}{L+q}\sum_{j,k} g_{k,j}\dot{Q}_k Q_j + \frac{\dot{q}^2}{2(L+q)^2}\sum_{j,k,l} g_{kj}g_{kl}Q_l Q_j. \end{aligned} \tag{I.9}$$

The canonical momenta conjugate to Q_k and q, P_k and p respectively, are obtained by Legendre transformation and are defined as follows:

$$P_k = \dot{Q}_k - \frac{\dot{q}}{L+q}\sum_j g_{kj}Q_j, \tag{I.10}$$

$$p = m\dot{q} - \frac{1}{L+q}\sum_{j,k} g_{k,j}P_k Q_j. \tag{I.11}$$

From here it is then possible to define a Hamiltonian H associated to L. It can be easily checked that H represents the total energy of the system (kinetic and potential energies associated to the mirror's motion and the energy stored by the electromagnetic field inside the cavity).

$$\begin{aligned} H(q,p,\{Q_k,P_k\}) &= p\dot{q} + \sum_k P_k\dot{Q}_k - L(q,\dot{q},\{Q_k,\dot{Q}_k\}) \\ &= \frac{1}{2m}\left(p + \frac{1}{L+q}\sum_{j,k} g_{kj}P_k Q_j\right)^2 + V(q) + \sum_k\left[\frac{1}{2}P_k^2 + \omega_k(q)^2 Q_k^2\right] \\ &= \frac{1}{2}m\dot{q}^2 + V(q) + \frac{1}{2}\int_0^{L+q(t)} dx\ \left[\left(\frac{\partial A(x,t)}{\partial t}\right)^2 + \left(\frac{\partial A(x,t)}{\partial x}\right)^2\right] \end{aligned} \tag{I.12}$$

I.1.2.2. Main approximations

From the Hamiltonian I.12 one could "quantize" the problem by following the canonical quantification procedure (replacing the variables q, p, Q_k and P_k with noncommuting operators on a Hilbert space). Doing so at this point would lead to a Hamiltonian describing additional physical phenomena going beyond the scope of this thesis. Let us now briefly discuss these phenomena and present the main approximations leading to the quantum optomechanics Hamiltonian used throughout this manuscript.

Taking the infinite summations over the field modes into the quantum realm leads to a divergent vacuum field energy arising from the vacuum fluctuations of each mode. In order to get rid of such divergence one would have to take into account the field modes outside the cavity and by doing so introduce the well known Casimir force [57]. This force, which results from a differential radiation pressure force applied on both the internal and external faces of the mirror, would introduce a term $-\hbar\pi/24(L+q)$ into the potential energy $V(q)$. In the following we assume the equilibrium cavity length is big enough so that the Casimir potential can be neglected with respect to the other energies of the problem (kinetic energy and harmonic potential of the mirror motion and the energy stored in the electromagnetic field inside the cavity).

The non-linearities in Hamiltonian I.12 also allow two photon emission and absorption processes as well as exchange of photons between the different cavity modes. In the following we neglect these non linear processes and assume that only one mode contributes dominantly to the cavity field. The mode subscripts k are replaced by a single subscript c. The cavity field variables are thus Q_c and P_c and the cavity mode eigenfrequency will be denoted ω_c. In order for this one mode approximation to be valid the mirror motion has to be adiabatically slow (with respect to the photon lifetime inside the cavity) so that no photon scattering between cavity modes is possible.

Finally we assume that the mirror displacement is small enough so that the dynamics can be well described by keeping terms only to second order on q. The potential energy $V(q)$ is thus set to a harmonic potential $V(q) = \frac{1}{2}m\omega_m^2 q^2$, where ω_m is the frequency of the mechanical oscillation in this potential.

I.1.2.3. Quantum optomechanics Hamiltonian

Taking into account these approximations we now move to a quantum mechanical frame by applying the canonical quantization procedure. We let the variables q, p, Q_c and P_c be operators obeying the commutation relations

$$[\hat{q}, \hat{Q}_c] = [\hat{q}, \hat{P}_c] = [\hat{p}, \hat{Q}_c] = [\hat{p}, \hat{P}_c] = 0 \tag{I.13}$$

$$[\hat{q}, \hat{p}] = [\hat{Q}_c, \hat{P}_c] = i\hbar. \tag{I.14}$$

From here it is possible to introduce the usual annihilation and creation operators, $\hat{a}$ and $\hat{a}^\dagger$ respectively, for the cavity field

$$\hat{a} = \sqrt{\frac{1}{2\hbar\omega_c}} \left[\omega_c \hat{Q}_c + i\hat{P}_c\right] \tag{I.15}$$

$$\hat{a}^\dagger = \sqrt{\frac{1}{2\hbar\omega_c}} \left[\omega_c \hat{Q}_c - i\hat{P}_c\right]. \tag{I.16}$$

We thus get the usual quantum optomechanics Hamiltonian for the system under consideration (single mode optical cavity field coupled to the motion of a mechanical harmonic oscillator via radiation pressure)

$$\hat{H} = \hbar\omega_c \left(\hat{a}^\dagger \hat{a} + \frac{1}{2}\right) + \frac{\hat{p}^2}{2m} + \frac{1}{2} m\omega_m^2 \hat{q}^2 - \hbar G_{cm} \hat{a}^\dagger \hat{a} \hat{q}, \tag{I.17}$$

where we have introduced the optomechanical coupling between the cavity and the mechanical oscillator $G_{cm} = -\partial\omega_c/\partial q|_{q=0}$ ($G_{cm} = k\pi c/L^2$ for the linear model introduced in this Chapter, k is the mode number associated to the cavity mode under consideration). Here again we can introduce annihilation and creation operators for the mechanical resonator,

$$\hat{b} = \sqrt{\frac{m\omega_m}{2\hbar}}\hat{q} + i\sqrt{\frac{1}{2m\hbar\omega_m}}\hat{p}, \tag{I.18}$$

$$\hat{b}^\dagger = \sqrt{\frac{m\omega_m}{2\hbar}}\hat{q} - i\sqrt{\frac{1}{2m\hbar\omega_m}}\hat{p}. \tag{I.19}$$

Introducing the newly defined operators into the Hamiltonian I.17 yields the standard form of the Hamiltonian used in quantum optomechanics

$$\hat{H} = \hbar\omega_c \left(\hat{a}^\dagger \hat{a} + \frac{1}{2}\right) + \hbar\omega_m \left(\hat{b}^\dagger \hat{b} + \frac{1}{2}\right) - \hbar g_{cm} \hat{a}^\dagger \hat{a} \left(\hat{b}^\dagger + \hat{b}\right), \tag{I.20}$$

where we introduced $g_{cm} = G_{cm}\sqrt{\hbar/2m\omega_m} = G_{cm}x_{zpf}$, the single photon optomechanical coupling strength. g_{cm} represents the cavity frequency shift due to a displacement equal to the zero point fluctuations of the mechanical resonator position ($x_{zpf} = \sqrt{\frac{\hbar}{2m\omega_m}}$).

Before moving to the next step of our description of the system (the description of the dissipative baths responsible for the decoherence of the system) we would like to introduce a new transformation on the Hamiltonian which will prove useful in the following. Let us consider the dimensionless position and momentum operators for the mechanical resonator

$$\begin{aligned} \hat{q}_m &= \frac{\hat{b} + \hat{b}^\dagger}{\sqrt{2}} = \sqrt{\frac{m\omega_m}{\hbar}}\hat{q} \\ \hat{p}_m &= \frac{\hat{b} - \hat{b}^\dagger}{i\sqrt{2}} = \sqrt{\frac{1}{m\hbar\omega_m}}\hat{p}. \end{aligned} \tag{I.21}$$

These operators satisfy the dimensionless commutation relation $[\hat{q}_m, \hat{p}_m] = i$. Injecting them into the hamiltonian I.17 leads to the following form

$$\hat{H} = \hbar\omega_c\left(\hat{a}^\dagger\hat{a} + \frac{1}{2}\right) + \hbar\omega_m\left(\frac{\hat{p}_m^2}{2} + \frac{\hat{q}_m^2}{2}\right) - \sqrt{2}\hbar g_{cm}\hat{a}^\dagger\hat{a}\hat{q}_m. \tag{I.22}$$

I.1.3. Open system dynamics

Since the optomechanical coupling term in the Hamiltonian I.20 is proportional to the number of photons in the cavity, reaching a large photonic population boosts the optomechanical effects. In usual experimental realizations this is achieved by driving the system with a coherent laser. This drive not only populates the cavity but it also enables acquisition of information on mechanical motion via the detection of the photons exiting the cavity. The optomechanical cavity is thus receiving and giving information from and to the exterior world. Taking into account these information exchanges and the noise intrinsic to them requires a proper description of the coupling to the environment.

Another reason for taking into account the environment is the inclusion of the effects of finite temperature on the mechanical resonator dynamics. Indeed, given the usual orders of magnitude of the mechanical frequency ($\omega_m \sim$ 1 kHz-1 GHz), even dilution cryostat environments lead to a mean thermal occupation of the mechanical resonator $n_{th} \gg 1$. Neglecting the effects of the thermal environment would give an incomplete description of the dynamics. Furthermore, as will be presented later on in this Chapter, by taking into account this two environments

(the cavity field environment and the mechanical resonator thermal environment) it is possible to show that the optomechanical interaction can reduce the pseudo-thermal occupation of the mechanical resonator taking it close to its ground state. In the following paragraphs we present a Hamiltonian description of the total system {optomechanical cavity + environment}. We first discuss in general terms the properties of the environment and of the coupling between it and the system, and then we give the hamiltonian formulation used during this research project.

I.1.3.1. Modelling the environment

Let us first consider a simple optical cavity. We showed before that a single cavity mode can be described in terms of a harmonic oscillator at frequency ω_c. It is a well known result [58] that in quantum mechanics such a closed system has a discrete energy spectrum with equidistant energy levels separated by $\hbar\omega_c$. If one was to linearly probe the spectral response of such a system the resulting spectrum would yield a delta peak at frequency ω_c. But in real life experiments the spectral response of the cavity does not present a Dirac delta shape, rather the delta peak is convoluted with a Lorentzian distribution thus giving rise to a finite linewidth. The same holds for the problem of an atom with discrete eigenstates but whose spectral lines (obtained by means of an absorption experiment for example) are not sharp. Gardiner and Zoller give the following interpretation of the finite linewidths of atomic spectra: "The origin of the spectral linewidth is the coupling of the atom to the electromagnetic field, which has infinitely many degrees of freedom, and it is only because of this infinity that the irreversible phenomenon of atomic decay takes place" [59]. In the following we follow this guideline in order to describe the coupling to the environment. We assume that the cavity mode can either absorb a photon from the environmental field thus creating a cavity photon or it can emit/destroy a cavity photon in order to excite one of the vacuum modes outside the cavity. The optical bath is described as a collection of harmonic oscillators coupled to the cavity mode of interest. We assume that the coupling is linear in the bath and cavity operators. On the mechanics side the dissipative processes at play can have diverse origins. They can result from clamping losses due to the structural connection of the mechanical resonator to its support, they can also arise from fluidic damping due to the motion in the surrounding fluid (air or liquid) for example. In any case, we assume that the mechanical resonator undergoes Brownian motion and we describe it by assuming that it is also linearly coupled to an infinity of harmonic oscillators.

I.1.3.2. Optical Bath

Let us first take into account the optical bath leading to dissipative processes on the cavity field. We assume the following form for the Hamiltonian of the system {optomechanical cavity + optical bath},

$$\hat{H} + \hat{H}_{bath}^{opt} = \hat{H} + \int_q dq \ \left\{ \hbar\omega_q \hat{\alpha}_q \hat{\alpha}_q^\dagger + i\sqrt{\kappa_q} \left(\hat{\alpha}_q \hat{a}^\dagger - \hat{\alpha}_q^\dagger \hat{a} \right) \right\}. \tag{I.23}$$

Each mode of the environment is indexed by the subscript q and $\hat{\alpha}_q$, $\hat{\alpha}_q^\dagger$ are annihilation and creation operators for each mode. The first term under the integral on the right hand side of equality I.23 amounts for the energy of each environmental mode, the other two terms give the coupling between the system and its bath. The system can absorb a photon from one of the modes thus creating a photon in the cavity mode ($\hat{\alpha}_q \hat{a}^\dagger$) or one cavity photon can be lost to the extra cavity field ($\hat{\alpha}_q^\dagger \hat{a}$). The reservoir exchanges excitations with the system, at zero temperature ($\hbar\omega_c \gg k_b T$, with k_b Boltzmann's constant and T the environment temperature) the reservoir only absorbs energy from the system.

Let us assume that mode p is driven by a coherent pump. We consider it is in a coherent state $|A(t)\rangle$ such that $\hat{\alpha}_p |A(t)\rangle = A(t)|A(t)\rangle$ with $A(t) \in \mathbb{C}$. Let us now consider the unitary transformation given by the displacement operator $\hat{D}\left(A(t)\right) = \exp\left[A(t)\hat{\alpha}_p^\dagger - A(t)^* \hat{\alpha}_p\right]$. Up to a constant scalar term which can be forgotten, the Hamiltonian now reads

$$\begin{aligned} \hat{H} + \hat{H}_{bath}^{opt} = \hat{H} &+ iF_p \left(e^{-i\omega_p t} \hat{a}^\dagger - e^{i\omega_p t} \hat{a} \right) \\ &+ \int_q dq \ \left\{ \hbar\omega_q \hat{\alpha}_q \hat{\alpha}_q^\dagger + i\sqrt{\kappa_q} \left(\hat{\alpha}_q \hat{a}^\dagger - \hat{\alpha}_q^\dagger \hat{a} \right) \right\}, \end{aligned} \tag{I.24}$$

where we assumed the amplitude of the coherent state has a constant norm such that $A(t) = F_p/\sqrt{\kappa_p} \exp(-i\omega_p t)$ and we have chosen $F_p \in \mathbb{R}$ without loss of generality. The Hamiltonian I.24 corresponds to an optomechanical cavity driven by a coherent laser at frequency ω_p and coupled to the vacuum electromagnetic field whose modes are all in their ground state.

I.1.3.3. Mechanical bath

Let us now propose a Hamiltonian description for the dissipative dynamics undergone by the mechanical resonator. The train of thought is similar to what was just discussed but with the major difference that the relevant frequencies of the

mechanical resonator are such that the thermal occupancy of the modes has to be taken into account ($\omega_m \sim k_b T/\hbar$).

As stated before, the dissipative processes acting on the moving mirror can have diverse and multiple origins. They can arise from clamping losses in which case the dissipative processes can be understood in terms of energy exchanges between the mechanical resonator and the vibrational modes of the structure on which it is attached. The dissipation can also result from the action of the surrounding fluid on the motion of the mechanical resonator. In both cases and at equilibrium the problem is well described in terms of Brownian motion [60].

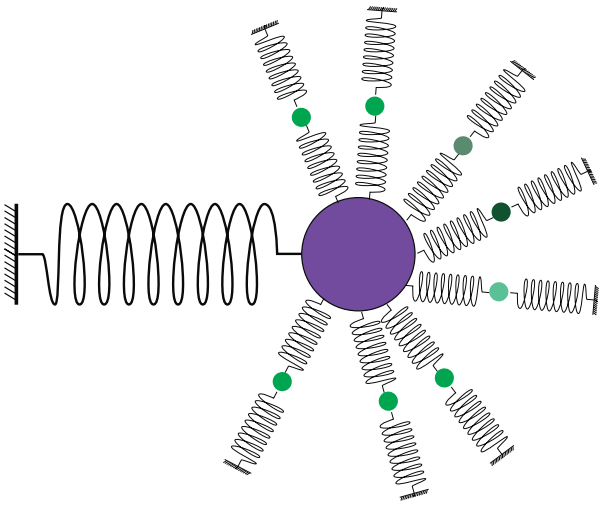

FIGURE I.2: A mechanical resonator linearly coupled to an infinity of oscillators. The coupling is mediated by the positions of the resonator and of the oscillators.

Looking for a Hamiltonian description for the dissipative processes undergone by the mechanical resonator amounts to choosing a microscopic description of the mechanical resonator's environment and of the coupling between the two of them. The picture we have chosen follows the schematics of Fig.I.2 : the mechanical resonator is coupled to an infinity of modes with a linear coupling via its position. We thus consider the following Hamiltonian for an optomechanical cavity whose moving mirror undergoes Brownian motion due to its coupling to a thermal environment of harmonic oscillators [61].

$$\hat{H} + \hat{H}_{bath}^{mech} = \hat{H} + \int_k dk \ \left\{ \hbar\omega_k \frac{\hat{p}_k^2 + (\hat{q}_k - g_k\hat{q})^2}{2} \right\}, \tag{I.25}$$

where k is an index for the modes of the bath, $\hat{q}_k$ and $\hat{p}_k$ are position and momentum operators for each mode, ω_k is the energy for mode k and g_k is the coupling

strength between the mechanical resonator and the mode. The Hamiltonian I.23 can be deduced from equation I.25 by introducing annihilation and creation operators and by neglecting the anti-resonant terms resulting from the coupling term.

I.1.4. Total Hamiltonian and extensions

The Hamiltonian of the complete system, optomechanical cavity and baths, is thus:

$$\begin{aligned}\hat{H}_{tot} =& \hbar\omega_c\left(\hat{a}^\dagger\hat{a}+\frac{1}{2}\right)+\hbar\omega_m\left(\hat{b}^\dagger\hat{b}+\frac{1}{2}\right)-\hbar g_{cm}\hat{a}^\dagger\hat{a}\left(\hat{b}^\dagger+\hat{b}\right)\\ &+iF_p\left(e^{-i\omega_p t}\hat{a}^\dagger-e^{i\omega_p t}\hat{a}\right)\\ &+\int_q dq\ \left\{\hbar\omega_q\hat{\alpha}_q\hat{\alpha}_q^\dagger+i\sqrt{\kappa_q}\left(\hat{\alpha}_q\hat{a}^\dagger-\hat{\alpha}_q^\dagger\hat{a}\right)\right\}\\ &+\int_k dk\ \left\{\hbar\omega_k\frac{\hat{p}_k^2+(\hat{q}_k-g_k\hat{q})^2}{2}\right\}.\end{aligned} \tag{I.26}$$

This Hamiltonian takes into account the dynamics of the closed optomechanical system (a cavity mode coupled to mechanical motion via radiation pressure), the driving of the cavity by a laser of frequency ω_p and intensity F_p, the cavity coupling to an optical bath modeled by a collection of harmonic oscillators in their ground state and the coupling of the mechanical resonator to a bath of thermally populated harmonic oscillators.

The Hamiltonian I.26 is the starting point of the physics studied in this thesis. In the following chapters we consider variations to this Hamiltonian, which are not derived in detail. Nevertheless, each time the modifications to the Hamiltonian are explicitly stated. In the case of the optomechanical arrays (Chapters II and III), each optical cavity is coupled to the same optical bath as in the Hamiltonian I.23 (they are subject or not to a coherent drive) and each mechanical resonator undergoes Brownian motion described by the Hamiltonian I.25. In the situation considered in Chapter IV, just as the cavity, an artificial atom is coupled to the vacuum electromagnetic field outside the cavity, which allows us to take into consideration the phenomenon of spontaneous emission from the atom.

At the beginning of this thesis, one of the guidelines of our work was to study the cooling mechanisms arising in optomechanical systems. The original description of this phenomenon can be found in Refs.[28–31]. The review [17] also presents the principles and limitations of optomechanical ground state cooling of the mechanical

resonator. In the following we present the main aspects of optomechanical cooling theory. We feel that this discussion provides an easy-to-follow scenario on which to discuss the relevant concepts in theoretical quantum optomechanics. Doing so also allows us to set-down important ideas that will be revisited in the following chapters.

I.2. Langevin equations

In this section we discuss the dynamics of the system within the Heisenberg representation. The time-varying behavior is carried by the operators while the state of the system remains unchanged. The time evolution for any given operator $\hat{O}(t)$, acting on the system or the environment, can be deduced from the Hamiltonian I.26 by simply applying the Heisenberg equation :

$$\hbar \frac{d\hat{O}(t)}{dt} = -i \left[\hat{O}(t), \hat{H}_{tot} \right]. \tag{I.27}$$

We thus get the following set of equations on the system's observables of interest,

$$\begin{aligned} \dot{\hat{a}} &= -i\omega_c \hat{a} + i g_{cm} \hat{a}(\hat{b} + \hat{b}^\dagger) + F_p e^{-i\omega_p t} + \int_q dq \ \sqrt{\kappa_q}\hat{\alpha}_q \\ \dot{\hat{b}} &= -i\omega_m \hat{b} + i g_{cm} \hat{a}^\dagger \hat{a} + \int_k dk \ \sqrt{\kappa_k}\hat{\beta}_k. \end{aligned} \tag{I.28}$$

The set of equations I.28 includes terms corresponding to the environment's dynamics, for which similar equations can be derived. Dealing with the complete set of dynamical equations would amount to follow at each time t the evolution of the whole system {optomechanical cavity + environment}. Given the size of the environment this would be impossible and inconvenient since in the end only the behavior of the optomechanical system is of interest. By using the Langevin equations formalism it is possible to overlook the environment's time evolution and keep track of its dissipative influence on the system altogether. We do not present the whole derivation of the Langevin equations [61–63] but rather give the essential assumptions, arguments and steps leading to the set of equations considered during this thesis.

By formally integrating the dynamical equations on the environment's observables one can rewrite the set I.28 in the following form

$$\begin{aligned}\dot{\hat{a}} &= -i\omega_c\hat{a} - \int_{-\infty}^{t} dt'\gamma_c(t-t')\hat{a}(t') + ig_{cm}\hat{a}(\hat{b}+\hat{b}^\dagger) + F_p e^{-i\omega_p t} + \hat{\xi}_c(t) \\ \dot{\hat{b}} &= -i\omega_m\hat{b} - \int_{-\infty}^{t} dt'\gamma_m(t-t')\hat{b}(t') + ig_{cm}\hat{a}^\dagger\hat{a} + \hat{\xi}_m(t).\end{aligned} \tag{I.29}$$

I.2.1. Dissipation and noise operators

The coupling to the environment leads to the presence of two terms in the equations of motion of the observables of interest. The first term ($\gamma_j(\tau)$, $j = c, m$), is responsible for the dissipation, which in general can be delayed (memory effect). The second term ($\hat{\xi}_j(t)$) is an operator acting on the environment, it represents the noise introduced by the environment onto the system.

By determining the properties of the memory kernel and the noise spectrum of the Langevin force it is possible to continue the study of the system dynamics. We assume that the optomechanical cavity is weakly coupled to the environment and that the environment is Markovian. The latter approximation implies that any system information dissipated to the environment is irreversibly lost. The markovian environment is thus memoryless and we set the memory kernel to $\gamma_j(t) = \gamma_j\delta(\tau)$, where γ_j is a constant amplitude decay rate for the cavity (γ_c) and for the mechanical resonator (γ_m) and $\delta(\tau)$ is the Dirac delta distribution.

The Langevin forces are treated as stochastic terms with zero mean value and their noise spectrum is determined by the following two relations

$$\langle[\hat{\xi}_j(t), \hat{\xi}_j^\dagger(t')]\rangle = \gamma_j\delta(t-t'), \tag{I.30}$$

$$\langle\hat{\xi}_j{}^\dagger(t)\hat{\xi}_j(t')\rangle = \gamma_j\frac{1}{\exp(\hbar\omega_j/kT)-1}\delta(t-t'). \tag{I.31}$$

In the correlation function in Eq.I.31 we see the appearance of a factor giving the average thermal occupation of an harmonic oscillator in equilibrium with a temperature T. As previously stated we assume that for the characteristic frequencies related to the cavity ($\omega_j \sim \omega_c$) this occupation factor is 0. For frequencies related to the mechanical resonator ($\omega_j \sim \omega_m$) we consider occupations given by a finite temperature.

The equations of motion for the cavity and mechanical degrees of freedom are thus

$$\begin{aligned}\dot{\hat{a}} &= -i\omega_c\hat{a} - \gamma_c\hat{a} + ig_{cm}\hat{a}(\hat{b}+\hat{b}^\dagger) + F_p e^{-i\omega_p t} + \hat{\xi}_c(t)\\ \dot{\hat{b}} &= -i\omega_m\hat{b} - \gamma_m\hat{b} + ig_{cm}\hat{a}^\dagger\hat{a} + \hat{\xi}_m(t).\end{aligned} \tag{I.32}$$

The equations of motion in terms of the mechanical resonator position will also be useful when discussing the effects of the radiation pressure coupling on the mechanical frequency and dissipation rate. Considering the normalized position operator the corresponding set of equations is :

$$\begin{aligned}\dot{\hat{a}} &= -i\omega_c\hat{a} - \gamma_c\hat{a} + i\sqrt{2}g_{cm}\hat{a}\hat{q}_m + F_p e^{-i\omega_p t} + \hat{\xi}_c(t)\\ \ddot{\hat{q}}_m &= -\omega_m^2\hat{q}_m - \gamma_m\dot{\hat{q}}_m + \sqrt{2}g_{cm}\omega_m\hat{a}^\dagger\hat{a} + \hat{\Xi}_m(t).\end{aligned} \tag{I.33}$$

Eq.I.32 and Eq.I.33 are not strictly equivalent as they result from two different Hamiltonians describing two different couplings to the thermal environment of the mechanical resonator. Eq.I.33 results from a coupling to the mechanical environment as described by the Hamiltonian in Eq.I.25. On the other hand Eq.I.32 arises from a coupling where the anti-resonant terms have been neglected, in which case the coupling to the mechanical bath is formally identical to that considered in Eq.I.23.
If the coupling to the mechanical environment is weak enough (in other terms if the mechanical quality factor is large enough, $Q_m = \omega_m/\gamma_m \gg 1$) both equations describe the same physics. The correlation function of the Langevin force acting on the mechanical resonator position is given by

$$\langle\hat{\Xi}_m(t)\hat{\Xi}_m(t')\rangle = \hbar\gamma_m\int_{\mathbb{R}} d\omega\ e^{i\omega(t-t')}coth\left(\frac{\hbar\omega}{2k_bT}\right). \tag{I.34}$$

The sets of differentials equations I.32 and I.33 contain a non-linear term proportional to $\hat{a}^\dagger\hat{a}$, which is treated with a mean field approach. By separating the mean fields and the fluctuations it is possible to linearize the optomechanical interaction and use a Fourier transform to analyze the cavity and mechanical spectral response.

I.3. Non-linear mean-field approach

Moving to the frame rotating at the pump frequency[1] we are able to eliminate the time dependance in the equations of motion. In this rotating frame the coherent pump term is now a constant F_p, and the cavity annihilation operator now oscillates at the cavity detuning defined as $\Delta = \omega_c - \omega_p$. Being coupled to the light field by the number of photons, the mechanical resonator is insensitive to this change of frame.

Having lost the time dependance in the equations we assume that the cavity and mechanical resonator reach a stationary state characterized by time-independent mean fields defined as : $\alpha = \langle \hat{a} \rangle$ and $\beta = \langle \hat{b} \rangle$. Injecting the definition of the mean fields into the equations of motion we obtain the following algebraic expressions:

$$\begin{aligned} 0 =& -(i\Delta + \gamma_c)\alpha + ig_{cm}\alpha(\beta + \beta^*) + F_p \\ 0 =& -(i\omega_m + \gamma_m)\beta + ig_{cm}|\alpha|^2. \end{aligned} \tag{I.35}$$

Absorbing the equation on the mechanical mean field we derive a third order polynomial equation relating the intra-cavity photon intensity $I_c = |\alpha|^2$ to the pump intensity $|F_p|^2$.

$$|F_p|^2 = (\Delta^2 + \gamma_c^2)I_c - 4\Delta\frac{g_{cm}^2\omega_m}{\omega_m^2 + \gamma_m^2}I_c^2 + 4\frac{g_{cm}^4\omega_m^2}{(\omega_m^2 + \gamma_m^2)^2}I_c^3. \tag{I.36}$$

Such third order equation can lead to multistable regimes, reminiscent of Kerr non-linearities, in which for a given intensity of the coherent pump one has more than one solution to the mean field equation I.36. By looking at the polynomial it is possible to show that the multistability appears if and only if $\Delta > \sqrt{3}\gamma_c$, which is to say only for a red-detuned pump with respect to the cavity resonance.

Let us now take into account the fluctuations of the system around its mean-field. We write $\hat{a} = \alpha + \delta\hat{a}$ and $\hat{b} = \beta + \delta\hat{b}$. We limit ourselves to terms up to first order in the fluctuations.

$$\begin{aligned} \delta\dot{\hat{a}} &= -(i\Delta_{nl} + \gamma_c)\delta\hat{a} + i\alpha g_{cm}(\delta\hat{b} + \delta\hat{b}^\dagger) + \hat{\xi}_c(t) \\ \delta\dot{\hat{b}} &= -(i\omega_m + \gamma_m)\delta\hat{b} + i\alpha g_{cm}(\delta\hat{a} + \delta\hat{a}^\dagger) + \hat{\xi}_m(t) \end{aligned} \tag{I.37}$$

[1]The change of frame is performed by applying a unitary transformation to the Hamiltonian defined by the unitary operator : $\hat{U}_p = e^{i\omega_p t\hat{a}^\dagger\hat{a}}$.

The average stationary number of photons in the cavity $|\alpha|^2$ displaces statically the equilibrium position of the mechanical resonator thus shifting the resonance frequency of the cavity. We take into account this mean-field effect by introducing the non-linear detuning of the cavity $\Delta_{nl} = \Delta - (\beta + \beta^*)g_{cm}$. In the set of equations I.37 we have assumed without loss of generality that the coherent pump phase is such that $\alpha \in \mathbb{R}$. Having linearized the equations on the fluctuations the non-linear optomechanical coupling $g_{cm}\hat{a}^\dagger\hat{a}(\hat{b}^\dagger + \hat{b})$ is reduced to an effective linear coupling between the quadratures of the light field and the mechanical resonator. This effective linear coupling can be described by an interaction term in the Hamiltonian of the form $\alpha g_{cm}(\delta\hat{a}^\dagger + \delta\hat{a})(\delta\hat{b}^\dagger + \delta\hat{b})$. The effective optomechanical coupling is enhanced by the square root of the average number of photons inside the cavity.

The linear set of equations I.37 can be solved by considering the Fourier transform of the operators. For any time dependent quantity $c(t)$ its Fourier transform is defined as follows

$$\tilde{c}(\omega) = F[c(t)](\omega) = \int dt e^{i\omega t} c(t). \tag{I.38}$$

The Fourier transform of the Hermitian conjugate of an operator will be noted $F[\hat{c}^\dagger(t)](\omega) = \tilde{\hat{c}}^\dagger(-\omega)$ [2].

In frequency space the equations of motion link linearly the operators of the system to the noisy inputs by the environment.

$$\mathbf{M}[\omega] \begin{bmatrix} \tilde{\delta}\hat{a}(\omega) \\ \tilde{\delta}\hat{b}(\omega) \\ \tilde{\delta}\hat{a}^\dagger(-\omega) \\ \tilde{\delta}\hat{b}^\dagger(-\omega) \end{bmatrix} + i \begin{bmatrix} \tilde{\hat{\xi}}_c(\omega) \\ \tilde{\hat{\xi}}_m(\omega) \\ \tilde{\xi}_c^\dagger(-\omega) \\ \tilde{\xi}_m^\dagger(-\omega) \end{bmatrix} = 0, \tag{I.39}$$

where we have introduced the Bogoliubov matrix of the system

$$\mathbf{M}[\omega] = \begin{bmatrix} \Delta_{nl} - \omega - i\gamma_c & -\alpha g_{cm} & 0 & -\alpha g_{cm} \\ -\alpha g_{cm} & \omega_m - \omega - i\gamma_m & -\alpha g_{cm} & 0 \\ 0 & \alpha g_{cm} & -\Delta_{nl} - \omega - i\gamma_c & \alpha g_{cm} \\ \alpha g_{cm} & 0 & \alpha g_{cm} & -\omega_m - \omega - i\gamma_m \end{bmatrix}. \tag{I.40}$$

The stability of the mean-fields α and β can be checked by looking at the eigenvalues of the Bogoliubov matrix $\mathbf{M}[\omega]$. The mean-fields are stable if and only if

[2] $\int_{-\infty}^{+\infty} dt e^{i\omega t}\hat{c}^\dagger(t) = \left(\int_{-\infty}^{+\infty} dt e^{-i\omega t}\hat{c}(t)\right)^\dagger = (\tilde{c}(-\omega))^\dagger$

all the eigenvalues of the matrix have strictly negative imaginary parts, which is reminiscent of the well knwon Routh-Hurwitz criterion for stability [64]. Fluctuations diverge in time if any imaginary part changes sign, one then moves from damped to amplified fluctuations.

I.3.1. Bistability

Having this stability criterion for the mean-field solutions it is possible to separate the stable from unstable solutions of the mean-field equations. As shown in Fig.I.3 it is possible to obtain multistable regimes where the curve $\alpha(F_p)$ has an "S"-like shape displaying unstable solutions for the middle branch. As soon as $\Delta < \sqrt{3}\gamma_c$ the multistability is lost, for every value of the pump intensity there is one and only one mean-field solution. In the case where the multistability is possible, the center of the "S"-like curve (the center of the two points at which the derivative of the function $F_p(\alpha)$ changes sign) corresponds to an intracavity intensity $I_c = |\alpha|^2 = (\gamma_b^2 + \omega_m^2)\Delta/3g_{cm}^2\omega_m$. Higher values of the optomechanical coupling lead to the appearance of the bistability for smaller number of photons. Inversely if the detuning between the cavity and the pump increases the bistability is pushed to larger values of the number of photons. For an early experimental demonstration of the bistable behavior of optomechanical systems the reader is invited to consult the reference [19].

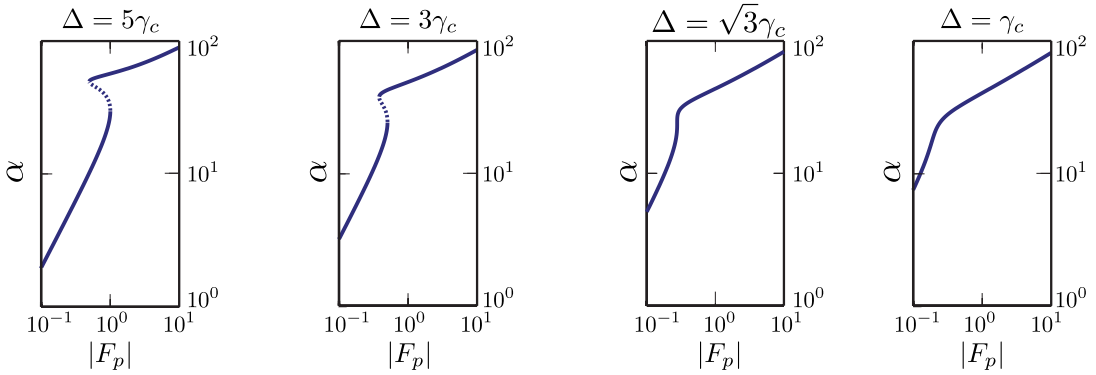

FIGURE I.3: Solutions of the mean-field equation for the cavity field α as a function of the coherent pump intensity F_p for different values of the cavity detuning $\Delta = \omega_c - \omega_p$. Stable (unstable) solutions are shown as solid (dashed) lines. $\gamma_m/\omega_m = 10^{-6}$, $\gamma_c/\omega_m = 10^{-3}$, $g_{cm}/\omega_m = 10^{-3}$.

In the following section we discuss cavity cooling of mechanical motion in the regime where the linearization with respect to the mean-field holds. We implicitly assume that the system reaches a stable stationary state and that it is far from bistability.

I.4. Cavity cooling of mechanical motion

I.4.1. Linearized optomechanics

The linear set of equations of motion I.37 can be recovered from an effective linear Hamiltonian,

$$\hat{H}_{lin} = \Delta\delta\hat{a}^\dagger\delta\hat{a} + \omega_m\delta\hat{b}^\dagger\delta\hat{b} - \alpha g_{cm}(\delta\hat{a}^\dagger + \delta\hat{a})(\delta\hat{b}^\dagger + \delta\hat{b}). \tag{I.41}$$

By performing an unitary transformation defined by the operator $\hat{U}(t) = \exp[i(\Delta\delta\hat{a}^\dagger \delta\hat{a} + \omega_m\delta\hat{b}^\dagger\delta\hat{b})t]$ it is easy to see that the optomechanical effects on the mechanical resonator are tailored by the cavity-pump detuning Δ [2]. For a pump red-detuned so that $\Delta = \omega_m$ the resonant terms in the optomechanical interaction are $\delta\hat{a}^\dagger\delta\hat{b} + h.c$, which allows transfer of excitations between the mechanical resonator and the cavity. Given that $\delta\hat{a}$ is an oscillator at zero temperature it is possible to cool down the mechanical resonator, the surplus thermal energy being extracted by the photons and dissipated into the vacuum electromagnetic field. For $g_{cm} \gg (\gamma_m, \gamma_c)$ $\delta\hat{a}$ and $\delta\hat{b}$ hybridize and it becomes possible to coherently transfer photonic information to mechanical states and vice-versa. On the other hand, for a blue detuned pump ($\Delta = -\omega_m$) the resonant interaction is $\delta\hat{a}^\dagger\delta\hat{b}^\dagger + H.c$, which can lead to two-mode squeezing, entanglement and even mechanical instabilities if the amplification rate is larger than the losses.

Starting from the Langevin equations on the fluctuations around the mean field we now study how optomechanical effects of light on mechanical motion lead to its modification. This is discussed by considering the equations coupling the light field fluctuations $\delta\hat{a}$ to the mechanical resonator position around the new equilibrium position $\delta\hat{q}$. We show how radiation pressure leads to the optical spring effect and to the introduction of an optomechanical damping rate, ultimately responsible for either cooling or amplification of mechanical motion.

I.4.2. Langevin equations on fluctuations

The set of equations of motion we consider is

$$\begin{aligned}
\dot{a} &= -(i\Delta_{nl} + \gamma_c)\hat{a} + i\sqrt{2}g_\alpha q_m + \xi_c(t) \\
\dot{a}^\dagger &= -(-i\Delta_{nl} + \gamma_c)\hat{a}^\dagger - i\sqrt{2}g_\alpha\hat{q}_m + \xi_c^\dagger(t) \\
\ddot{q}_m &= -\omega_m^2 q_m - \gamma_m\dot{q}_m + \sqrt{2}g_\alpha\omega_m(a + a^\dagger) + \Xi_m(t),
\end{aligned} \tag{I.42}$$

where we have omitted the δ's and the hats in the fluctuation operators for simplicity and we have introduced the coherently enhanced optomechanical coupling $g_\alpha = \alpha g_{cm}$. Just as we did before, we move to Fourier space in order to obtain an equivalent set of algebraic equations:

$$\begin{aligned}
\tilde{a}(\omega) &= i\sqrt{2}g_\alpha \chi_c(\omega)\tilde{q}_m(\omega) + \chi(\omega)\tilde{\xi}(\omega) \\
\tilde{a}^\dagger(-\omega) &= i\sqrt{2}g_\alpha \chi_c^*(-\omega)\tilde{q}_m(\omega) + \chi_c^*(-\omega)\tilde{\xi}^\dagger(-\omega) \\
\tilde{q}_m(\omega) &= \sqrt{2}g_\alpha \omega_m \chi_m(\omega)\left(\tilde{a}(\omega) + \tilde{a}^\dagger(-\omega)\right) + \chi_m(\omega)\tilde{\Xi}_m(\omega)
\end{aligned} \tag{I.43}$$

Here we see the appearance of the optical and mechanical susceptibilities, $\chi_c(\omega)$ and $\chi_m(\omega)$ respectively, which define the cavity and the mechanical resonator spectral response to the inputs. This suceptibilites are

$$\begin{aligned}
\chi_c^{-1}(\omega) &= i(\Delta_{nl} - \omega) + \gamma_c \\
\chi_m^{-1}(\omega) &= \omega_m^2 - \omega^2 - i\gamma_m\omega.
\end{aligned} \tag{I.44}$$

The cavity displays an usual Lorentzian response while the spectral response of the mechanical resonator is that of a well-known damped harmonic oscillator.

By eliminating the cavity degrees of freedom it is possible to get an equation only on the mechanical position fluctuation. These equations can be written in the form

$$\chi_{eff}^{-1}(\omega)\tilde{q}_m(\omega) = \tilde{\Xi}_{opt}(\omega) + \tilde{\Xi}_m(\omega) \tag{I.45}$$

As can be seen in Eq.I.45 the coupling to the light field has two major consequences. First, a modification of the mechanical spectral response, which is taken into account by the effective mechanical susceptibility

$$\chi_{eff}^{-1}(\omega) = \chi_m^{-1}(\omega) - i2g_\alpha^2\omega_m\left(\chi_c(\omega) - \chi_c^*(-\omega)\right). \tag{I.46}$$

Second, the mechanical resonator is effectively coupled to an additional noise source of optical origin $\tilde{\Xi}_{opt}(\omega)$. This Langevin force describes how the fluctuations arising from the coupling between the cavity photons and their environment affect mechanical motion. This additional noise can be cast in terms of the noise operators acting on the cavity as follows:

$$\tilde{\Xi}_{opt}(\omega) = \sqrt{2}g_\alpha\omega_m\left(\chi_c(\omega)\tilde{\xi}_c(\omega) + \chi_c^*(-\omega)\tilde{\xi}_c^\dagger(-\omega)\right). \tag{I.47}$$

The effective susceptibility in Eq.I.46 can be interpreted as resulting in a modification of the mechanical resonance frequency and of the mechanical damping rate, such that one can write $\chi_{eff}^{-1} = \omega_{eff}^2(\omega) - \omega^2 - i\omega\gamma_{eff}(\omega)$. This modification leads to what is known as the optical spring effect, in which the stiffness of the mechanical resonator can be controlled by the laser pumping of the cavity [65]. Of particular interest is the modification of the mechanical damping rate:

$$\gamma_{eff}(\omega) = \gamma_m + 2g_\alpha^2 \frac{\gamma_c \omega_m}{\omega} \left[\frac{1}{(\Delta_{nl} - \omega)^2 + \gamma_c^2} - \frac{1}{(\Delta_{nl} + \omega)^2 + \gamma_c^2} \right]. \tag{I.48}$$

For weak optomechanical coupling and large enough mechanical quality factors, this effect can be analyzed by just considering the problem at the unperturbed mechanical frequency ($\omega = \omega_m$). For red-detuned pumps $\Delta_{nl} > 0$ one obtains extra-damping that for strong enough pump intensities should completely eliminate the effects of thermal noise thus cooling down the mechanical resonator's motion. Blue-detuned pumps $\Delta_{nl} < 0$ on the contrary induce anti-damping leading to heating or even instability if the effective mechanical damping rate becomes negative.

In a classical approach to the cooling problem, we can assume that the optical environment is at zero temperature whereas the mechanical environment is at temperature T. The mechanical resonator couples with strength γ_m to its thermal environment and, due to the optomechanical coupling, is effectively coupled to the optical bath with a strength Γ_{opt}. The mechanical resonator total decay rate is thus $\gamma_{eff} = \gamma_m + \Gamma_{opt}$, and its final effective temperature should be given by $T_{eff} = \gamma_m T/(\gamma_m + \Gamma_{opt})$. By red-detuning the cavity and increasing sufficiently the laser power the optical damping Γ_{opt} should overcome the intrinsic damping rate γ_m and take the mechanical resonator down to its quantum ground state. Nevertheless with this approach we are not taking into account the fluctuations of the electromagnetic field, which will prevent us from getting exactly to the ground state. In the following section we present a rate equation approach to optomechanical cooling that gives a more precise insight into these fluctuations effects.

I.4.3. Optically induced transitions

The cooling of mechanical motion can be treated with rate equations for the populations of the mechanical resonator density matrix. In order to take into account

the optomechanical coupling it is necessary to know how it enters these rate equations. Based on usual time-dependent perturbation theory, we first derive a Fermi Golden Rule in terms of the spectral noise density of the perturbation. With this form of the Fermi Golden Rule we describe the optomechanically excited transitions of the mechanical resonator, which ultimately allows us to calculate the final occupancy of the mechanical resonator, thus giving the quantum limits of optomechanical cooling.

I.4.3.1. Fermi Golden Rule for noisy perturbations

Let us consider a system described by the following time-dependent Hamiltonian: $\hat{H} = \hat{H}_0 + \lambda\hat{\Theta}.\hat{F}(t)$. $\hat{H}_0$ is the unperturbed Hamiltonian, which we assume has a discrete diagonalization basis labeled $\{|n\rangle\}$ that verifies $\hat{H}_0|n\rangle = \omega_n|n\rangle$. $\hat{\Theta}$ is an operator acting on the system. $\hat{F}(t)$ is a noisy external operator perturbing the system. At any given time t the system is in a state $|\psi\rangle_t = \sum_n C_n(t)|n\rangle$ and we assume that initially its state is $|q\rangle$, meaning $C_n(t = t_0) = \delta_{nq}$. The objective of the calculation is to derive the probability to find the system in the $|n\rangle$ state after some small period of time $t > t_0$. We do so by performing an usual perturbative treatment on the coupling strength λ [66].

Let us introduce the probability amplitude of finding the state in the state $|n\rangle$, $b_n(t) = C_n(t)e^{i\omega_n t}$. The Schrödinger equation leads to the following set of equations on these amplitudes:

$$\forall n,\ \dot{b}_n = -i\lambda \sum_m \hat{F}(t)\Theta_{nm}e^{-i\omega_{mn}t}b_m, \tag{I.49}$$

where $\Theta_{mn} = \langle n|\hat{\Theta}|m\rangle$ is the matrix element between two coupled states, and $\omega_{mn} = \omega_m - \omega_n$ is the energy difference between the two states. Developing the perturbative treatment up to first order one finds that the probability amplitudes are given by:

$$\forall n \neq q,\ b_n(t) = -i\lambda\Theta_{nq}\int_{t_0}^{t} d\tau e^{-i\omega_{qn}\tau}\hat{F}(\tau) + \mathrm{O}\big(\lambda^2\big), \tag{I.50}$$

By averaging over the noise source we obtain that the probability to find the system in the state $|n\rangle$ at time t is,

$$\forall n \neq q,\ P_n(t) = \lambda^2|\Theta_{nq}|^2\int_{t_0}^{t}\int_{t_0}^{t} d\tau d\tau' e^{-i\omega_{qn}(\tau-\tau')}\langle\hat{F}(\tau)\hat{F}(\tau')\rangle. \tag{I.51}$$

If we assume that the whole system is in a stationary state so as to have $\langle \hat{F}(\tau)\hat{F}(\tau')\rangle = \langle \hat{F}(\tau-\tau')\hat{F}(0)\rangle$ we can introduce the spectral noise density for the noisy perturbation

$$S_{FF}[\omega] = \frac{1}{2\pi}\int d\tau e^{i\omega\tau}\langle \hat{F}(\tau)\hat{F}(0)\rangle, \tag{I.52}$$

which then leads to

$$P_n(t) = \lambda^2|\Theta_{nq}|^2 \int d\omega \int_{t_0}^{t}\int_{t_0}^{t} d\tau d\tau' e^{-i(\omega+\omega_{qn})(\tau-\tau')} S_{FF}[\omega]. \tag{I.53}$$

By performing two variable changes on the integrals over τ and τ' the previous expression can be rewritten

$$P_n(t) = \lambda^2|\Theta_{nq}|^2 \int d\omega S_{FF}[\omega] e^{-i(\omega+\omega_{qn})t/2} \left(2\frac{\sin((\omega+\omega_{qn})t)}{\omega+\omega_{qn}}\right)^2. \tag{I.54}$$

The last factor under the integral is well approximated by $\pi t\delta(\omega+\omega_{qn})$, which gives us the result we were looking for: the rate at which the state $|n\rangle$ is populated from the initial state $|q\rangle$

$$\Gamma_{q\mapsto n} = \frac{dP_n(t)}{dt} = \lambda^2|\Theta_{nq}|^2 S_{FF}[\omega_n - \omega_q] \tag{I.55}$$

I.4.3.2. Optically induced phonon transitions

For weak values of g_{cm} we can treat the optomechanical interaction perturbatively. In this case the noisy external perturbation is applied by the number of photons inside the cavity, $\hat{F} = \hat{a}^\dagger\hat{a}$. The spectral noise density of interest is thus the spectral density of the number of photons. The corresponding operator acting on the system is in this case $\hat{b}^\dagger + \hat{b}$, which couples an initial mechanical Fock state $|l\rangle$ to its neighbouring states $|l+1\rangle$ and $|l-1\rangle$.

In order to use the previously derived perturbative formula we need an expression for the spectral density of noise for the number of photons in the cavity. This can be obtained by using $\hat{a} = (\alpha+\delta\hat{a})\exp(-i\omega_p t)$ and $\langle \delta\hat{a}(t)\delta\hat{a}(0)\rangle = \exp(i\Delta_{nl}t - \gamma_c|t|)$ thus leading to

$$S_{nn}[\omega] = \frac{2\gamma_c|\alpha|^2}{(\omega+\Delta_{nl})+\gamma_c^2}. \tag{I.56}$$

Let us for a moment consider a simple mechanical resonator at frequency ω_m only coupled to a thermal environment at temperature T. At equilibrium the oscillator

has a mean number of excitations n_{th} given by the Boltzmann distribution: $n_{th} = 1/(\exp(\hbar\omega_m/k_bT) - 1)$. The dynamics of such a system can be described (as is discussed in further details in chapter II and in appendices A and B) by the following master equation on its density marix $\hat{\rho}$:

$$\dot{\hat{\rho}} = -i[\omega_m \hat{b}^\dagger \hat{b}, \hat{\rho}] + \gamma_m(n_{th}+1)D[\hat{b}]\hat{\rho} + \gamma_m n_{th} D[\hat{b}^\dagger]\hat{\rho}, \tag{I.57}$$

where $\gamma_o D[\hat{O}]\hat{\rho}$ is a Lindbladian super-operator acting on the density matrix. It describes a dissipative process characterized by a rate γ_o and a jump operator $\hat{O}$. From this master equation we can obtain equations of motion for the probability $P_l(t) = Tr(|l\rangle\langle l|\hat{\rho})$ of finding the mechanical resonator in the Fock state $|l\rangle$.

$$\begin{aligned}\dot{P}_l =& \gamma_m(n_{th}+1)(l+1)P_{l+1} - \gamma_m(n_{th}+1)lP_l \\ &+\gamma_m n_{th} l P_{l-1} - \gamma_m n_{th}(l+1)P_l.\end{aligned} \tag{I.58}$$

In the thermal rate equation Eq.I.58 we see that the state $|l\rangle$ is populated by decay of the state $|l+1\rangle$ (upper left term) or excitation of the state $|l-1\rangle$ (lower left). Similarly, decay of the state $|l\rangle$ populates $|l-1\rangle$ (upper right) and excitation of $|l\rangle$ populates $|l+1\rangle$ (lower right).

The optomechanical coupling proportional to $(\hat{b}^\dagger + \hat{b})$ induces similar transitions. The Fermi Golden Rule previously derived allows us to define optical transition rates corresponding to the optically induced excitation and decay of a Fock state. These rates are noted $\gamma_{opt}^{\uparrow}$ and $\gamma_{opt}^{\downarrow}$ respectively. They are defined as follows:

$$\begin{aligned}\gamma_{opt}^{\uparrow} &= g_{cm}^2 S_{nn}[\omega_m] = \frac{2\gamma_c|\alpha|^2 g_{cm}^2}{(\Delta_{nl}+\omega_m)^2 + \gamma_c^2} \\ \gamma_{opt}^{\downarrow} &= g_{cm}^2 S_{nn}[-\omega_m] = \frac{2\gamma_c|\alpha|^2 g_{cm}^2}{(\Delta_{nl}-\omega_m)^2 + \gamma_c^2}.\end{aligned} \tag{I.59}$$

Once again we see that the cavity-pump detuning plays a central role in determining how the mechanical resonator statistics will be modified by the photons in the cavity. Introducing this optical rates to Eq.I.58 we obtain the following optomechanical rate equation for the mechanical resonator.

$$\begin{aligned}\dot{P}_l =& \gamma_m(n_{th}+1)(l+1)P_{l+1} - \gamma_m(n_{th}+1)lP_l \\ &+\gamma_m n_{th} l P_{l-1} - \gamma_m n_{th}(l+1)P_l \\ &+\gamma_{opt}^{\downarrow}(l+1)P_{l+1} - \gamma_{opt}^{\downarrow} l P_l \\ &+\gamma_{opt}^{\uparrow} l P_{l-1} - \gamma_{opt}^{\uparrow}(l+1)P_l\end{aligned} \tag{I.60}$$

We introduce an optical decay rate $\Gamma_{opt} = \gamma_{opt}^{\downarrow} - \gamma_{opt}^{\uparrow}$ that yields the effective decay rate of the mechanical resonator $\gamma_{eff} = \gamma_m + \Gamma_{opt}$. By doing so we can rewrite Eq.I.60 as the rate equation of an harmonic oscillator coupled with strength γ_{eff} to a thermal environment at an effective temperature T_{eff}. The stationary state thus has an effective occupancy given by

$$n_{eff} = \frac{\gamma_m n_{th} + \gamma_{opt}^{\uparrow}}{\gamma_m + \Gamma_{opt}}. \tag{I.61}$$

This treatment allows us to correctly compute the stationary number of phonons in the optomechanical resonator. In particular we are able to recover the effects of the photon number noise on the final phonon population. Even in the case where the coupling and the pump are strong enough to erase the thermal effects on the phonons, $\Gamma_{opt} \gg n_{th}\gamma_m$, there is an inferior limit to the final occupation of the mechanical resonator, reached when the red-detuning matches the mechanical frequency $\Delta_{nl} = \omega_m$. The minimal number of phonons in this situation is given by: $n_{min} = (S_{nn}[-\omega_m]/S_{nn}[\omega_m] - 1)^{-1} = \gamma_c^2/\omega_m^2$. Approaching the quantum ground state by radiation pressure optomechanical cooling should hence be feasible in systems placed in what is known as the "resolved-sideband" or "good cavity" regime where $\omega_m \gg \gamma_c$.

I.5. Amplified motion of a mechanical resonator

So far we have discussed red-detuned pumping regimes, which lead to extra-damping of mechanical motion $\Gamma_{opt} > 0$ and ultimately cooling close to the ground state. Blue-detuned pumps on the other hand lead to anti-damping $\Gamma_{opt} < 0$ that results in heating-amplification of mechanical motion. For strong enough pump intensities (or strong enough effective optomechanical couplings) a blue-detuned pump can lead to an overall negative damping $\gamma_{eff} = \gamma_m + \Gamma_{opt} < 0$, thus setting unstable dynamics. In this case any small mechanical perturbation will exponentially grow in time until non-linear effects saturate the growth of mechanical motion amplitude. In this regime, parametric instability sets in giving rise to self-sustained oscillations of the mechanical resonator, which oscillates at frequency ω_m with constant amplitude A.

This mechanical instability was first discussed in classical terms [6]. In that work the position x of the mechanical resonator was assumed to evolve in time according to $x(t) = \bar{x} + A\cos(\omega_m t)$. By comparing the power injected to the system P_{inj} to the power dissipatedP_{diss} the authors showed that a classical optomechanical

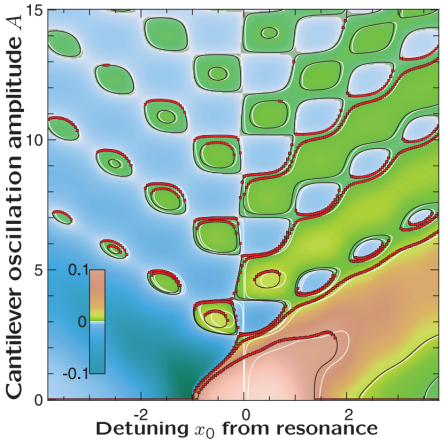

FIGURE I.4: Dynamical multistability in classical optomechanical systems. Density plot of the ratio of injected power to dissipated power as a function of mechanical oscillation amplitude A and cavity detuning x_0. The contour plots indicate possible oscillation amplitudes. Figure from [6].

system should display a rich array of dynamical attractors as seen in Fig.I.4. This figure shows a density plot of the ratio P_{inj}/P_{diss} as a function of the mechanical oscillation amplitude A and the cavity detuning x_0. The white contour plots displayed in the figure correspond to values for which this ratio goes to one thus yielding suitable solutions to the equations of motion.

The mechanical instability has also been studied in the quantum regime [46, 67, 68]. The signatures of the instability on the quantum statistics have been studied by considering the mechanical Wigner distribution. The cross-over from below-threshold to above-threshold statistics have been discussed [46]. It has been shown that above the instability threshold the mechanical resonator is in "a coherent state undergoing circular motion in phase space but with an undetermined phase" [67]. The possibility to attain non-classical states for the mechanical resonator, corresponding to Wigner functions presenting negative values, has been discussed both numerically [67] and analytically [68].

In this chapter we presented the theoretical framework within which this thesis was undertaken. Starting from the classical equations of motion for a deformable Fabry Perot cavity we derived the Hamiltonian formulation of the standard optomechanics system. We presented some of the main tools used in order to describe the dissipative behavior of such systems and reviewed briefly the cooling capabilities of optomechanical systems.

The following chapters present the work and results that were obtained during this PhD. They include the application of the tools presented in this chapter to other cooling mechanisms (see chapter III), the implementation of numerical resolution methods for optomechanical systems (see chapter II) and the study of a hybrid cQED-optomechanics system (see chapter IV).

Chapter II

Numerical methods for optomechanical systems

In this chapter we present the numerical methods used and implemented during this thesis. The methods under discussion rely on the Lindblad master equation for the density matrix of the optomechanical cavity. We start by quickly reviewing the basic properties of the density matrix and we present the master equation studied during this thesis. We then present the methods used to numerically solve the Lindblad master equation in order to acquire information about the stationary state and dynamical behavior of the system. These methods rely on a truncation of the Hilbert space of an harmonic oscillator and are thus best suited for problems exploring a low number of excitations. In the second part of this chapter we present the truncated Wigner Monte Carlo method we implemented in order to explore semi-classical regimes of parameters by solving stochastic differential equations on scalar fields.

II.1. Density matrix and master Equation

So far we have discussed the coupling of the system to its environment with quantum Langevin equations on the observables of the system. Within a Heisenberg representation, the dynamical behavior has been carried on by the operators while implicitly assuming that the state vector (of both the system and the environment) remains constant in time. We assumed a memory-less, Markovian, environment and by doing so we arrived to a set of damped first order non-linear differential

equations. In chapter I the equations were tackled with a mean-field approximation and we described the effect of the noisy environment in terms of spectral densities of noise.

Here we change the point of view and switch to the Schrödinger representation in which the observables are constant operators and the time dependance is encoded on the system state. Given the coupling to the environment the system is no longer described by a one dimensional vector state but rather by a density matrix operator $\hat{\rho}$. In this chapter we start by introducing the main properties of a proper density matrix [1]. Then we present and discuss the master equation on $\hat{\rho}$, a first-order differential equation with time-independent terms that takes into account the coupling of the system to its environment. The form of the Lindblad master equation can be recovered from very general assumptions on the structure and the properties of the time dynamics of a proper density matrix. This discussion can be found in [69], we present a brief summary in appendix A. The master equation and the coefficients on the dissipative terms can also be recovered from a microscopic Hamiltonian describing the interaction between the system and its environment. We present the corresponding derivation for a harmonic oscillator coupled to a finite temperature environment in appendix B.

II.1.1. Density Matrix

The density matrix is an hermitian operator describing statistical mixtures of states. Given its hermiticity it can be rewritten under its diagonalized form

$$\hat{\rho} = \sum_k p_k \hat{\rho}_k, \tag{II.1}$$

where $\{\hat{\rho}_k = |\psi_k\rangle\langle\psi_k|\}_k$ is a set of projectors into the vectors $|\psi_k\rangle$ which form an orthonormal basis of the Hilbert space. p_k is the probability to find the statistical mixture in the state $|\psi_k\rangle$, and thus we have

$$Tr[\hat{\rho}] = \sum_k p_k = 1. \tag{II.2}$$

The expectation value of any observable $\hat{O}$ is given by

$$\langle \hat{O} \rangle = Tr\left[\hat{O}\hat{\rho}\right]. \tag{II.3}$$

[1] Reference [58] was a wise companion throughout this thesis and an avid reader will find in it deep insight into more general considerations on density matrices.

If the dynamics of the system under consideration is ruled by some Hamiltonian $\hat{H}$, then the time evolution of the density matrix is determined by the Schrödinger equation

$$i\hbar\frac{d\hat{\rho}}{dt} = \left[\hat{H}, \hat{\rho}\right]. \tag{II.4}$$

Finally, for any given density matrix one has $Tr[\hat{\rho}^2] \leq 1$ where the equality is met if and only if there is only one $p_k = 1$, the other probabilities being zero, in which case the system is said to be in the pure state $|\psi_k\rangle\langle\psi_k|$.

II.1.2. Lindblad Master Equation

In the previous chapter we described the dynamics of an optomechanical cavity coupled to its environment by means of the total Hamiltonian defined in eq.I.26. The environment dynamics are of little or no interest and thus we formally integrated it. Doing so we obtained a set of quantum Langevin equations for the photon and phonon operators. In the set of equations I.29 the coupling to the environment leads to a causal memory kernel and to the introduction of an stochastic force acting on the system operators. When assuming weak coupling to a Markovian environment the memory kernel results in a time independent dissipative term related to the noise by the fluctuation-dissipation theorem. From there the expectation value of any operator $\hat{o}(t)$ can be computed by solving the Langevin equations and calculating the average over the total system state.

The system density matrix $\hat{\rho}$ is obtained by averaging over the environment degrees of freedom via a partial trace operation. If we assume that the system is weakly coupled to a Markovian environment, the dynamics of the optomechanical cavity under consideration is ruled by the following master equation

$$\frac{d\hat{\rho}}{dt} = -\frac{i}{\hbar}\left[\hat{H}, \hat{\rho}\right] + \gamma_c D[\hat{a}]\hat{\rho} + \gamma_m(n_{th}+1)D[\hat{b}]\hat{\rho} + \gamma_m n_{th} D[\hat{b}^\dagger]\hat{\rho}, \tag{II.5}$$

where $\hat{H}$ is the optomechanics Hamiltonian defined in Eq.I.20. $D[\hat{o}]\hat{\rho} = \hat{o}\hat{\rho}\hat{o}^\dagger - 1/2(\hat{o}^\dagger\hat{o}\hat{\rho} + \hat{\rho}\hat{o}^\dagger\hat{o})$ is the Lindbladian super operator with an associated quantum jump operator $\hat{o}$. n_{th} is the mean thermal occupancy of the mechanical resonator when at equilibrium at temperature T,

$$n_{th} = \frac{1}{e^{\frac{\hbar\omega_m}{k_b T}} - 1}. \tag{II.6}$$

The Lindbladian terms in the master equation II.5 account for the dissipative processes enforced by the memory-less environment on the system. The irreversible loss of a photon to the electromagnetic vacuum field outside the cavity at a rate γ_c is described by the term $\propto D[\hat{a}]$. The term $\propto D[\hat{b}]$ describes the process of losing a phonon to the mechanical resonator environment. Finally, the term $\propto D[\hat{b}^\dagger]$ accounts for the fact that at finite temperature ($n_{th} \neq 0$) the environment can excite thermal phonons. While the set of Langevin equations I.29 contains stochastic forces the master equation is a time independent equation. The effects of the environment noise are here averaged by the partial trace operation over the environment degrees of freedom.

II.2. Numerical resolution of the Liouvillian operator

We now present the numerical tools used to study the master equation II.5. We begin by presenting the matrix representation chosen to numerically describe the system density matrix and the corresponding operators.

II.2.1. Truncation of a discrete Fock Hilbert space

Both the phonons and the photons evolve in infinite and discrete Hilbert spaces. Let us consider a pair of annihilation and creation operators $\hat{a}$ and $\hat{a}^\dagger$. In the Fock states basis $\{|l\rangle\}_{l\in\mathbb{N}}$ (which we label by increasing number of excitations) they are represented by the following infinite matrices

$$\hat{a} \equiv \begin{bmatrix} 0 & \sqrt{1} & 0 & \dots & 0 & \dots \\ \vdots & \ddots & \sqrt{2} & \ddots & \vdots & \\ \vdots & & \ddots & \ddots & 0 & \\ 0 & \dots & \dots & 0 & \sqrt{l} & \ddots \\ \vdots & & & & \ddots & \ddots \end{bmatrix}, \; \hat{a}^\dagger \equiv \begin{bmatrix} 0 & \dots & \dots & 0 & \dots \\ \sqrt{1} & \ddots & & \vdots & \\ 0 & \sqrt{2} & \ddots & \vdots & \\ \vdots & \ddots & \ddots & 0 & \\ 0 & \dots & 0 & \sqrt{l} & \ddots \\ \vdots & & & \ddots & \ddots \end{bmatrix}. \tag{II.7}$$

In order to perform the numerical calculations we introduce a cutoff to the Hilbert space dimension. Let l_{max} be the maximum number of excitations taken into account. We truncate the Hilbert space to the subspace spanned by the set of states $\{|l\rangle\}_{0\leq l\leq l_{max}}$. We then introduce numerical annihilation and creation operators,

$\hat{a}_{num}$ and $\hat{a}^{\dagger}_{num}$, defined by truncating the actual operators. These numerical operators are represented by the following matrices in the truncated Hilbert space of dimension $l_{max}+1$.

$$\hat{a}_{num} \equiv \begin{bmatrix} 0 & \sqrt{1} & 0 & \dots & 0 \\ \vdots & \ddots & \sqrt{2} & \ddots & \vdots \\ \vdots & & \ddots & \ddots & 0 \\ \vdots & & & \ddots & \sqrt{l_{max}} \\ 0 & \dots & \dots & \dots & 0 \end{bmatrix}, \; \hat{a}^{\dagger}_{num} \equiv \begin{bmatrix} 0 & \dots & \dots & \dots & 0 \\ \sqrt{1} & \ddots & & & \vdots \\ 0 & \sqrt{2} & \ddots & & \vdots \\ \vdots & \ddots & \ddots & \ddots & \vdots \\ 0 & \dots & 0 & \sqrt{l_{max}} & 0 \end{bmatrix}. \quad \text{(II.8)}$$

While the real annihilation and creation operators follow the commutation relation $[\hat{b}, \hat{b}^{\dagger}] = \mathbb{1}$, their numerical representations present a slightly different commutator:

$$[\hat{a}_{num}, \hat{a}^{\dagger}_{num}] \equiv= \begin{bmatrix} 1 & 0 & \dots & \dots & 0 \\ 0 & 1 & \ddots & & \vdots \\ \vdots & \ddots & \ddots & \ddots & \vdots \\ \vdots & & \ddots & 1 & 0 \\ 0 & \dots & \dots & 0 & -l_{max} \end{bmatrix}. \quad \text{(II.9)}$$

Except for the terms acting on the last vector of the truncated basis, $|l_{max}\rangle$, the numerical operators verify the proper commutation relation. As long as the system does not populate this last vector the numerical operators verify the algebraic properties necessary to properly simulate the system. The choice of l_{max} is dependent on the kind of statistics considered for the system. Describing a coherent or thermal state requires a bigger cut-off than the one needed to describe a Fock state with few excitations. In the following we choose values of l_{max} ensuring that the system state is accurately described by states in the truncated Hilbert space. In some cases, mainly when there is amplification of mechanical motion, the system can be driven out of the truncation thus leading to incorrect results from the numerical treatment. Choosing an *a priori* big enough cut-off is not sufficient and one should ensure that at every step of the numerical treatment the truncation of the Hilbert space is adequate.

II.2.2. Stationary state of the master equation

In the most general case the dynamics of a system weakly coupled to a Markovian environment can be cast under the form of a Lindblad master equation of the

form:

$$\frac{d\hat{\rho}}{dt} = -i\left[\hat{H}, \hat{\rho}\right] + \sum_o \gamma_o L[\hat{O}]\hat{\rho}, \tag{II.10}$$

with $\hat{H}$ the Hamiltonian of the system and $\{\hat{O}, \gamma_o\}_o$ a set of jump operators and their corresponding dissipative rates. Eq.II.10 is a first order linear differential equation for the density matrix which can be rewritten:

$$\dot{\hat{\rho}} = \mathcal{L}\hat{\rho}, \tag{II.11}$$

where we have introduced the linear Liouvillian superoperator $\mathcal{L}$ acting on the density matrix. If the system Hamiltonian is time-independent then the superoperator $\mathcal{L}$ is a constant operator. If the master equation II.10 has a stationary state $\hat{\rho}_{stat}$ it verifies $\dot{\hat{\rho}}_{stat} = 0$. Such a state is thus an eigenvector of the superoperator $\mathcal{L}$ with zero eigenvalue. We can thus recover the stationary state by diagonalizing the Liouvillian super operator and considering the zero-eigenvalued matrix.

This procedure presents a few mathematical problems which go beyond the scope of this thesis. First, the problem of the existence of such a stationary state is not an easy question. Even if there exists one such state the system could present multiple stationary states. Second, the superoperator being non-hermitian the usual discussions in terms of a basis of diagonalizing eigenvectors is not straightforward and so the general methods for first order differential equations do not necessarily apply to this problem. Finally, even if such a zero-eigenvalue matrix exists there is no *a priori* way of knowing if it defines a proper density matrix for a physical system. We thus make the following assumptions which were never violated during this thesis. First, the physical systems under consideration do possess a stationary state. Second, such a stationary state can be found by diagonalizing the Liouvillian superoperator and taking the zero-eigenvalue density matrix (which we assume to be unique).

Given that we are dealing with infinite Hilbert spaces (spanned by the infinite basis of Fock states for the mechanical resonator) there is no simple way to tackle the diagonalization of the corresponding superoperator. We thus opted for a numerical diagonalization. With the numerical representation previously discussed it is rather straightforward to construct the superoperator $\mathcal{L}_{num}$ corresponding to the numerical version of the hamster equation II.5. The density matrix is mapped into a finite size vector and the superoperator is represented by a matrix which is then numerically diagonalized. For small dimensions of the numerical Hilbert space it

is possible to implement an exact and complete diagonalization of the super operator. When the dimension becomes too big it is possible to exploit the sparsity of $\mathcal{L}_{num}$ and use the ARPACK library [70] in order to obtain the eigenvectors with the smallest eigenvalues.

By diagonalizing this matrix and extracting the corresponding zero-eigenvalued eigenmatrix we get the stationary density matrix of the system. This matrix contains all the information necessary to calculate the system statistics, observable mean values, equal time correlation functions between observables and the stationary Wigner density function of the mechanical resonator. In chapter IV we present the results obtained concerning the stationary statistics of the mechanical resonator when coupled to a Jaynes-Cummings atom-cavity system.

II.2.3. Time resolved dynamics

Let us now present the method used to study the time dependent evolution of the system. Looking into the dynamical evolution of the system we are able to gain additional insight into how the system evolves from one state to another thus completing the knowledge we obtain from the study of the stationary state.

The master equation under consideration is a first order differential equation that can be numerically solved with usual Runge-Kutta algorithms [71]. A fine tuning of the resolution parameters (mainly those controlling the tolerance of the integration step) is required in order to ensure the "unitary" evolution of the master equation. The conservation of the density matrix norm, $Tr[\hat{\rho}] = 1$, for every time step was chosen as a first validity check on the resolution precision. When tuning the values of the resolution tolerances a compromise has to be made. Too-big tolerances lead to non unitary evolutions. Too-small values conserve the trace but imply an integration time which is way too long making the method unusable in practice. The tuning of these parameters is strongly dependent on the numerical values of the system parameters considered (frequencies, couplings and dissipative constants). In the case of optomechanical systems, the orders of magnitude of difference between the photon and mechanical time scales may also lead to a stiff problem which should be handled with care. In the end we chose a set of parameters (parameters inherent to the physical problem and parameters inherent to the numerical resolution itself) allowing unitary evolution within a reasonable range (comparable to the unavoidable numerical noise rising from the finite number of available decimals), and integration times that for the biggest Hilbert spaces considered, $l_{max} \sim 100$, were of the order of a few hours.

We created a set of functions and data structures in order to calculate, store and treat the produced numerical data. We also established parallel computing routines in order to take full advantage of the material at hand (two 48-cores servers where acquired by the theory group of Laboratoire Matériaux et Phénomènes Quantiques in 2011). Parallel computing was not used directly in the solving routine but was rather implemented in order to accelerate the study for different sets of parameters, each iteration calculating a distinct set of parameters.

II.3. Truncated Wigner distribution and Monte Carlo simulations of stochastic equations on scalar fields

The numerical resolution methods presented this far rely on the truncation of the Hilbert space. In principle if the truncation is big enough then the numerical resolution yields the proper results. In practice the computational power of a machine is finite and thus there is a limit on the dimension of the Hilbert space that can be handled. We now present a numerical resolution based on stochastic differential equations for scalar fields rather that on a master equation for a density matrix. The equations for the scalar fields are obtained by mapping the problem from a matricial point of view (master equation for the density matrix) to a partial derivative equation for a quasi-probability distribution on the system fields (the truncated Wigner function of the photons and phonons).

We start by introducing quasi-probability distributions for a quantum system. We then draw the equivalence between the master equation II.5 and a partial derivative equation on the Wigner function of the system. Under certain assumptions this partial derivative equation becomes a Fokker-Planck equation. The problem is then well described by a set of first order stochastic differential equations which we solve numerically with a Monte Carlo code. Finally, we present the principle of the numerical resolution and the results obtained during this thesis on single cavity optomechanics and arrays of coupled optomechanical cavities.

II.3.1. Quasi-probability distributions

Let us consider a classical system consisting of n interacting particles with masses, positions and momenta $\{m_i, q_i, p_i\}_{1\leq i\leq n}$. The system dynamics is ruled by the

classical Halmiltonian

$$H(\{x_i, p_i\}) = \frac{p_1^2}{2m_1} + \frac{p_2^2}{2m_2} + \ldots + \frac{p_n^2}{2m_n} + V(x_1, \ldots, x_n). \tag{II.12}$$

If the system is at thermodynamic equilibrium at temperature T it is possible to introduce a probability distribution $P(x_1, \ldots, x_n; p_1, \ldots, p_n)$ such that the probability of finding each particle i at a position x_i with momentum p_i within the ranges $x_i \in [x_i, x_i + dx_i]$ and $p_i \in [p_i, x_i + dp_i]$ [2] respectively is given by

$$P(x_1, \ldots, x_n; p_1, \ldots, p_n) dx_1 \ldots dx_n dp_1 \ldots dp_n. \tag{II.13}$$

The probability distribution is given by the Gibbs-Boltzmann formula

$$P(\{x_i, p_i\}) = \exp\left[-\frac{H(\{x_i, p_i\})}{k_b T}\right]. \tag{II.14}$$

The average value of any function of the positions and momenta of the particles can then be calculated by integrating it all over the parameter phase space as follows

$$\langle f(\{x_i, p_i\})\rangle = \int_{\mathbb{R}^n} f(\{x_i, p_i\}) P(\{x_i, p_i\}) \prod_{1 \leq i \leq n} dx_i dp_i. \tag{II.15}$$

In 1932 Eugene Wigner published an article [72] where he explored the possibility to introduce a similar probability distribution for a quantum mechanical version of the system. It is far from a trivial problem since the non-commutation of position and momentum operator, $[\hat{x}_i, \hat{p}_j] = i\hbar\delta_{i,j}$, excludes the definition of simultaneous probabilities for both position and momentum. Nevertheless he managed to introduce a quasi-probability distribution presenting similar properties as in Eq.II.15. This distribution is nowadays known as the Wigner quasi-probability distribution and since then quasi-probability distributions in phase space have become important tools for the study of quantum optics systems [73].

Defining a probability distribution in order to describe a quantum system statistics as in Eq.II.15 poses a number of problems among which the non-commutation of operators in a Hilbert space. The introduction of a scalar representation for non-commuting operators of a harmonic oscillator was thoroughly tackled in a series of papers by Cahill and Glauber in 1969 [74, 75]. They discussed the existence and convergence of a Taylor series expansion of any given operator $\hat{o}$ in terms of

[2] dx_i and dp_i being the differential elements in phase space.

powers of the creation and annihilation operators, $\hat{a}^\dagger$ and $\hat{a}$, of the system,

$$\hat{o} = \sum_{m,n} c_{n,m} (\hat{a}^\dagger)^n \hat{a}^m. \tag{II.16}$$

In Eq.II.16 we chose a normally ordered expansion on the creation and annihilation operators where powers of $\hat{a}^\dagger$ are always to the left. Antinormal ordering, $\hat{a}^\dagger$ to the right, or symmetric ordering, where $\hat{a}^\dagger$ and $\hat{a}$ are in equal footing with respect to order, are also possible. In [74, 75] the authors discuss such power series expansions by introducing a continuous ordering parameter s which for $s = 1, 0, -1$ yields normal, symmetric and anti-normal ordering respectively. Here we quickly review the results presented in those references.

Let us consider a system described by a single pair of operators $\hat{a}$, $\hat{a}^\dagger$ verifying the commutation relation $[\hat{a}, \hat{a}^\dagger] = 1$. Such a system evolves in an infinite Hilbert space spanned by a discrete and complete set of orthonormal eigenvectors of the hermitian operator $\hat{a}^\dagger\hat{a}$, the Fock basis $\{|n\rangle\}_{n\in\mathbb{N}}$:

$$\forall n \in \mathbb{N},\ \hat{a}^\dagger\hat{a}|n\rangle = n|n\rangle. \tag{II.17}$$

Let us now introduce the unitary operator

$$\forall \alpha \in \mathbb{C},\ \hat{D}(\alpha) = \exp\left(\alpha\hat{a}^\dagger - \alpha^*\hat{a}\right), \tag{II.18}$$

which obeys the relation $\hat{D}(\alpha)^{-1} = \hat{D}^\dagger(\alpha) = \hat{D}(-\alpha)$. Usually called a "displacement operator", its action on the annihilation operator is

$$\hat{D}(\alpha)^{-1}\hat{a}\hat{D}(\alpha) = \alpha + \hat{a}. \tag{II.19}$$

It displaces the Fock state $|0\rangle$ into an eigenvector of $\hat{a}$ with eigenvalue α, the coherent state $|\alpha\rangle$:

$$\hat{a}|\alpha\rangle = \hat{a}\hat{D}(\alpha)|0\rangle = \alpha|\alpha\rangle. \tag{II.20}$$

The overlap between two coherent states is

$$\langle\beta|\alpha\rangle = \exp\left[-\frac{1}{2}|\alpha|^2 - \frac{1}{2}|\beta|^2 + \beta^*\alpha\right]. \tag{II.21}$$

Two coherent states are not orthogonal but their overlap vanishes if $|\alpha - \beta|^2 \mapsto +\infty$. The set of coherent states forms a continuous and overcomplete set of vectors

of the Hilbert space as

$$\int_{\mathbb{C}} |\alpha\rangle\langle\alpha|\pi^{-1}d^2\alpha = \mathbb{1}, \tag{II.22}$$

where the differential element of phase space is given by $\pi^{-1}d^2\alpha = \pi^{-1}d\Re(\alpha)d\Im(\alpha)$.

We define the s-ordered product $\{(\hat{a}^\dagger)^n\hat{a}^m\}_s$ by means of a Taylor series expansion of the operator

$$\begin{aligned}\hat{D}(\alpha,s) &= \hat{D}(\alpha)e^{s|\alpha|^2/2} \\ &= \exp\left[\alpha\hat{a}^\dagger - \alpha^*\hat{a} + \frac{1}{2}s|\alpha|^2\right] \\ &= \sum_{n,m=0}^{\infty}\frac{\alpha^n(-\alpha^*)^m}{n!m!}\{(\hat{a}^\dagger)^n\hat{a}^m\}_s.\end{aligned} \tag{II.23}$$

The normal and anti normally ordered products are recovered by setting $s = 1, -1$ respectively,

$$\{(\hat{a}^\dagger)^n\hat{a}^m\}_1 = (\hat{a}^\dagger)^n\hat{a}^m \tag{II.24}$$

$$\{(\hat{a}^\dagger)^n\hat{a}^m\}_{-1} = \hat{a}^m(\hat{a}^\dagger)^n. \tag{II.25}$$

The symmetrically ordered product $\{(\hat{a}^\dagger)^n\hat{a}^m\}_0$ is the average of all ways of ordering the product of n factors of $\hat{a}^\dagger$ and m factors of $\hat{a}$. For example we have

$$\{\hat{a}^\dagger\hat{a}\}_0 = \frac{1}{2}\left(\hat{a}^\dagger\hat{a} + \hat{a}\hat{a}^\dagger\right) \tag{II.26}$$

$$\{\hat{a}^\dagger\hat{a}^2\}_0 = \frac{1}{3}\left(\hat{a}^\dagger\hat{a}^2 + \hat{a}\hat{a}^\dagger\hat{a} + \hat{a}^2\hat{a}^\dagger\right). \tag{II.27}$$

From the completeness of the coherent states basis $\{|\alpha\rangle\}_{\alpha\in\mathbb{C}}$ it is possible to introduce a set of complete operators $\{\hat{T}(\alpha,s)\}_{\alpha\in\mathbb{C}}$ spanning the Hilbert space of operators. This set of operators is obtained by complex Fourier transform of the operators $\hat{D}(\alpha,s)$ as follows

$$\forall\alpha\in\mathbb{C},\ \hat{T}(\alpha,s) = \int_{\mathbb{C}}\hat{D}(\epsilon,s)e^{\alpha\epsilon^*-\alpha^*\epsilon}\pi^{-1}d^2\epsilon. \tag{II.28}$$

It is then possible to expand any arbitrary operator $\hat{o}$ over phase space in the following form

$$\hat{o} = \int_{\mathbb{C}} O(\alpha,-s)\hat{T}(\alpha,s)\pi^{-1}d^2\alpha. \tag{II.29}$$

The weight function is given by

$$O(\alpha, -s) = Tr\left[\hat{o}\hat{T}(\alpha, -s)\right]. \tag{II.30}$$

For a given value of s it is then possible to establish a one to one correspondence between operators and functions of scalar $\mathbb{C}$-numbers[3].

An operator of particular interest is the density matrix $\hat{\rho}$ of a system. It encodes the statistical information about the system so that the expectation value of any observable $\hat{o}$ is given by $\langle\hat{o}\rangle = Tr[\hat{\rho}\hat{o}]$. By means of the previous one-to-one correspondence between operators and functions we are able to obtain an expression of the average value of an observable in terms of an integral over phase space of some "probability" distribution.

$$Tr\left[\hat{o}\hat{\rho}\right] = \int_{\mathbb{C}} O(\alpha, -s)R(\alpha, s)\pi^{-1}d^2\alpha, \tag{II.31}$$

where $O(\alpha, -s)$ is the weight function associated to $\hat{o}$ by Eq.II.30 and $R(\alpha, s)$ is the scalar function associated to $\hat{\rho}$ by $R(\alpha, s) = Tr[\hat{\rho}\hat{T}(\alpha, s)]$. In general the function $R(\alpha, s)$ can have negative values forbidding us to treat it as an actual probability distribution. Nevertheless, given the relation in Eq.II.31 we will call it a quasi-probability distribution over the phase space of eigenvalues of the annihilation operator $\hat{a}$. For a given value of the ordering parameter s we have in particular

$$Tr[\{(\hat{a}^\dagger)^n\hat{a}^m\}_s\hat{\rho}] = \int_{\mathbb{C}} (\alpha^*)^n\alpha^m R(\alpha, s)\pi^{-1}d^2\alpha. \tag{II.32}$$

II.3.2. Fokker-Planck like equation for the Wigner Distribution

Let us now move back to the problem at hand, an optomechanical cavity coupled both to an electromagnetic environment, treated as if it were at zero temperature, and to a thermal environment at finite temperature T for the mechanical resonator. As previously stated the dynamics of such system can be described by dealing with

[3] Here we present a very brief discussion on this correspondence. The convergence domain of the expansion of Eq.II.23 depends on the value of the ordering parameter s. This translates into different domains of validity for the phase space expansion of Eq.II.29. For more details the reader should refer to [74, 75].

the following master equation

$$\begin{aligned}\frac{d\hat{\rho}}{dt} =& -i\left[\omega_c\hat{a}^\dagger\hat{a} + \omega_m\hat{b}^\dagger\hat{b} - g_{cm}\hat{a}^\dagger\hat{a} + iF_p(e^{-i\omega_p t}\hat{a} - e^{i\omega_p t}\hat{a}^\dagger), \hat{\rho}\right] \\ &+ \gamma_c\left(\hat{a}\hat{\rho}\hat{a}^\dagger - \frac{1}{2}(\hat{a}^\dagger\hat{a}\hat{\rho} + \hat{\rho}\hat{a}^\dagger\hat{a})\right) \\ &+ \gamma_m(n_{th}+1)\left(\hat{b}\hat{\rho}\hat{b}^\dagger - \frac{1}{2}(\hat{b}^\dagger\hat{b}\hat{\rho} + \hat{\rho}\hat{b}^\dagger\hat{b})\right) \\ &+ \gamma_m n_{th}\left(\hat{b}^\dagger\hat{\rho}\hat{b} - \frac{1}{2}(\hat{b}\hat{b}^\dagger\hat{\rho} + \hat{\rho}\hat{b}\hat{b}^\dagger)\right),\end{aligned} \tag{II.33}$$

where we have taken into account a coherent drive of the photons at frequency ω_p. Now we use the density matrix to quasi-probability distribution mapping we just presented to derive a partial differential equation on the corresponding function representing our system. We have two coupled harmonic oscillators represented by the operators $\hat{a}$ and $\hat{b}$ and their adjoint operators. We thus have two scalar fields α and β and two ordering parameters s and u for the cavity and the mechanical resonator respectively. The corresponding time-dependent quasi-probability distribution is noted $R(\alpha, \beta; s, u; t)$.

Given the linearity of the mapping, we derive the corresponding partial differential equation by calculating the quasi-probability distribution associated to each term in Eq.II.33. In order to do so we establish a series of correspondences to obtain the quasi-probability distribution associated to the product of some arbitrary operator $\hat{o}$ and a system operator ($\hat{a}$, $\hat{a}^\dagger$, $\hat{b}$, or $\hat{b}^\dagger$) [76]. With $f^\pm = s \pm 1/2$ and $g^\pm = u \pm 1/2$ the necessary correspondences are given by

$\hat{a}\hat{o} \longleftrightarrow (\alpha - f^-\partial_{\alpha^*})\, O(\alpha, \beta; s, u)$	$\hat{b}\hat{o} \longleftrightarrow (\beta - g^-\partial_{\beta^*})\, O(\alpha, \beta; s, u)$
$\hat{a}^\dagger\hat{o} \longleftrightarrow (\alpha^* - f^+\partial_{\alpha})\, O(\alpha, \beta; s, u)$	$\hat{b}^\dagger\hat{o} \longleftrightarrow (\beta^* - g^+\partial_{\beta})\, O(\alpha, \beta; s, u)$
$\hat{o}\hat{a} \longleftrightarrow (\alpha - f^+\partial_{\alpha^*})\, O(\alpha, \beta; s, u)$	$\hat{o}\hat{b} \longleftrightarrow (\beta - g^+\partial_{\beta^*})\, O(\alpha, \beta; s, u)$
$\hat{o}\hat{a}^\dagger \longleftrightarrow (\alpha^* - f^-\partial_{\alpha})\, O(\alpha, \beta; s, u)$	$\hat{o}\hat{b}^\dagger \longleftrightarrow (\beta^* - g^-\partial_{\beta})\, O(\alpha, \beta; s, u)$

(II.34)

From now on we only consider the case of the Wigner distribution of the system, $W(\alpha, \beta) = R(\alpha, s = 0; \beta, u = 0)$, which is obtained by considering symmetrical ordering[4] of the operators and thus setting $s = u = 0$. In this case the time-dependent Wigner distribution of the system $W(\alpha, \beta; t)$ follows the Fokker-Planck like equation defined in Eq.II.35.

[4] More details on the derivation for arbitrary ordering parameters can be found in Appendix C

$$\begin{aligned}\frac{\partial}{\partial t}W(\alpha,\beta;t) = &\partial_\alpha\left[i\omega_c\alpha - ig_{cm}\alpha(\beta+\beta^*) + \frac{\gamma_c}{2}\alpha + F_p e^{-i\omega_p t}\right]W(\alpha,\beta,t)\\ &+\partial_{\alpha^*}\left[-i\omega_c\alpha^* + ig_{cm}\alpha^*(\beta+\beta^*) + \frac{\gamma_c}{2}\alpha^* + F_p e^{i\omega_p t}\right]W(\alpha,\beta,t)\\ &+\partial_\beta\left[i\omega_m\beta - ig_{cm}\left(|\alpha|^2 - \frac{1}{2}\right) + \frac{\gamma_m}{2}\beta\right]W(\alpha,\beta,t)\\ &+\partial_{\beta^*}\left[-i\omega_m\beta^* + ig_{cm}\left(|\alpha|^2 - \frac{1}{2}\right) + \frac{\gamma_m}{2}\beta^*\right]W(\alpha,\beta,t)\\ &+\frac{\gamma_c}{2}\partial^2_{\alpha^*\alpha}W(\alpha,\beta,t) + \gamma_m\left(n_{th}+\frac{1}{2}\right)\partial^2_{\beta^*\beta}W(\alpha,\beta,t)\\ &+i\frac{g_{cm}}{4}\partial^3_{\beta\alpha^*\alpha}W(\alpha,\beta,t) - i\frac{g_{cm}}{4}\partial^3_{\beta^*\alpha^*\alpha}W(\alpha,\beta,t)\end{aligned} \tag{II.35}$$

Phase space approaches have been recently used to successfully study the quantum regime of optomechanical limit cycles appearing when the blue-detuned optical pump leads to mechanical self-sustained oscillations [68]. In that work only the mechanical Wigner distribution is introduced and analytical results on the mechanical resonator statistics show that it should be possible to obtain quantum statistics (negative values of the mechanical Wigner distribution) when exciting the mechanical resonator to a limit cycle. In the following we consider a Wigner distribution over the photons and phonons and use the Fokker-Planck like equation to derive a set of stochastic differential equations on the scalar fields α and β which can be numerically solved with Monte Carlo algorithms.

II.3.3. Equivalent stochastic equations on scalar fields

Eq.II.35 contains first order terms corresponding to a drift term determined by the system Hamiltonian $\hat{H}$. It should be noted that in the drift terms of the phonon field the optomechanical coupling is represented by a term $\propto |\alpha|^2 - 1/2$. This comes from the fact that the Wigner distribution favors symmetrical ordering of operators in which the number of photons operator is written as $\hat{a}^\dagger\hat{a} = 1/2(\hat{a}^\dagger\hat{a} + \hat{a}\hat{a}^\dagger - \mathbb{1}) = \{\hat{a}^\dagger\hat{a}\}_0 - \mathbb{1}/2$. The second order terms are responsible for the diffusion of the Wigner distribution in phase space. They rise from the dissipative coupling to the environment. Finally the non-linear radiation pressure coupling between the photons and phonons yields third order terms. Whenever the coupling constant is stronger than the dissipative effects of the environment these third order terms lead to the appearance of non-classical correlations in the system. In such a regime the Wigner function presents negative values which forbid any interpretation in

terms of actual probability distributions. In the following we neglect these terms. Doing so we limit ourselves to positive gaussian distributions which in return can be interpreted as probability distributions over phase space.

Without the third order terms we recover a Fokker-Planck equation with a definite positive diffusion matrix. The dynamical and statistical behaviour of such an equation can be recovered by considering the following set of stochastic equations on the scalar fields

$$\frac{d}{dt}\alpha = -i\omega_c\alpha + ig_{cm}\alpha(\beta+\beta^*) - \frac{\gamma_c}{2}\alpha + F_p e^{-i\omega_p t} + \sqrt{\frac{\gamma_c}{2}}\xi_c(t), \quad \text{(II.36)}$$

$$\frac{d}{dt}\beta = -i\omega_m\beta + ig_{cm}\left(|\alpha|^2 - \frac{1}{2}\right) - \frac{\gamma_m}{2}\beta + \sqrt{\gamma_m\left(n_{th}+\frac{1}{2}\right)}\xi_m(t), \quad \text{(II.37)}$$

where $\xi_c(t)$ and $\xi_m(t)$ are gaussian random variables with mean values to zero and whose correlators are given by $\langle\xi_c(t)\xi_c^*(t')\rangle = \langle\xi_m(t)\xi_m^*(t')\rangle = \delta(t-t')$. Such a set of equations has been used to numerically study amplitude noise suppression in cavity-driven oscillations of a mechanical resonator [77].

During this thesis we developed a numerical Monte Carlo code in order to numerically solve the set of equations II.36 and II.37 . A similar procedure had been developed in the theory group at Laboratoire Matériaux et Phénomènes Quantiques in order to successfully study light-matter interactions in semiconductor microcavities [78] and polariton super-fluidity [79–81]. We designed and tested an implementation able to study the physics in an array of coupled optomechanical cavities. Great effort was spent in order to tackle the stiffness of the corresponding numerical problem. The orders of magnitude separating the mechanical and cavity time scales lead to simulations requiring very precise integration time steps (in order to have enough resolution to follow the photon dynamics) over a very large time window (in order to properly describe the "slow" mechanical dissipation). The procedure crafted during this thesis also implements parallel computing structures in order to best exploit the equipment at hand.

In the following we present the Monte Carlo code developed. We study the convergence of the simulation and present the work undertaken in order to validate this numerical resolution method. We tested incrementally the different physical phenomena we wanted to study with our calculations and compared them to what is obtained by analytical treatment of the equations of motion. First we study the noise statistics for a system with no optomechanical coupling, $g_{cm} = 0$, for which the cavity and the mechanical resonator are described by coherent and thermal

states respectively. Second, we consider the mean field behaviour of an optomechanical cavity under coherent pumping and show that our resolution method is able to properly follow the bistable diagram solution discussed in Chapter I. Then we take into account the fluctuations around the mean fields and show that we are able to properly describe the cooling capabilities of a single optomechanical cavity. Finally, the numerical resolution was conceived to simulate an array of optomechanical cavities, we thus consider the auxiliary cavity scenario depicted in Chapter III for which we get excellent agreement between the numerical and analytical results and we present our results on synchronization of amplified mechanical motion in a 30×30 optomechanical array.

II.3.4. Truncated Wigner Montecarlo simulations

II.3.4.1. Principle

The numerical integration of equations Eq.II.36 and Eq.II.37 is performed by introducing a time step dt chosen small enough (we set $dt^{-1} \gg \omega_{max}$, where ω_{max} is the largest frequency at play in the system) so that we can write

$$\begin{aligned}
\alpha(t+dt) =& \alpha(t) + dt \times \Big[-(i\omega_c + \frac{\gamma_c}{2})\alpha(t) + ig_{cm}\big(\beta(t) + \beta^*(t)\big)\alpha(t) + F_p(t)\Big] \\
&+ \xi_c(t)\sqrt{\frac{\gamma_c}{4}dt} \\
\beta(t+dt) =& \beta(t) + dt \times \left[-(i\omega_m + \frac{\gamma_m}{2})\beta(t) + ig_{cm}\left(|\alpha(t)|^2 - \frac{1}{2}\right)\right] \\
&+ \xi_m(t)\sqrt{\gamma_m \frac{n_{th} + 1/2}{2}dt}.
\end{aligned} \tag{II.38}$$

For a single run of the integration we obtain a set of vectors $\alpha(t)$ and $\beta(t)$ containing the time evolution of the system fields. The Monte Carlo implementation calculates N configurations, each configuration corresponding to a statistically independent trajectory. As seen in Fig.II.1 we obtain a set of N independent trajectories $\{\alpha_k(t), \beta_k(t)\}_{1 \leq k \leq N}$.

The quantities of interest are the mean values of the observables of the system. For any given observable $\hat{o}\left(\hat{a}, \hat{a}^\dagger, \hat{b}, \hat{b}^\dagger\right)$ the correspondence between operators and

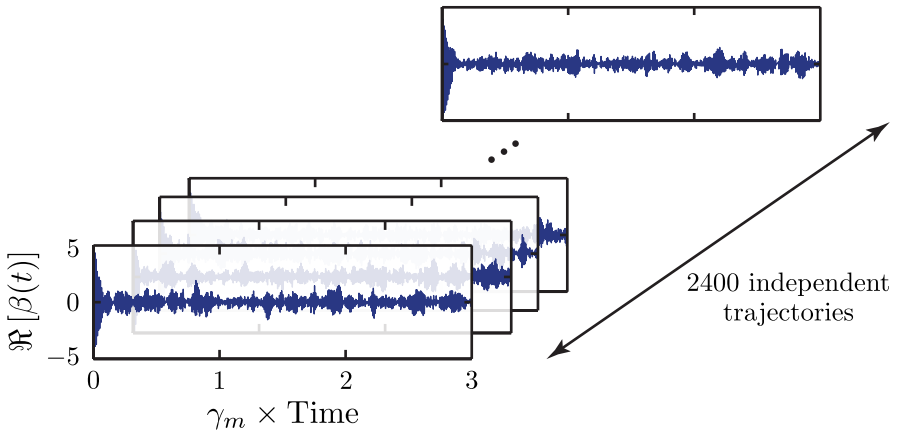

FIGURE II.1: Schematics of the data structure produced by the Monte Carlo algorithm. Here the simulation provides $N = 2400$ independent trajectories. We represent for each trajectory the real part of the phonon field $\Re[\beta(t)]$ as a function of time.

distributions over phase space yields the following relation:

$$\begin{aligned}\left\langle \hat{o}\left(\hat{a},\hat{a}^\dagger,\hat{b},\hat{b}^\dagger\right)\right\rangle &= Tr[\hat{o}\hat{\rho}] \\ &= \int_{\mathbb{C}} O(\alpha,\beta)W(\alpha,\beta)\pi^{-2}d^2\alpha d^2\beta.\end{aligned} \tag{II.39}$$

With the Monte Carlo procedure the average over phase space is recovered by averaging over the N independent configurations, so that

$$\left\langle \hat{o}(\hat{a},\hat{a}^\dagger,\hat{b},\hat{b}^\dagger)\right\rangle = \lim_{N\to+\infty}\frac{1}{N}\sum_{k=1}^{N} O(\alpha_k,\beta_k). \tag{II.40}$$

Let us now consider the field corresponding to the number of phonons after an average over N configurations:

$$\langle|\beta(t)|^2 - 1/2\rangle_N = \frac{1}{N}\sum_{k=1}^{N}|\beta_k(t)|^2 - \frac{1}{2}. \tag{II.41}$$

Fig.II.2 presents $\langle|\beta|^2-1/2\rangle_N$ as a function of time for increasing values of N. The set of parameters in Fig.II.2 corresponds to an optomechanical cavity pumped as to have cooling of mechanical motion. $\langle|\beta(t)|^2\rangle_N$ reaches a stationary state at a time t_{stat}. For times $t > t_{stat}$ the system fluctuates around this stationary state. We then calculate the N-dependent mean value and standard deviation over time

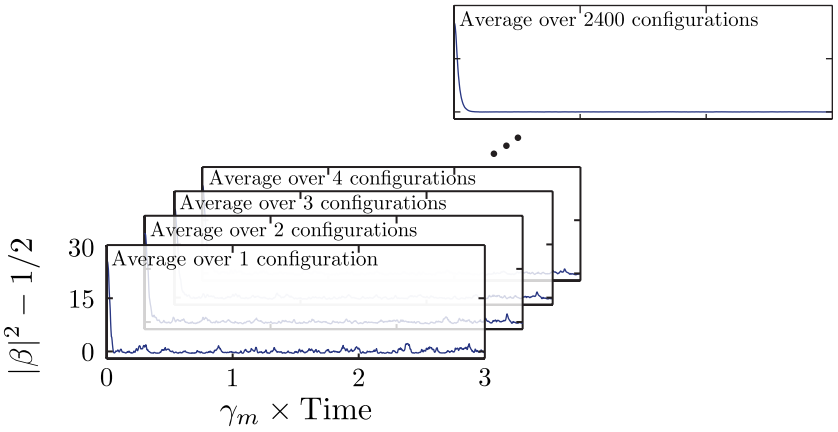

FIGURE II.2: Number of phonons as a function of time. The set of parameters has been set to yield optomechanical cooling of mechanical motion. The different plots correspond to results after averaging over an increasing number of configurations.

of the field in the stationary state as follows

$$\begin{aligned}\overline{\langle|\beta|^2\rangle_N} &= \frac{1}{t_{end}-t_{stat}}\int_{t_{stat}}^{t_{end}} d\tau \langle|\beta(\tau)|^2\rangle_N, \\ \sigma_{|\beta|^2}(N) &= \sqrt{\frac{1}{t_{end}-t_{stat}}\int_{t_{stat}}^{t_{end}} d\tau \frac{\left(\langle|\beta(\tau)]^2\rangle_N - \overline{\langle|\beta|^2\rangle_N}\right)^2}{\left(\overline{\langle|\beta|^2\rangle_N}\right)^2}},\end{aligned} \tag{II.42}$$

where t_{end} is the final time of the integration window.

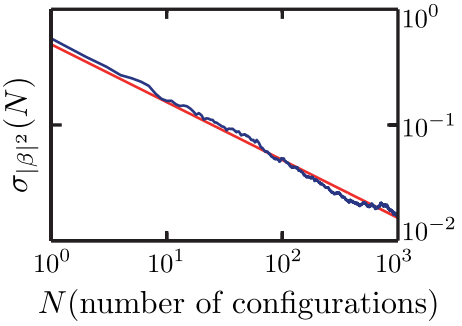

FIGURE II.3: N-dependent standard deviation of the number of phonons in the stationary state as function of the number of calculated configurations. The blue line corresponds to numerical results. The red line gives a fit proportional to the expected behavior $\propto 1/\sqrt{N}$.

Fig.II.3 presents the evolution of the standard deviation $\sigma_{|\beta|^2}(N)$ as a function of the number of calculated configurations. As expected from a Monte Carlo

algorithm computing statistically independent trajectories, the standard deviation decreases as $\propto 1/\sqrt{N}$.

II.3.4.2. Noise statistics

We now look closely at the noise statistics yielded by the truncated Wigner Monte Carlo simulation. Let us discuss a scenario in which there is no optomechanical coupling ($g_{cm} = 0$), no coherent excitation of the cavity photons ($\forall t,\ F_p(t) = 0$) and the mechanical resonator is at equilibrium with a bath at zero temperature ($T = 0$). Under this conditions the system density matrix is a product of the two ground states and the Wigner distribution of the total system is a product of two gaussians centered around 0.

$$W(\alpha, \beta) = \frac{4}{\pi^2} e^{-2|\alpha|^2} \times e^{-2|\beta|^2}. \tag{II.43}$$

Given that we expect a gaussian distribution for the fields of both the cavity and the mechanical resonator we only study the distribution moments up to second order. In order to characterize the gaussian states of the cavity and the mechanical resonator we consider the mean value of the number of photons and phonons and the mean value of the square of one of the quadratures. The two harmonic oscillators being in the ground state we should get

$$\begin{aligned} \langle \hat{a}^\dagger \hat{a} \rangle = \langle \hat{b}^\dagger \hat{b} \rangle = 0 \\ \langle (\hat{a}^\dagger + \hat{a})^2 \rangle = \langle (\hat{b}^\dagger + \hat{b})^2 \rangle = 1. \end{aligned} \tag{II.44}$$

In terms of an integral over phase space this expectation values are given by

$$\langle \hat{a}^\dagger \hat{a} \rangle = \int_{\mathbb{C}} \left(|\alpha|^2 - \frac{1}{2} \right) W(\alpha, \beta) d^2\alpha d^2\beta \tag{II.45}$$

$$\langle (\hat{a}^\dagger + \hat{a})^2 \rangle = \int_{\mathbb{C}} (\alpha + \alpha^*)^2 W(\alpha, \beta) d^2\alpha d^2\beta \tag{II.46}$$

$$\langle \hat{b}^\dagger \hat{b} \rangle = \int_{\mathbb{C}} \left(|\beta|^2 - \frac{1}{2} \right) W(\alpha, \beta) d^2\alpha d^2\beta \tag{II.47}$$

$$\langle (\hat{b}^\dagger + \hat{b})^2 \rangle = \int_{\mathbb{C}} (\beta + \beta^*)^2 W(\alpha, \beta) d^2\alpha d^2\beta. \tag{II.48}$$

Fig.II.4 presents the results yielded by the numerical resolution. Averaging over 4800 configurations we obtain an excellent agreement between the expected theoretical value and the numerics, with differences of the order $\sim 10^{-2}$, showing that

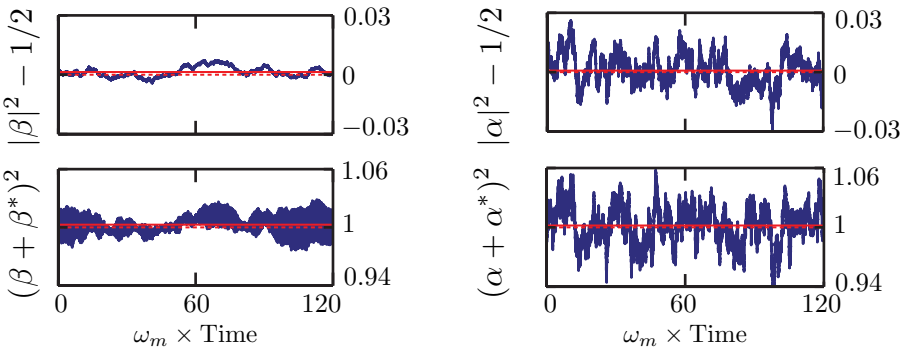

FIGURE II.4: Average values of the mechanical resonator (left column) and cavity (right panel) number of excitations (upper panel) and squared quadrature (lower panel). In blue the time evolution of the observables. Red-solid and red-dotted lines correspond to the average value over time and the expected theoretical value respectively. Results after averaging over 4800 configurations, $g_{cm} = 0,\ F_p = 0,\ T = 10^{-8},\ \Delta = 0,\ \gamma_m/\omega_m = 10^{-3},\ \gamma_c/\omega_m = 10^{-1}$.

the simulation is able to describe the proper statistics of a harmonic oscillator in its ground state coupled to the vacuum fluctuations.

We also checked the noise statistics for a cavity subject to non-zero coherent pumps and for a mechanical resonator at equilibrium with an environment at temperature $T \neq 0$. Under these conditions the cavity photons should be in a coherent state and the mechanical resonator in a thermal state. The corresponding Wigner distribution is then given by

$$W(\alpha,\beta) = \frac{4}{\pi^2} e^{-2|\alpha-\alpha_0|^2} \tanh\left(\frac{\hbar\omega_m}{k_b T}\right) \exp\left[-2|\beta|^2 \tanh\left(\frac{\hbar\omega_m}{k_b T}\right)\right], \tag{II.49}$$

where the photons are assumed to be in a coherent state $|\alpha_0\rangle$. The expected values for the mean values of the observables are in this case

$$\begin{aligned} \langle \hat{a}^\dagger \hat{a} \rangle &= |\alpha_0|^2 \\ \langle (\hat{a}^\dagger + \hat{a})^2 \rangle &= 1 \\ \langle \hat{b}^\dagger \hat{b} \rangle &= n_{th} = \frac{e^{-\hbar\omega_m/k_b T}}{1 - e^{-\hbar\omega_m/k_b T}} \\ \langle (\hat{b}^\dagger + \hat{b})^2 \rangle &= 2n_{th} + 1. \end{aligned} \tag{II.50}$$

Fig.II.5 presents the stationary state standard deviation between the numerical results and the expected theoretical values for different temperatures and different coherent pump intensities. The standard deviation for any given observable o is

defined as

$$\sigma[o] = \sqrt{\left\langle \frac{(o(t) - o_{theory})^2}{o_{theory}^2} \right\rangle_{erg}}, \tag{II.51}$$

where $\langle . \rangle_{erg}$ corresponds to the ergodic time average over the stationary state as discussed before.

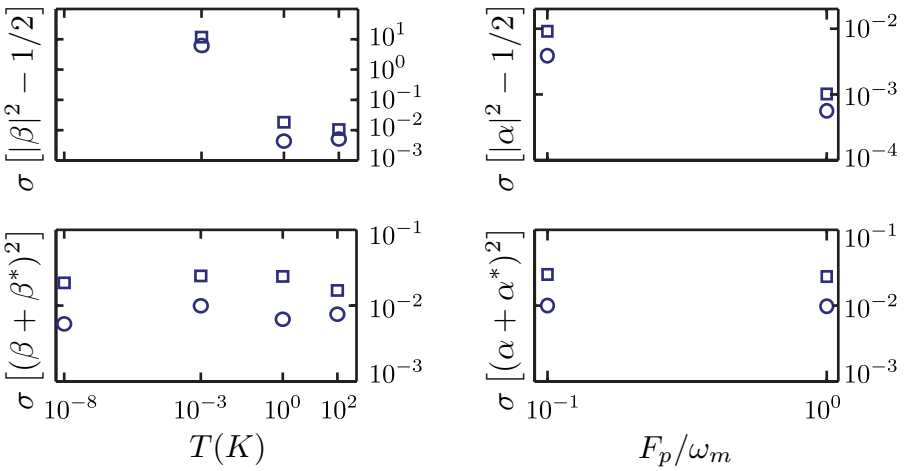

FIGURE II.5: Stationary state standard deviation of the observables of interest for an uncoupled system as a function of the equilibrium temperature (for the phonons) and the coherent pump intensity (for the photons). Squares and circles correspond to averaging over 800 or 4800 configurations respectively. $g_{cm} = 0,\ \Delta = 0,\ \gamma_m/\omega_m = 10^{-3},\ \gamma_c/\omega_m = 10^{-1}$.

Fig.II.5 displays the standard deviations obtained for averages over 800 configurations (squares) and 4800 configurations (circles). The calculations with 800 configurations display relative differences of the order of the percent and were obtained after roughly 2 hours of calculations using 12 parallelized processors. With 4800 configurations it is possible to reduce these differences by one or two orders of magnitude and the calculation time needed was of about six hours when using the same 12 processors. The deviation to the expected theoretical values is more important for lower values of the temperature and the pump intensity. This rises from the fact that properly describing such low number of excitations requires a much bigger number of configurations. The quadratures on the other hand have a lower bound ≥ 1, we thus get excellent an agreement with just 800 configurations.

These results show that the numerical resolution gives a proper description of the coherent and thermal statistics as long as the average is performed over a big enough number of independent configurations. Now we demonstrate it is also

able to describe accurately the mean field behavior rising from the non-linear optomechanical coupling.

II.3.4.3. Bistable mean-field behavior

In Chapter I we showed that the non-linear coupling between the photons and phonons leads to multistable solutions to the mean-field equations of the system. In particular we showed that for red-detuned pumps it is possible to reach a regime in which there are two stable solutions and an unstable one. Increasing and decreasing the pump intensity can lead to an hysteresis cycle (for an experimental observation of the optomechanical bistability see [19]). Fig.II.6 presents a numerical simulation in which we slowly change the pump intensity in order to scan the bistability diagram back and forth. We chose a pump with a gaussian shape over time as to ensure an intensity modification over time as adiabatic as possible. The blue line depicts the numerical dependance of the photon field absolute value as a function of the changing pump intensity. The red line corresponds to the analytical curve described by Eq.I.36. We have an excellent agreement between the analytical and numerical results.

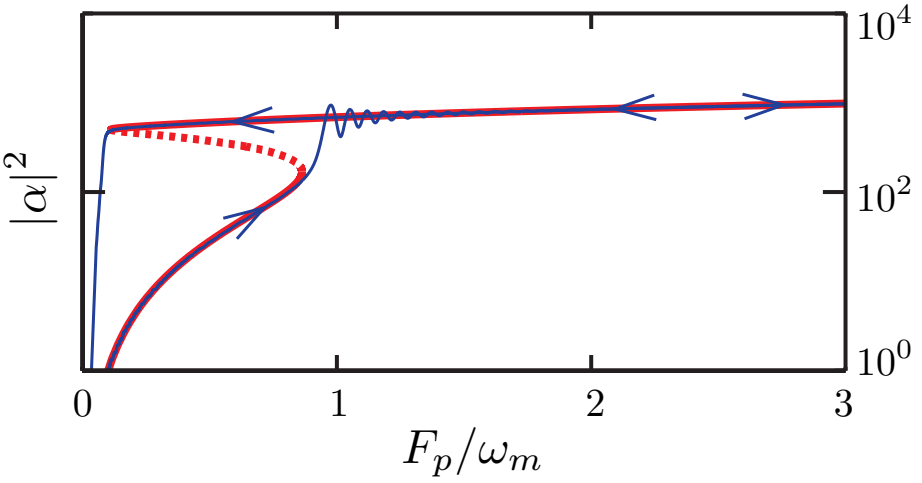

FIGURE II.6: Numerical bistability of the optomechanical mean-field equations. Squared absolute value of the photon field as a function of the time dependent pump intensity F_p. The red line depicts the expected theoretical bistable relation obtained from the mean field equations. The blue line corresponds to the numerical results. The width of the gaussian profile pump is given by $t_w\gamma_c = 5/3$. $\Delta/\omega_m = 10^{-1}$, $\gamma_m/\omega_m = 10^{-3}$, $\gamma_c/\omega_m = 10^{-2}$, $g_{cm}/\omega_m = 10^{-2}$, $T = 4mK, \omega_m = 1GH_z$. Results after averaging over 800 configurations.

The oscillations after the sudden jump on the cavity field are probably related to a transient regime excited by the abrupt change in the number of photons leading to a non adiabatic excitation of the mechanical resonator position.

II.3.4.4. Single cavity cooling

We now discuss the results of our numerical method beyond the mean fields. In particular we want to determine whether or not the numerical resolution takes properly into account the dynamics of the fluctuations around the mean field. Fig.II.7 presents the time evolution of the number of phonons inside the mechanical oscillator for a set of parameters chosen to give cooling from an initial thermal occupation of 130 phonons. According to Eq.I.61 the stationary state of the system should contain on average 1.44 phonons. The numerical treatment displays cooling of the mechanical resonator as expected. Averaging over time in the stationary state and over 800 configurations, the numerics yield a final occupation ~ 1.61.

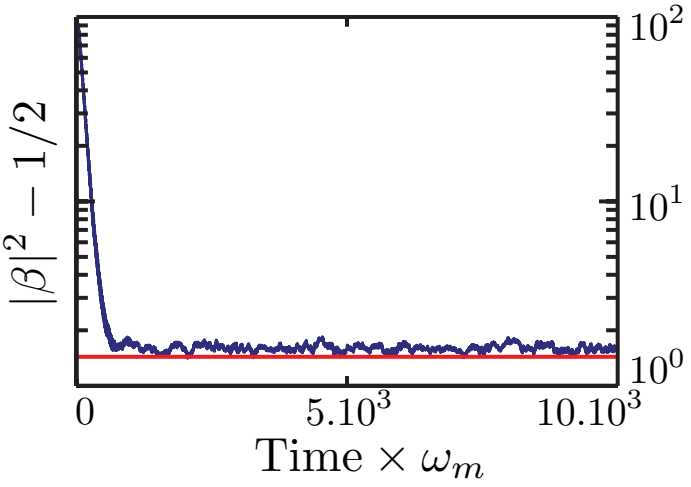

FIGURE II.7: Mechanical resonator number of phonons as a function of time. The red line corresponds to the final mechanical occupation computed with the theoretical results of Chapter I. The set of parameters ($\Delta/\omega_m = 1$, $\gamma_m/\gamma_m = 10^{-3}$, $\gamma_c/\omega_m = 10^{-1}$, $g_{cm}/\omega_m = 10^{-3}$, $F_p/\omega_m = 15$, $n_{th} = 130$) has been chosen to lead to cooling of the mechanical resonator down to ~ 1.44 excitations.

The disagreement between the theoretical value and the numerical result cannot be explained by the number of configurations which should be enough to obtain accuracy up to the percent. Given the pump intensity considered in the parameters of Fig.II.7 we believe that the system is being excited to a point close to the unstable solutions of the mean field approximation thus breaking the validity of the linearized approach. We obtain better agreement for less intense coherent pumps. Nevertheless we decided to show this figure for consistency with what is

presented in Fig.II.9. Both figures share the same parameters and Fig.II.9 presents our numerical results for the auxiliary cavity cooling scenario discussed in chapter III.

The final phonon occupation is related to the intrinsic dynamical behavior of the mechanical resonator (through γ_m), to the modifications to the mechanical damping rate introduced by the coupling to the photons (through Γ_{opt}) and to the effects of the optical noise (through $S_{opt}[\omega]$). The fact that our numerical resolution yields a result corresponding to what is expected from a theoretical treatment shows that the resolution is capable of properly taking into account the dynamical behavior of the fluctuations around the mean fields.

II.3.4.5. Linear optical coupling between cavities

We have stated before that the numerical implementation is well suited for the study of an optomechanical array comprising many optomechanical cavities. The scalar stochastic equations for the photon and phonons fields of the i-th optomechanical cavity are given by

$$\begin{aligned}
\frac{d}{dt}\alpha_i &= -i\omega_{ci}\alpha_i + ig_i\alpha_i(\beta_i + \beta_i^*) + i\sum_{j\neq i} J_{ij}\alpha_j - \frac{\gamma_{ci}}{2}\alpha_i + F_{pi}e^{-i\omega_{pi}t} + \sqrt{\frac{\gamma_{ci}}{2}}\xi_{ai}(t), \\
\frac{d}{dt}\beta_i &= -i\omega_{mi}\beta_+ ig_i\left(|\alpha_i|^2 - \frac{1}{2}\right) + i\sum_{j\neq i} K_{ij}\beta_j - \frac{\gamma_{mi}}{2}\beta_i + \sqrt{\gamma_{mi}\left(n_{th,i} + \frac{1}{2}\right)}\xi_{mi}(t),
\end{aligned} \tag{II.52}$$

where the matrices $\{J_{ij}\}$ and $\{K_{ij}\}$ determine the coupling between cavities which can be mediated by photons and/or phonons respectively.

Fig.II.8 presents a comparison between the analytical and numerical spectral response of a double cavity system with no optomechanical coupling ($g_1 = g_2 = 0$) and a site to site optical coupling ($\{J_{ij}\} \neq 0$, $\{K_{ij}\} = 0$). We obtain the spectral response of cavity 1 by applying a gaussian pulse to both cavities and deconvoluting the spectrum of the system excitation (coherent pump and white noise) from the photons spectrum. The numerical results are in excellent agreement with the theoretical predictions from Eq.III.24.

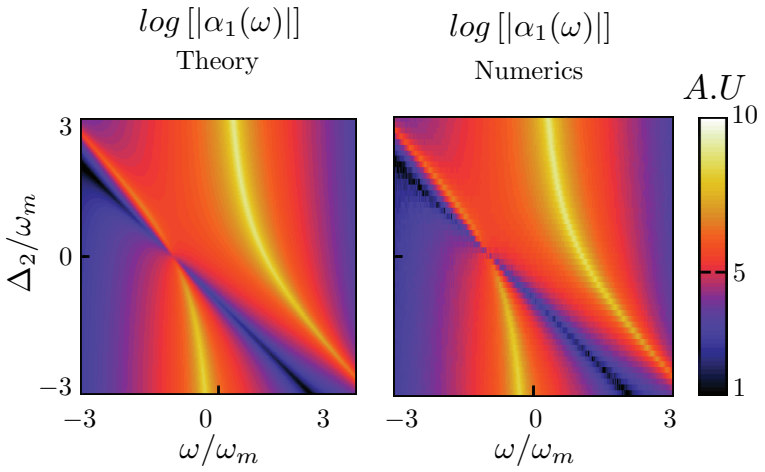

FIGURE II.8: Double cavity system spectral response. Absolute value of cavity 1 field Fourier transform as a function of frequency and cavity 2 detuning. The spectral response of the cavities is studied by applying a gaussian pulse of width $t_w \sim 6\gamma_c$. The other parameters are $\Delta_1 = 0,\ J = 10\gamma_c,\ \gamma_c/\omega_m = 10^{-1},\ g_{cm} = 0,\ F_p/\omega_m = 20,\ \{K_{ij}\} = 0$. The numerical results, obtained by averaging over 800 configurations, are in excellent agreement with the theory.

II.3.4.6. Auxiliary cavity cooling

In order to test if the numerics is capable of describing properly both a linear coupling between cavity photons and the optomechanical coupling we tested it with the auxiliary cavity cooling presented in Chapter III. Fig.II.9 displays the corresponding results for a calculation averaging over 1200 configurations. The set of parameters has been chosen so that theoretically the mechanical resonator reaches a stationary population of 14.4 phonons. Numerically (after ergodic average over the stationary state) we obtain a final occupation of 14.1 which is in good agreement with the analytical values.

II.3.4.7. Synchronization of optomechanical arrays

Finally we would like to present some preliminary results on the study of optomechanical arrays. It has been shown [82] that an array of optomechanical cavities coupled through the mechanical degrees of freedom can present synchronization of the limit cycle oscillations of the mechanical resonators.

We consider an all to all coupling scenario for an array of identical optomechanical cavities. We assume that the cavities are coupled via the mechanical degrees of

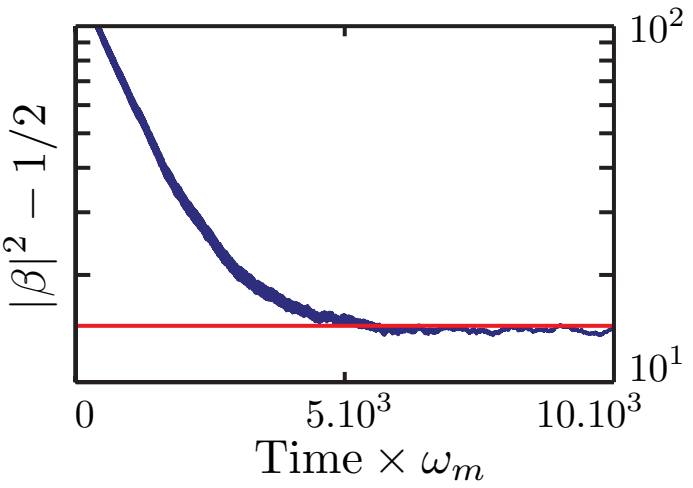

FIGURE II.9: Numerical results for the auxiliary cavity cooling of Chapter III. Number of phonons in cavity 1 as a function of time after averaging over 1200 configurations. The red line corresponds to the expected theoretical value. $\Delta_1/\omega_m = 10^{-2},\ \Delta_2/\omega_m = 7.10^{-1},\ \gamma_m/\omega_m = 10^{-4},\ \gamma_{ci}/\omega_m = 10^{-1},\ J/\omega_m = 1,\ g_1/\omega_m = 10^{-3},\ g_2 = 0,\ F_{pi}/\omega_m = 15,\ T = 1K,\ \omega_m = 1GH_z.$

freedom. The equations of motion of the i-th optomechanical cavity are then

$$\begin{aligned}
\frac{d}{dt}\alpha_i &= -i\omega_c\alpha_i + ig_{cm}\alpha_i(\beta_i + \beta_i^*) - \frac{\gamma_c}{2}\alpha_i + F_p e^{-i\omega_p t} + \sqrt{\frac{\gamma_c}{2}}\xi_{ai}(t), \\
\frac{d}{dt}\beta_i &= -i\omega_m\beta_i + ig_{cm}\left(|\alpha_i|^2 - \frac{1}{2}\right) + iK\sum_{j\neq i}\beta_j - \frac{\gamma_m}{2}\beta_i + \sqrt{\gamma_m\left(n_{th} + \frac{1}{2}\right)}\xi_{mi}(t).
\end{aligned} \tag{II.53}$$

In order to quantify the synchronization of the mechanical resonators we introduce the phase coherence

$$\chi_\phi = \left\langle \left| \frac{1}{N}\sum_j e^{i\phi_j} \right|^2 \right\rangle, \tag{II.54}$$

where N is the number of cavities in the array. The average is performed over the configurations. ϕ_j is the argument of the mechanical field in the j-th cavity:

$$e^{i\phi_j} = \frac{\beta_j}{|\beta_j|}. \tag{II.55}$$

Complete synchronization of the mechanical resonators corresponds to having $\forall j, \phi_j = \phi$ in which case χ_ϕ goes to 1. On the contrary, if there is no synchronization the phases of all the resonators are independent from each other in which case we have $\chi_\phi = 1/N$.

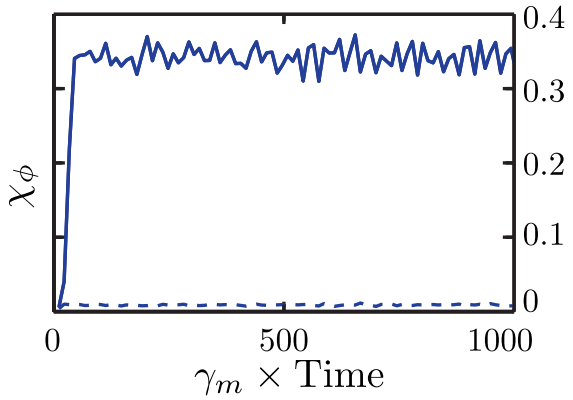

FIGURE II.10: Phase coherence of a 30×30 optomechanical array as a function of time. We consider an all to all mechanical coupling scenario in which $K_{ij} = K = \omega_m/4$. The other parameters are: $g_{cm} = \gamma_c = 0.3\omega_m$, $\gamma_m = 0.074\omega_m$ and $F_p = 1.1\gamma_c$. Solid blue line corresponds to a synchronized array with $\Delta = \omega_c - \omega_p = -\omega_m/2$. Dashed blue line corresponds to an unsynchronized array with $\Delta = -3\omega_m/4$.

Fig.II.10 presents the phase coherence of a 30×30 optomechanical array. The set of parameters are identical to those considered in [82]. Fig.II.10 presents the transition from synchronized to unsynchronized dynamics of the optomechanical array as the detuning between the coherent pump and the cavities frequency increases. Our numerical results are in good agreement with the results from [82].

The numerical methods for the resolution of the Lindblad master equation are extensively used in chapter IV in order to study the open system dynamics and statistics of a hybrid architecture combining optomechanics and quantum electrodynamics. The semi-classical truncated Wigner Monte Carlo approach is still a work in progress but given the promising results presented here we are confident that it will prove to be an useful tool for the study of disordered optomechanical arrays.

Chapter III

Non conventional optomechanical cooling: dissipative forces and auxiliary cavities

In chapter I we went through the theory of optical self cooling of mechanical motion in an optomechanical cavity coupled via radiation pressure [28–31]. The calculations show that for systems in the resolved-sideband regime, where the mechanical frequency is larger than the cavity linewidth, it is possible to cool mechanical motion down to the mechanical quantum ground state if the photons are pumped with a coherent pump red-detuned from the cavity resonance by an amount equal to the mechanical frequency. In this chapter we present two different cooling mechanisms for optomechanical systems. First we present our work on photothermal-based cooling [1]. We show that it is possible to cool mechanical motion without relying on the resolved-sideband regime by considering photothermal forces. We also present our work on an optomechanical cavity coupled to an auxiliary cavity. These new geometry modifies the optomechanical cavity spectral response thus allowing cooling close to the ground state while pumping almost resonantly the photons in the optomechanical cavity.

III.1. Limits of cavity optomechanical cooling by photothermal forces

In usual optomechanical setups the coupling between mechanical motion and cavity photons results from the reflection of photons on the mirror. The reflection

of a photon with wave vector k induces a momentum exchange $2\hbar k$ with the mirror, thus leading to radiation pressure. If instead of reflecting every incoming photon the moving mirror absorbs some energy from the light field, this extra energy can be converted into thermoelastic deformation of the mirror yielding a coupling between light and mechanics. The associated optically generated force is call the photothermal (or bolometric) force. Actually, the first experimental realizations of optomechanical self-cooling of mechanical motion were obtained in setups where this kind of photothermal force was dominating the dynamical effects [23, 83–85]. More recently several experimental groups have shown photothermal coupling between light and a variety of mechanical resonators such as semiconductor nanomembranes [86], grating reflectors [87], silicon nanowires [88] and graphene [89] among others.

When deriving a Hamiltonian formulation of the radiation pressure coupling we assumed the two cavity mirrors to be perfectly reflective. Later, in order to take into account the environment dissipative effects, we relaxed that approximation by introducing an optical decay rate γ_c measuring the rate at which photons leak out of the cavity. In the picture of a linear Fabry-Perot cavity this decay rate can be understood as resulting from the finite transmission coefficient $\mathcal{T}$ of the fixed mirror. The transmission decay rate of the amplitude γ_t is related to the fixed mirror transmission coefficient and to the photons round-trip time τ_0 by the relation $\gamma_t = \mathcal{T}/\tau_0$. In the following we consider that the moving mirror absorbs photons with an absorption coefficient A, thus introducing an additional loss channel described by a decay rate $\gamma_{abs} = A/\tau_0$. The cavity photons are then lost at a total decay rate $\gamma_c = \gamma_t + \gamma_{abs}$.

The absorbed photons transfer thermal energy to the mirror thus inducing a temperature field within the material. If this field is not uniform thermoelastic deformation of the mirror bulk material is possible and eventually leads to a modification of the cavity length. This mechanical effect is called photothermal or bolometric force. This additional optomechanical coupling has been extensively studied in the field of interferometric gravitational waves detection, where in order to reach the precision required to measure gravitational waves one needs to bound the different noise sources acting on the system. In particular, thermoelastic noise induced by heat diffusion in the mirror material after the absorption of photons has been taken into account [90, 91]. The noise on the number of absorbed photons has to be considered if one is to describe cooling to the ground state with photothermal forces.

We just discussed radiation pressure as resulting from momentum exchange between the photons and the mechanical resonator. Following the same guideline to

compute the amplitude of the photothermal force leads to the wrong conclusion that the latter is half as intense as radiation pressure (the absorption of a photon leads to a momentum exchange $\hbar k$). This was the scenario considered in a paper discussing photothermal forces before the beginning of this PhD work [92]. By doing so one fails to take into account the total energy transfer from the photon to the mechanical resonator. It has been shown experimentally that in case of absorption photothermal forces can actually overcome radiation pressure by several orders of magnitude [85]. The work we present here tackles a more general picture in which the difference of magnitude between the two forces is not fixed and where we take fully into account the effects of both radiation pressure and photothermal forces on the cooling of mechanical motion close to the ground state.

III.1.1. Description of a dissipative force

It has been stated that photothermal forces arise from heat generation due to photon absorption. Describing such a dissipative process from a Hamiltonian point of view is a difficult if not impossible task. To do so we would have to describe an infinite amount of degrees of freedom in order to describe the dissipative heat diffusion within the phonon modes of the bulk. Even though we do not have a Hamiltonian formulation of the problem, we tackle it with a quantum Langevin approach where the photothermal force acts as a time-delayed force depending on the number of photons absorbed by the mechanical resonator, and where the shot noise of the absorption process is taken into account. This approach is theoretically self-consistent and is supported by the fact that its classical limit has been shown to reproduce the dynamics of a large number of bolometric optomechanical settings.

III.1.1.1. Time-delayed photothermal force

At any time the number of absorbed photons by the mirror per unit time depends on the total number of photons in the cavity. Nevertheless the thermoelastic deformation will only change the position of the mechanical resonator after the extra thermal energy has diffused across the resonator. We assume that this diffusion has a characteristic finite time-scale τ_{th}. The photothermal force at time t thus depends on the number of absorbed photons in the past. We describe this time delayed force in terms of a convolution of the flux of absorbed photons with some causal memory kernel reflecting the thermal relaxation process :

$$\hat{F}_{photothermal}(t) \propto \int_{-\infty}^{+\infty} du \frac{1}{\tau_{th}} \Theta(t-u) e^{-\frac{t-u}{\tau_{th}}} \hat{I}_{abs}(u), \tag{III.1}$$

where $\tau \mapsto \Theta(\tau)$ is the Heaviside function and $\hat{I}_{abs}(\tau)$ is the rate of absorbed photons at time τ. This memory kernel plays an essential role in the discussion of photothermal cavity cooling. As we will see, in the case where photothermal force overcomes radiation pressure the thermal relaxation time τ_{th} replaces the photons life time $1/\gamma_c$ as the typical time scale of the dynamical optomechanical self-cooling process.

III.1.1.2. Fluctuation and dissipation

We assume that the equation of motion of the mechanical resonator can still be written in the standard form

$$\ddot{\hat{q}}_m = -\omega_m^2 \hat{q}_m - \gamma_m \dot{\hat{q}}_m + \hat{F}_{opt} + \hat{\Xi}_m(t), \tag{III.2}$$

where $\hat{F}_{opt}$ accounts here for the radiative forces (radiation pressure and photothermal force) applied by the light field. The mechanical damping rate γ_m and the stochastic Langevin force $\hat{\Xi}_m(t)$ are linked to each other via the fluctuation-dissipation theorem. The fluctuation and dissipation described by this quantities account for contributions from different noisy channels. On one hand the effects due to the campling of the mechanical resonator to a support at finite temperature. On the other hand the thermoelastic noise [90, 91] which finds its origin in the steady state temperature fluctuations of the oscillator body. Finally, any steady-state increase of the equilibrium temperature due to photon absorption will also be included in this terms. It will simply translate into a shifted environment temperature T. The Langevin force is thus still defined by the correlation function:

$$\langle \hat{\Xi}_m(t) \hat{\Xi}_m(t') \rangle = \hbar \gamma_m \int_{\mathbb{R}} d\omega \; e^{i\omega(t-t')} coth\left(\frac{\hbar\omega}{2k_b T}\right). \tag{III.3}$$

One last key element is necessary to discuss optomechanical cooling close to the ground state. As stated before, we have to take into account the effects of the fluctuations in the number of absorbed photons, which enforce fluctuations of the photothermal force. We do so by treating the absorbing mirror as an effective transmission channel with transmission coefficient A. Under these circumstances the photons in the cavity, the absorbed photons and the absorption shot noise are

related by the following input-output relation [63]

$$\begin{aligned}\hat{a}_{abs} &= \sqrt{\frac{A}{\tau_0}}\hat{a} - \hat{\xi}_{abs} \\ &= \sqrt{\gamma_{abs}}\hat{a} - \hat{\xi}_{abs},\end{aligned} \tag{III.4}$$

where $\hat{\xi}_{abs}$ is the noise operator corresponding to vacuum fluctuations entering the cavity through the absorption process. The intensity of absorbed photons is given by $\hat{I}_{abs} = \hat{a}^\dagger_{abs}\hat{a}_{abs}$. We also introduce the operator corresponding to the shot noise entering from the fixed mirror $\hat{\xi}_t$.

Now we have all the ingredients to write down the set of equations of motion for an optomechanical cavity subject both to radiation pressure and photothermal forces:

$$\begin{aligned}\dot{\hat{a}} =& -(i\omega_c + \gamma_c)\,\hat{a} + i\sqrt{2}g_{cm}\hat{a}\hat{q}_m + F_p e^{-i\omega_p t} + \sqrt{\gamma_t}\hat{\xi}_t(t) + \sqrt{\gamma_{abs}}\hat{\xi}_{abs}(t) \\ \ddot{\hat{q}}_m =& -\omega_m^2\hat{q}_m - i\gamma_m\dot{\hat{q}}_m + \sqrt{2}g_{cm}\omega_m\left(\hat{a}^\dagger\hat{a} + \tau_0\beta\int_{\mathbb{R}} du\frac{1}{\tau_{th}}\Theta(t-u)e^{-\frac{t-u}{\tau_{th}}}\hat{I}_{abs}(u)\right) \\ &+ \hat{\Xi}_m(t).\end{aligned} \tag{III.5}$$

Here we have introduced a phenomenological parameter β that quantifies the difference of amplitudes between the photothermal and radiation pressure forces. Under constant illumination and for a fixed cavity this ratio would be given by $F_{photothermal}/F_{rad} = \beta A$ (reference [85] reports values of βA between 10^2 and 10^4).

III.1.2. Photothermal cavity cooling

The set of equations III.5 is dealt with in the same way we used to describe radiation pressure cooling in chapter I. Using a mean field approach we linearize the equations of motion, which can then be treated as algebraic equations by moving to Fourier space.

Moving to the frame rotating at the frequency of the pump we find that the stationary mean values of the position and the photon field are given by

$$\begin{aligned}\langle\hat{q}_m\rangle &= \sqrt{2}\frac{g_{cm}}{\omega_m}\,(1+\beta A)\,\alpha^2 \\ \alpha = \langle\hat{a}\rangle &= \frac{F_p}{i\Delta_{nl} + \gamma_c},\end{aligned} \tag{III.6}$$

where once again we assume that the pump phase is set to have $\alpha \in \mathbb{R}$ and we have introduced the effective detuning of the cavity $\Delta_{nl} = \omega_c - \omega_p - 2g_{cm}^2/\omega_m(1+\beta A)\alpha^2$. We also introduce the non linear frequency shift induced by the steady-state intracavity photon pressure on the movable mirror $\omega_{nl} = 2g_{cm}^2\alpha^2/\omega_m(1+\beta A)$, the effective detuning can then be rewritten $\Delta_{nl} = \omega_c - \omega_{nl} - \omega_p$.

Let us now consider the fluctuations around these mean fields : $\delta\hat{c} = \hat{c} - \langle\hat{c}\rangle$. For clarity in the expressions we will omit the hats on the operators. Only keeping terms up to first order we get the set of coupled linear equations

$$\begin{aligned}
\delta\dot{a} =& -(i\Delta_{nl} + \gamma_c)\delta a + i\sqrt{2}g_\alpha\delta q_m + \sqrt{\gamma_t}\xi_t + \sqrt{\gamma_{abs}}\xi_{abs} \\
\delta\ddot{q}_m =& -\omega_m^2\delta q_m - \gamma_m\delta\dot{q}_m + \sqrt{2}g_\alpha\omega_m\left(\delta a + \delta a^\dagger + \beta A\int du\ h(u-t)\left(\delta a(u) + \delta a^\dagger(u)\right)\right) \\
&- \sqrt{2}g_\alpha\omega_m\beta\tau_0\sqrt{\gamma_{abs}}\int du\ h(u-t)\left(\xi_{abs}(u) + \xi_{abs}^\dagger(u)\right) + \Xi_m(t),
\end{aligned} \tag{III.7}$$

$h(\tau)$ being the memory kernel introduced in Eq.III.1. At this point the set of equations III.7 presents a major difference with what we encountered with radiation pressure. Given the nature of the photothermal force the mechanical resonator is directly (without the formal integration of the photonic degree of freedom) sensitive to the optical absorption shot noise,which is convoluted by the thermal relaxation memory kernel $h(u)$. The differences appear more clearly when moving to Fourier space where, after integration of the equations on a and $a^\dagger$, the equation on the mechanical resonator position can be rewritten

$$\begin{aligned}
\chi_m^{-1}(\omega)\tilde{q}_m(\omega) =& \ i2g_\alpha^2\omega_m\left(1 + \beta A\frac{1}{1+i\omega\tau_{th}}\right)(\chi_c(\omega) - \chi_c^*(-\omega))\tilde{q}_m(\omega) \\
&+ \tilde{\Xi}_m(\omega) \\
&- \sqrt{2}g_\alpha\omega_m\beta\tau_0\frac{1}{1+i\omega\tau_{th}}\sqrt{\frac{A}{\tau_0}}\left(\xi_{abs}(\omega) + \xi_{abs}^\dagger(-\omega)\right) \\
&+ \sqrt{2}g_\alpha\omega_m\left(1 + \beta A\frac{1}{1+i\omega\tau_{th}}\right)\sqrt{\frac{A}{\tau_0}}\left(\chi_c(\omega)\tilde{\xi}_{abs}(\omega) + \chi_c^*(-\omega)\tilde{\xi}_{abs}^\dagger(-\omega)\right) \\
&+ \sqrt{2}g_\alpha\omega_m\left(1 + \beta A\frac{1}{1+i\omega\tau_{th}}\right)\sqrt{\frac{\overline{\gamma}}{\tau_0}}\left(\chi_c(\omega)\tilde{\xi}_t(\omega) + \chi_c^*(-\omega)\tilde{\xi}_t^\dagger(-\omega)\right),
\end{aligned} \tag{III.8}$$

where we have introduced the cavity and mechanical bare suceptibilities : $\chi_m^{-1}(\omega) = \omega_m^2 - \omega^2 + i\omega\gamma_m$ and $\chi_c^{-1}(\omega) = i(\Delta_{nl} - \omega) + \gamma_c$.

We have obtained a result reminiscent of what was obtained for the radiation pressure case in Eq.I.45. By integrating the photonic degrees of freedom we see that the mechanical oscillator responds with an effective susceptibility to a modified noise term. The first line of the right hand term in Eq.III.8 is responsible for the mechanical resonator effective suceptibility. Once again, if the initial mechanical quality factor $Q_m = \omega_m/\gamma_m$ is big enough this effects can be understood in terms of both an optical spring effect (modification of the mechanical resonance frequency $\omega_{eff} = \omega_m + \delta\omega_m$) and the appearance of an optical damping rate (the decay rate is then given by $\gamma_{eff} = \gamma_m + \Gamma_{opt}$). Given the additional damping rate, the fluctuation-dissipation theorem tells us that there has to be an additional noise term on the equation of motion of the mechanical resonator. This additional optical noise has a slightly more convoluted form than what was discussed in chapter I for radiation pressure. Indeed here we have taken into account the absorption shot noise which is described by the third and fourth lines. But most importantly, the thermal relaxation memory kernel introduces a "thermal low-pass frequency filter" $\propto \beta/(1+\omega\tau_{th})$ that completely modifies the optical force spectral density with respect to the radiation pressure case. Setting the absorption rate A to zero yields the exact same equations we obtained for radiation pressure cooling.

The normalized motional variance of the mechanical resonator is given by

$$\langle q_m^2 \rangle = \int_{-\infty}^{+\infty} \frac{d\omega}{2\pi} \, \langle \tilde{q}_m(\omega)\tilde{q}_m(-\omega)\rangle. \tag{III.9}$$

Using Eq.III.8 this variance can be recast in the following form:

$$\langle q_m^2 \rangle = \int_{-\infty}^{+\infty} \frac{d\omega}{2\pi} \, |\chi_{eff}(\omega)|^2 \left(S_{th}[\omega] + S_{opt}[\omega]\right), \tag{III.10}$$

where $S_{th}[\omega]$ and $S_{opt}[\omega]$ are the spectral noise densities of the thermal Langevin and optical noise forces respectively. The effective susceptibility of the mechanical oscillator is given by

$$\chi_{eff}^{-1}(\omega) = \chi_m^{-1}(\omega) - 4\Delta_{nl} g_\alpha^2 \omega_m \left(1 + \beta A \frac{1}{1 + i\omega\tau_{th}}\right) \chi_c(\omega)\chi_c^*(-\omega). \tag{III.11}$$

Before discussing the cooling limits let us introduce the following set of normalized variables.

Normalized variable	Physical Meaning
$b = \frac{\omega_m}{\gamma_c}$	Normalized mechanical frequency
$\varphi = \frac{\Delta_{nl}}{\gamma_c}$	Normalized cavity detuning
$\varphi_{nl} = \frac{\omega_{nl}}{\gamma_c(1+\beta A)} = \frac{2g_\alpha^2}{\omega_m \gamma_c}$	Normalized non-linear frequency shift
$d = \omega_m \tau_{th}$	Normalized thermal relaxation time
$\Omega = \frac{\omega}{\omega_m}$	Normalized frequency

With this normalized notations the spectral density of optical noise $S_{opt}[\Omega]$ (including both radiation pressure and photothermal contributions) is given by:

$$((1-b^2\Omega^2+\varphi^2)^2+4b^2\Omega^2)S_{opt}[\Omega] = \left(\frac{2T}{T+A}\left|1+\frac{\beta A}{1+i\Omega d}\right|^2(1+\varphi^2+b^2\Omega^2-2b\Omega\varphi) + \frac{2A}{T+A}\left|(1+i\Omega b-i\varphi)\left[1+\beta\frac{T+A}{2(1+i\Omega d)}\left(\frac{A-T}{T+A}-i\varphi-ib\Omega\right)\right]\right|^2\right), \tag{III.12}$$

The effective damping of the mechanical resonator is given by

$$\gamma_{eff} = \gamma_m\left[1+\varphi_{nl}\frac{2\varphi Q_m}{(1-b^2+\varphi^2)^2+4b^2}\left((1-b^2+\varphi^2)d\frac{\beta A}{1+d^2}+2b\left(1+\frac{\beta A}{1+d^2}\right)\right)\right]. \tag{III.13}$$

We are only interested in discussing the quantum limits of strong optomechanical cooling, where the optical spring effect remains moderate but the effective mechanical damping of motion allows efficient quenching of the mechanical oscillator Brownian fluctuations ($\gamma_{eff} \gg \gamma_m$). In this regime, and if the effective mechanical susceptibility has a sharp frequency response, the normalised position variance of the mechanical resonator reduces to

$$\langle q_m^2\rangle \cong \frac{\gamma_m}{\gamma_{eff}}\left(1+2n_{th}+\frac{\varphi_{nl}}{2}Q_m(S_{opt}[\Omega=1]+S_{opt}[\Omega=-1])\right) \tag{III.14}$$

Fig.III.1 displays the normalised variance $\langle q_m^2\rangle$ as a function of the normalized cavity detuning $\varphi = \Delta_{nl}/\gamma_c$ and the normalized thermal relaxation time $d = \omega_m\tau_{th}$ in the regime of strong cooling and in the limit of strong optomechanical coupling $\varphi_{nl} \gg 1$. As can be seen in the figure, the quantum ground state is approached (which corresponds to variances $\langle q_m^2\rangle \sim 1$) for a large set of values of the detuning and thermal relaxation time. Large values of the detuning reduce the influence of radiation-pressure noise and could be a favourable route to approach the ground state in this configuration. But the system exhibits other regimes of interest. For

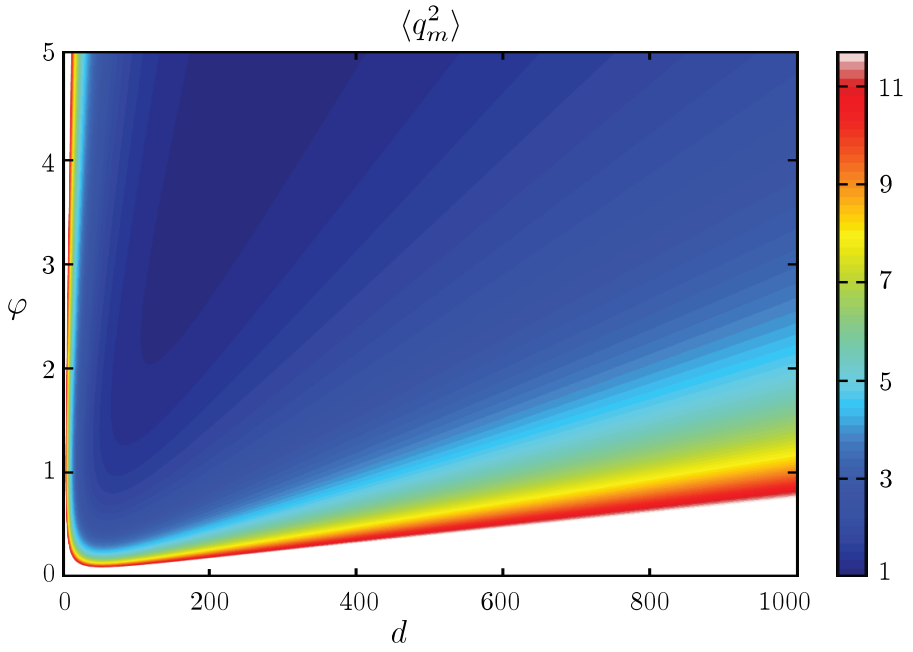

FIGURE III.1: Normalized variance of the mechanical resonator as a function of the normalized cavity detuning $\varphi = \Delta_{nl}/\gamma_c$ and the normalized thermal relaxation time $d = \omega_m \tau_{th}$. The other parameters of the system $A = 10^{-2}$, $T = 10^{-3}$, $\beta = 10^4$, $b = 10^{-2}$.

example, for $\varphi = 1$ increasing d from 0 to 100 gets the system closer to its ground state. For values of d much bigger than 100 (that is values bigger than βA in the specific case of Fig.III.1) the variance increases again reflecting the fact that the optomechanical effects of photothermal origin no longer damp the mechanical motion response to radiation-pressure noise. Taking into account the noise originating from radiation pressure and the noise of photothermal origin leads to an optimum value of the parameter d. We used a numerical bound constrained minima search algorithm to get statistical insights into the final mechanical resonator phonon occupation. We found for example that it is possible to reach a state containing $\sim 4.10^{-2}$ phonons for a set of parameters putting the system in the bad cavity limit and for a slightly detuned pump ($\varphi \sim 1.2,\ b \sim 0.6,\ d \sim 10^5,\ \beta \sim 10^5,\ A \sim 0.45$). However, because of the complexity of Eq.III.12 we were unable to find a simple expression allowing an analytical survey of the minimal occupancy dependence on all the involved parameters.

Just as we did in chapter I, the minimum number of phonons that can be reached by optomechanical cavity cooling is computed by assuming that the thermal effects become negligible due to optical damping ($\gamma_{eff} \gg \gamma_m$) and by applying a detailed balance condition on the spectral density of optical noise [28, 29] (we assume that the optical noise leads the mechanical resonator to a state described by an usual

Boltzmann distribution at thermal equilibrium). The minimal occupancy is in that case given by

$$n_{min} = \left[\frac{S_{opt}[-1]}{S_{opt}[+1]} - 1\right]^{-1}. \tag{III.15}$$

Fig.III.2 plots n_{min} as a function of $d = \omega_m \tau_{th}$, for a detuning $\varphi = 1$, in the bad cavity limit $b = 10^{-1}$ and for different values of βA. Occupation factors well below one are obtained here by an appropriate choice of the parameter d. For example, an occupancy of about 10^{-1} is reached for $A = 10^{-1}$ and $\beta = 10^4$. More generally, very small occupations are obtained in the "bad-cavity" ($\omega_m < \gamma_c$) regime by a proper choice of the A and β parameters compatible with experimentally reported values.

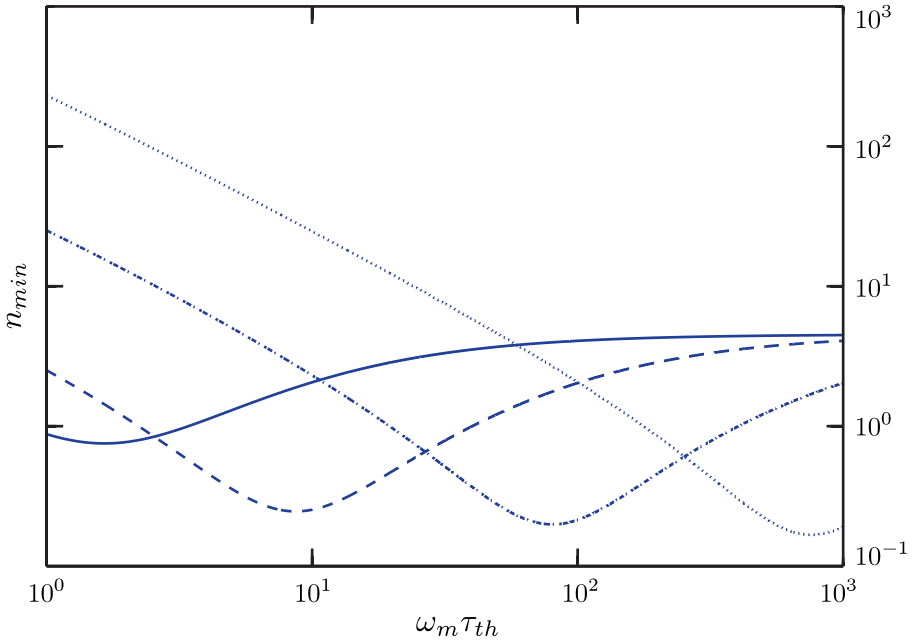

FIGURE III.2: Minimum phonon occupancy as a function of the normalized thermal relaxation time $d = \omega_m \tau_{th}$ for a normalized detuning $\varphi = 1$ and for different values of A and β. **solid line:** $A = 10^{-2}$, $\beta = 10^2$, **dashed line:** $A = 10^{-2}$, $\beta = 10^3$, **dashe-dotted line:** $A = 10^{-2}$, $\beta = 10^4$, **dotted line:** $A = 10^{-1}$, $\beta = 10^4$.

Photothermal cooling of mechanical motion allows to closely approach the quantum ground state of the mechanical resonator even in the so-called bad-cavity limit where the life time of cavity photons is smaller than the mechanical oscillation period. This is very different from the standard radiation pressure cooling scenario and opens interesting new experimental perspectives. Using photothermal cooling the ground state can be reached without having to fulfill the good cavity condition and for moderate detunings where a large number of incident photons can be more

easily injected in the cavity. From a theoretical point of view, our calculations are valid for any semi-classical force that can be written under the form of Eq.III.1 such as radiometric pressure or optoelectronic stresses.

Another theoretical paper [93] explored the quantum limits of photothermal cavity cooling and reached similar conclusions to ours. The authors limited themselves to the unresolved-sideband regime in which the dynamical modifications induced by radiation pressure can be neglected. In [94] the authors describe exciton-mediated photothermal coupling in GaAs membranes via a microscopic formulation of the couplings between light, excitons and mechanics. Self-oscillation regimes of mechanical motion have also been discussed theoretically for semi-classical resonators under photothermal forces [95].

III.2. Cooling with an auxiliary cavity

In recent years, a growing interesting for coupled cavity systems has emerged. A few publications have discussed theoretically the physics of "optomechanical arrays" [82, 96, 97]. Here we consider a scenario in which an optomechanical cavity is coupled to a passive (without optomechanical coupling) auxiliary cavity. By doing so we show that it should be possible to cool the mechanical resonator close to its ground state while pumping the optomechanical cavity near its optical resonance thus allowing to inject more easily a large number of intracavity photons.

The system under consideration is described by the following Hamiltonian.

$$\begin{aligned}\hat{H} &= \omega_{c1}\hat{a}_1^\dagger\hat{a}_1 + \omega_{c2}\hat{a}_2^\dagger\hat{a}_2 + \omega_m\hat{b}^\dagger\hat{b} \\ &\quad - g_{cm}\hat{a}_1^\dagger\hat{a}_1(\hat{b}^\dagger + \hat{b}) + J(\hat{a}_1^\dagger\hat{a}_2 + \hat{a}_1\hat{a}_2^\dagger) \\ &\quad + iF_p(\hat{a}_1^\dagger e^{-i\omega_p t} - \hat{a}_1 e^{i\omega_p t}) + \hat{H}_{bath},\end{aligned} \tag{III.16}$$

where we use subscripts $1, 2$ to distinguish the two cavities. g_{cm} is the optomechanical coupling strength between cavity 1 and the mechanical resonator. The two cavity modes are coupled with a coupling strength J (this coupling could result from evanescent overlap between the optical modes for example). Cavity 1 is pumped by a coherent pump of intensity F_p and frequency ω_p. Finally $\hat{H}_{bath}$ is responsible for the coupling to the baths.

Moving to the frame rotating at frequency ω_p with respect to the photons and integrating the Markovian environment we get to the Langevin equations describing

our system:

$$\begin{aligned}
\dot{\hat{a}}_1 &= -(i\Delta_1 + \gamma_{c1})\hat{a}_1 - iJ\hat{a}_2 + i\sqrt{2}g_{cm}\hat{a}_1\hat{q}_m + F_p + \hat{\xi}_{c1}(t), \\
\dot{\hat{a}}_2 &= -(i\Delta_2 + \gamma_{c2})\hat{a}_2 - iJ\hat{a}_1 + \hat{\xi}_{c2}(t), \\
\ddot{\hat{q}}_m &= -\omega_m^2 - \gamma_m\dot{\hat{q}}_m + \sqrt{2}\hat{a}_1^\dagger\hat{a}_1 + \hat{\Xi}_m(t),
\end{aligned} \tag{III.17}$$

where Δ_i, γ_{ci} and $\hat{\xi}_{ci}$ are the detuning ($\Delta_i = \omega_{ci} - \omega_p$), amplitude decay rate and shot noise operator for the i-th cavity respectively. We deal with the optomechanical non-linearity with a mean field approach. The mean fields $\alpha_i = \langle\hat{a}_i\rangle$, $Q_m = \langle\hat{q}_m\rangle$ are linked by the following set of algebraic equations:

$$F_p = \left[i\left(\Delta_1 - \sqrt{2}\frac{g_{cm}^2}{\omega}|\alpha_1|^2 - \Delta_2\frac{J^2}{\Delta_2^2+\gamma_{c2}^2}\right) + \gamma_{c1} + \gamma_{c2}\frac{J^2}{\Delta_2^2+\gamma_{c2}^2}\right]\alpha_1 \tag{III.18}$$

$$\alpha_2 = \frac{-iJ}{i\Delta_2 + \gamma_{c2}}\alpha_1 \tag{III.19}$$

$$Q_m = \sqrt{2}\frac{g_{cm}}{\omega_m}|\alpha_1]^2. \tag{III.20}$$

As can be seen in Eq.III.18 the level splitting induced by the coupling J introduces an effective detuning for cavity 1

$$\Delta_1^{eff} = \Delta_1 - \Delta_2\frac{J^2}{\Delta_2^2+\gamma_{c2}^2}. \tag{III.21}$$

The amplitude decay rate is modified according to

$$\gamma_{c1}^{eff} = \gamma_{c1}\left(1 + \frac{\gamma_{c2}}{\gamma_{c1}}\frac{J^2}{\Delta_2^2+\gamma_{c2}^2}\right). \tag{III.22}$$

Linearizing the set of equations of motion III.17 around the mean fields and moving to Fourier space we can reduce the set of equations to a single equation on the Fourier transform of the mechanical resonator position operator

$$\chi_{eff}(\omega)^{-1}\tilde{q}_m(\omega) = \tilde{\Xi}_m(\omega) + \tilde{\Xi}_{opt}(\omega). \tag{III.23}$$

Eq.III.23 is formally identical to what we have encountered this far. Just as for the photothermal force, the coupling to the second cavity modifies the spectral response of the photons in cavity 1 leading to a modification of the spectral density of optical noise acting on the mechanical resonator. Keeping similar notations as in chapter I the susceptibility of cavity 1 is $\chi_{1e}^{-1}(\omega) = i(\Delta_{1e}(\omega) - \omega) + \gamma_{1e}(\omega))$, where the frequency-dependent effective detuning and amplitude decay rate are

given by

$$\begin{aligned}\Delta_{1e}(\omega) &= \Delta_{nl} - J^2 \frac{\Delta_2 - \omega}{(\Delta_2 - \omega)^2 + \gamma_{c2}^2} \\ \gamma_{1e}(\omega) &= \gamma_{c1}\left(1 + \frac{\gamma_{c2}}{\gamma_{c1}} \frac{J^2}{(\Delta_2 - \omega)^2 + \gamma_{c2}^2}\right).\end{aligned} \tag{III.24}$$

Δ_{nl} is the non-linear detuning of cavity 1 when one takes into account the frequency shift arising from the static shift of the mechanical resonator equilibrium position. From these expressions we then get the optical force spectral density of noise on the mechanical resonator and the effective mechanical damping:

$$S_{opt}[\omega] = 2(g_\alpha \omega_m)^2 \left(|\chi_{1e}(\omega)|^2 \left(\langle \tilde{\xi}_{c1}(\omega)\tilde{\xi}_{c1}^\dagger(\omega)\rangle + J^2 |\chi_{c2}(\omega)|^2 \langle \tilde{\xi}_{c2}(\omega)\tilde{\xi}_{c2}^\dagger(\omega)\rangle\right)\right) \tag{III.25}$$

$$\gamma_{eff}(\omega) = \gamma_m \left(1 + \sqrt{2} g_\alpha^2 \frac{\omega_m}{\omega}\left[\frac{\gamma_{1e}(\omega)}{\gamma_m}|\chi_{1e}(\omega)|^2 - \frac{\gamma_{1e}(-\omega)}{\gamma_m}|\chi_{1e}(-\omega)|^2\right]\right), \tag{III.26}$$

where $g_\alpha = \alpha_1 g_{cm}$ and $\chi_{c2}^{-1}(\omega) = i(\Delta_2 - \omega) + \gamma_{c2}$.

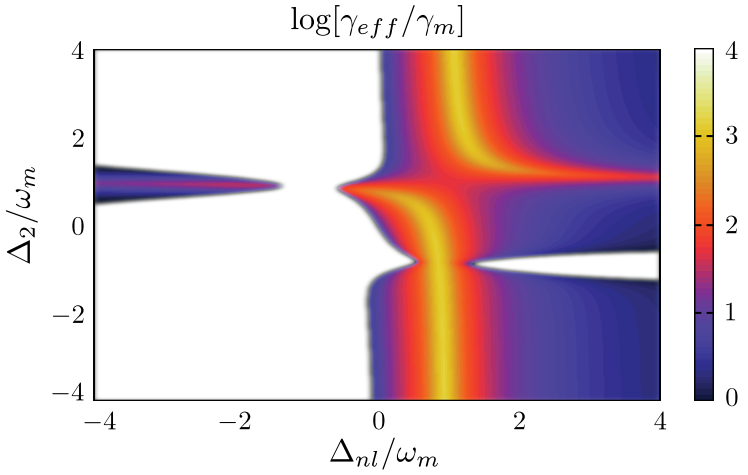

FIGURE III.3: Effective mechanical damping rate in a double cavity as a function of the cavity detunings Δ_{nl} and Δ_2. The white regions correspond to unstable regimes where $\gamma_{eff} < 0$. The other parameters are given by $\gamma_{c1} = \gamma_{c2} = 10^{-1}\omega_m$, $\gamma_m/\omega_m = 10^{-4}$, $g_\alpha/\omega_m = 10^{-1}$, $J/\gamma_{c1} = 5$.

Fig.III.3 plots the effective mechanical damping rate as a function of the cavity detunings Δ_{nl} and Δ_2. It is obtained by assuming that the initial mechanical quality factor is high enough as to evaluate Eq.III.26 on $\omega = \omega_m$. The regions where $\gamma_{eff} < 0$, which correspond to the onset of mechanical instability, are depicted in white. The coupling between cavities yields a rather complicated stability diagram

but it shows that it is possible to obtain optomechanical cooling ($\gamma_{eff} \gg \gamma_m$) for a set of parameters for which cavity 1 is pumped near resonance $\Delta_{nl} \sim 0$. In the following we assume $\Delta_{nl} = 0$ and investigate the limits of optomechanical cooling as a function of the auxiliary cavity detuning Δ_2.

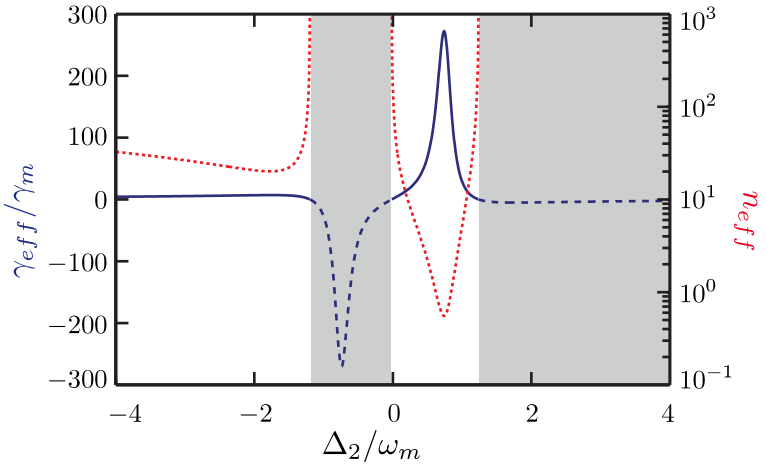

FIGURE III.4: Effective mechanical damping rate (blue solid and dashed line) and final phonon occupancy (red dotted line) as a function of the auxiliary cavity detuning Δ_2. Gray areas correspond to unstable solutions ($\gamma_{eff} < 0$, dashed blue line), white areas to stable solutions ($\gamma_{eff} > 0$, solid blue line). $\Delta_{nl} = 0$, the temperature has been chosen so that the average number of thermally excited phonons is $n_{th} = 130.45$, all other parameters as in Fig.III.3.

Fig.III.4 presents the effective damping rate and the final number of phonons under optomechanical cooling as a function of Δ_2. The final number of phonons n_{eff} is computed by assuming the optical noise leads the mechanical resonator to a pseudo-thermal state and thus applying a detailed balance condition as in Eq.I.61. The instability regions are colored in gray, they correspond to negative values of the effective mechanical damping and their boundaries correspond to points where the final occupancy of the mechanical resonator goes to infinity thus breaking the validity of the linearization procedure. We consider an environment at finite temperature T exciting an average number of thermal phonons $n_{th} = 130.45$ (for a mechanical resonator in the GHz range this correspond to a temperature of $1K$). For $\Delta_2/\omega_m = 0.74$ the mechanical resonator is cooled down to a state containing $n_{eff} \sim 0.6$ phonons with a cavity 1 that can be pumped exactly at its Lorentzian resonance ($\Delta_1^{eff} \sim -2.3\gamma_{c1}^{eff}$). According to these calculations it should be possible to cool down the mechanical resonator close to its ground state while pumping the optomechanical cavity near its resonance which allows more efficient injection of photons into the cavity. These results might be useful to experimentalists limited by undesirable absorption in their devices when faced to strong out-of-resonance pumping of the cavity in the resolved-sideband regime.

Chapter IV

Hybrid cavity quantum electrodynamics - optomechanics

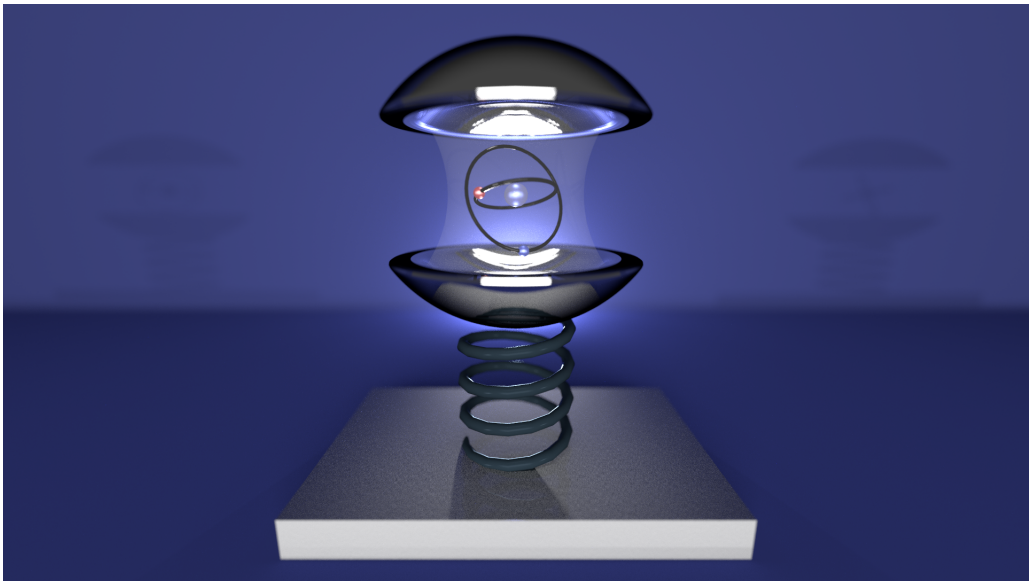

FIGURE IV.1: Conceptual illustration of a system combining cavity quantum electrodynamics and optomechanics.

Until recently the theoretical description of optomechanical systems was based on a single optomechanical cavity strongly pumped in order to enhance, via the cavity mean field, the effective optomechanical interaction. In this regime the optomechanical interaction is linearized around the cavity mean field. Such treatment predicts important and already achieved results such as optical cooling of mechanical motion close to the ground state [28–31, 33, 34], mechanical instability and self sustained oscillations [6, 46, 67], pondemorotive squeezing of light [98] and entanglement between photons and phonons [40, 42, 42]. More recently, confident

on the promising future of experimental optomechanics, theoretical studies have started exploring more ambitious configurations. Regimes of strong optomechanical coupling in which a single photon is sufficient to yield a visible effect on the mechanics [47, 99–101] have been discussed. There have been works exploring the pathway to non-classical states (other than the gaussian ground state) for the mechanical resonator [43]. And recently the problem of hybrid optomechanical setups comprising more complex systems, such as optomechanical arrays [82, 96, 102] or hybrid cold-atoms-optomechanics systems have been proposed [50, 51, 103–105].

In this chapter we present our contribution to these new perspectives for future hybrid optomechanical systems. We detail our results on the physics of a quantum system where a cavity photon mode is coupled to an artificial two-level atom and to a mechanical resonator. The coupling between a cavity mode and an atom has been explored within the field of cavity Quantum Electrodynamics (QED), which has undertaken experiments exploring light-matter interactions at the quantum level [69, 106]. Similar physics have been successfully studied in solid state implementations such as semiconductor systems [107, 108] or superconducting circuits [109, 110]. Experimental optomechanical systems have successfully coupled cavity photons to mesoscopic mechanical resonators [17, 111]. Given these experimental results the maturity of solid-state quantum devices will soon allow to bridge cavity and circuit QED and cavity optomechanics.

The basic principle of inserting a two-level artificial atom in an optomechanical setting was discussed in classical terms for fine tuning of dispersive and dissipative optomechanical interactions [111]. The coupling of an optomechanical cavity to an atom motion [105] or to collective excitations of an ensemble of atoms [112] was also discussed, resulting in the physical situation of two linearly coupled harmonic oscillators. In that case the anharmonic internal structure of a single atom and its corresponding nonlinear dynamics, a key feature of cavity and circuit QED, is absent. Since optomechanical systems progressively move towards regimes where single photon coupling exceeds dissipation [33, 45, 47, 48, 113, 114] we decided to study a scenario in which artificial atoms, photons and phonons are all strongly coupled at the quantum level.

In the following we present our findings reported in [3] concerning such a hybrid system. We start by introducing the system Hamiltonian, which combines Jaynes-Cummings coupling between the cavity mode and a two-level artificial atom and radiation pressure coupling between the cavity mode and mechanical motion. At the expense of some reasonable approximations, we are able to analytically diagonalize the Hamiltonian. We discuss the dynamics in presence of losses and driving. We show atom-assisted cooling of mechanical motion close to the ground

state, atom-assisted unusual mechanical amplification and the appearance of non-classical states for the mechanical resonator. Last, we discuss the emission of strongly antibunched phonons in such tripartite atom-cavity-mechanics systems.

IV.1. The system under consideration

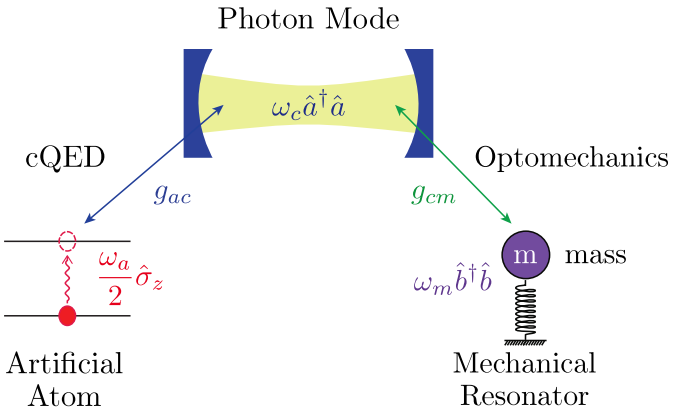

FIGURE IV.2: Scheme of the considered hybrid system. A confined photon mode of frequency ω_c couples both to a two-level system (ω_a is its transition frequency) and to a mechanical resonator of frequency ω_m. g_{ac} (g_{cm}) is the coupling strength of the Jaynes-Cummings (radiation pressure) atom-cavity (cavity-mechanics) coupling.

As depicted in Fig.IV.2 the system under consideration consists of a single cavity mode at frequency ω_c, a mechanical resonator at frequency ω_m and an artificial two-level atom with a transition energy ω_a. We assume that the cavity is coupled both to the artificial atom and the mechanical resonator.

IV.1.1. Uncoupled Hilbert space

The Hilbert space on which the cavity photon operators act can be spanned by an infinite and discrete set of orthogonal Fock states which we label $\{|k\rangle\}_{k\in\mathbb{N}}$, the same holds for the mechanical resonator Hilbert space which is spanned by a set of Fock states labeled $\{|l\rangle\}_{l\in\mathbb{N}}$.
The artificial two-level atom evolves in a two dimensional Hilbert space spanned by the vector states corresponding to the ground, $|g\rangle$, and excited, $|e\rangle$, states of the atom. Any operator acting on the artificial atom can be written as a combination

of the Pauli matrices, which in the basis $\{|g\rangle, |e\rangle\}$ are defined as follows:

$$\hat{\sigma}_z = \begin{bmatrix} -1 & 0 \\ 0 & 1 \end{bmatrix}, \ \hat{\sigma}_x = \begin{bmatrix} 0 & 1 \\ 1 & 0 \end{bmatrix}, \ \hat{\sigma}_y = \begin{bmatrix} 0 & i \\ -i & 0 \end{bmatrix}. \tag{IV.1}$$

We also define atomic lowering and raising operators as follows:

$$\hat{\sigma}_- = |g\rangle\langle e| = \begin{bmatrix} 0 & 1 \\ 0 & 0 \end{bmatrix}, \ \hat{\sigma}_+ = |e\rangle\langle g| = \begin{bmatrix} 0 & 0 \\ 1 & 0 \end{bmatrix}. \tag{IV.2}$$

A hybrid system combining these three subsystems is described in a Hilbert space obtained by tensor product of the three separate Hilbert spaces just discussed. These new Hilbert space is spanned by a basis labeled $\{|\xi\rangle \otimes |k\rangle \otimes |l\rangle\}_{\xi\in\{g,e\},k\in\mathbb{N},l\in\mathbb{N}}$ that diagonalizes the uncoupled Hamiltonian of the system:

$$\hat{H}_{uncoupled} = \omega_c \hat{a}^\dagger \hat{a} + \omega_m \hat{b}^\dagger \hat{b} + \frac{\omega_a}{2} \hat{\sigma}_z. \tag{IV.3}$$

IV.1.2. Closed system Hamiltonian

Let us now discuss the couplings between the different sub-systems. First, the cavity is coupled to the two-level atom via a dipolar electric coupling of the form $\propto \vec{d}.\vec{E}$, where $\vec{d}$ is the atom electric dipole and $\vec{E}$ is the electric quadrature of the electromagnetic field. By quantizing the operators of both the atom and the field and neglecting the resulting counter-rotating terms we obtain the Jaynes-Cummings Hamiltonian [69, 115, 116]. The interaction term between the cavity mode and the two-level system can be cast in the following form:

$$\hat{V}_{ac} = i g_{ac} \left(\hat{\sigma}_+ \hat{a} - \hat{\sigma}_- \hat{a}^\dagger \right). \tag{IV.4}$$

The mechanical resonator can be coupled to the atom-cavity system either by a radiation pressure coupling to the photons, which is described by an interaction term of the form $\propto \hat{a}^\dagger \hat{a} (\hat{b}^\dagger + \hat{b})$, or it could be directly coupled to the artificial atom. A promising experimental candidate to explore the physics described in this chapter is a miniature Gallium-Arsenide optomechanical resonator combining strong optomechanical coupling [45, 113, 114] with strong cavity QED couplings [107, 108]. In such architectures the artificial atom is a semiconductor quantum dot embedded in the crystalline optical-mechanical resonator. The strain in the lattice induced by the resonator mechanical movement can modify the spatial

properties of the quantum dot thus modifying the energy splitting between ground and excited states. Such an effect can be accounted for by introducing a term in the Hamiltonian of the form $\propto \hat{\sigma}_z(\hat{b}^\dagger + \hat{b})$. Here we only consider the radiation pressure term.

The closed system Hamiltonian for our hybrid atom-cavity mechanics system is thus:

$$\begin{aligned}\hat{H} =&\omega_c \hat{a}^\dagger \hat{a} + \frac{\omega_a}{2}\hat{\sigma}_z + i g_{ac}\left(\hat{\sigma}_+ \hat{a} - \hat{\sigma}_- \hat{a}^\dagger\right) \\ &+ \omega_m \hat{b}^\dagger \hat{b} - g_{cm}\hat{a}^\dagger \hat{a}\left(\hat{b} + \hat{b}^\dagger\right).\end{aligned} \tag{IV.5}$$

IV.2. Hamiltonian diagonalization

In this section we present the steps of the analytical diagonalization of the Hamiltonian IV.5.

IV.2.1. Diagonalization of the atom-cavity Hamiltonian

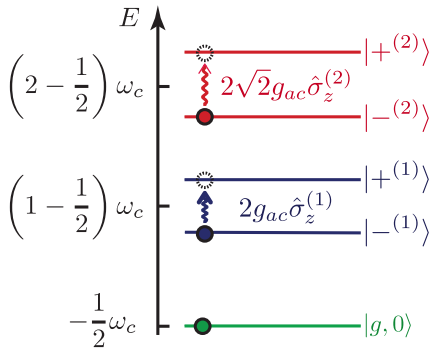

FIGURE IV.3: Polariton energy levels of the Jaynes-Cummings Hamiltonian. Restriction to the subspaces $\mathcal{H}_n, n \leq 2$.

Our hybrid Hamiltonian shares an important symmetry with the usual Jaynes-Cummings one (without the optomechanical part). Let us define a "number of polaritons" operator as follows:

$$\hat{N}_{polariton} = \hat{a}^\dagger \hat{a} + \hat{\sigma}_+ \hat{\sigma}_-. \tag{IV.6}$$

This operator counts the number of photons and atomic excitations inside the cavity. Its commutation with the total Hamiltonian ($[\hat{N}_{polariton}, \hat{H}] = 0$) tells us

that the two operators can share a common basis. We now introduce the following set of states:

$$\begin{aligned} &\forall n \in \mathbb{N},\ n \neq 0 \\ &\qquad |+^{(n)}\rangle = \frac{1}{2}\left(|g\rangle|k=n\rangle + i|e\rangle|k=n-1\rangle\right) \\ &\qquad |-^{(n)}\rangle = \frac{1}{2}\left(|g\rangle|k=n\rangle - i|e\rangle|k=n-1\rangle\right) \\ &n = 0 \\ &\qquad |G\rangle = |g\rangle|k=0\rangle \end{aligned} \tag{IV.7}$$

This set of vectors constitutes an orthogonal basis of the atom-cavity Hilbert space, which diagonalizes $\hat{N}_{polariton}$ ($\hat{N}_{polariton}|\pm^{(n)}\rangle = n|\pm^{(n)}\rangle$). In the following we assume that the atom and the cavity mode are at resonance $\omega_a = \omega_c$. Under this condition the previously defined basis of polaritons also diagonalizes the Jaynes-Cummings part of the Hamiltonian, thus yielding the well known Jaynes-Cummings ladder of states:

$$\begin{aligned} \hat{H}_{JC}|\pm^{(n)}\rangle &= \left(\omega_c\hat{a}^\dagger\hat{a} + \frac{\omega_a}{2} + ig_{ac}(\hat{\sigma}_+\hat{a} - \hat{\sigma}_-\hat{a}^\dagger\right)|\pm^{(n)}\rangle \\ &= \left(\left(n-\frac{1}{2}\right)\omega_c \pm \frac{\Omega^{(n)}}{2}\right)|\pm^{(n)}\rangle, \end{aligned} \tag{IV.8}$$

where $\Omega^{(n)} = \sqrt{n}g_{ac}$. Taking into account an asymmetry between the atom and cavity frequencies ($\omega_a \neq \omega_c$) leads to more cumbersome expressions for the eigenvectors of the total Hamiltonian. For this reason we restrict the analytical diagonalization presented here to the resonant case. Nevertheless the numerical exploration of the system was performed in order to allow non-resonant configurations for the Jaynes-Cummings sub-system.

From this point on the atomic and cavity degrees of freedom will be discussed in terms of upper, $|+^{(n)}\rangle$, and lower, $|-^{(n)}\rangle$, polaritons. The second and final part of the diagonalization is performed by switching to the polariton-phonon basis $\{|\pm^{(n)}\rangle \otimes |l\rangle\}_{n\in\mathbb{N},l\in\mathbb{N}}$ and projecting the optomechanical interaction into each subspace containing n polaritons.

IV.2.2. Atom-cavity-mechanics polarons

Given the comutation relation $[\hat{H}, \hat{N}_{polariton}] = 0$, the two operators share a common diagonalization basis. The set $\{|\pm^{(n)}\rangle \otimes |l\rangle\}_{n,l\in\mathbb{N}}$ diagonalizes the Jaynes-Cummings part of the Hamiltonian. In this basis the total Hamiltonian has a block-diagonal structure that allows us to treat the projection of $\hat{H}$ into each n-polariton subspace $\mathcal{H}_n$ independently. We present in the following how the radiation pressure coupling is projected into the polariton basis, giving rise to a coupling between the mechanical resonator and a series of polariton doublets. By restricting ourselves to a single subspace $\mathcal{H}_n$ the system can be seen as an effective two-level system (upper and lower polaritons with n excitations) coupled to a harmonic oscillator (the mechanical resonator). The effective coupling between this two level system and the harmonic resonator is reminiscent in its form of the original coupling between the artificial atom and the light field.

IV.2.2.1. Polaron eigenstates

After performing the change of basis we can study the system in each subspace $\mathcal{H}_n$. If put in any state $|\psi\rangle \in \mathcal{H}_n$ the system remains within this subspace unless an additional perturbation (coherent pump or dissipative processes acting on the Jaynes-Cummings subsystem) is taken into account.

In the basis $\{|+^{(n)}\rangle, |-^{(n)}\rangle\}$ the Jaynes-Cummings Hamiltonian, the number of photons operator and the atomic $\hat{\sigma}_z$ operator are represented by the following 2×2 matrices:

$$\hat{H}_{JC} \equiv \begin{bmatrix} (n-1/2)\omega_c + \frac{\Omega^{(n)}}{2} & 0 \\ 0 & (n-1/2)\omega_c - \frac{\Omega^{(n)}}{2} \end{bmatrix}, \tag{IV.9}$$

$$\hat{a}^\dagger\hat{a} \equiv \begin{bmatrix} n-\frac{1}{2} & \frac{1}{2} \\ \frac{1}{2} & n-\frac{1}{2} \end{bmatrix}, \tag{IV.10}$$

$$\hat{\sigma}_z \equiv \begin{bmatrix} 0 & -1 \\ -1 & 0 \end{bmatrix}. \tag{IV.11}$$

We introduce the corresponding Pauli matrices for this dimension 2 subspace $\hat{\sigma}_z^{(n)}$, $\hat{\sigma}_x^{(n)}$, $\hat{\sigma}_y^{(n)}$ as well as the two polaritonic lowering and raising operators $\hat{\sigma}_+^{(n)}, \hat{\sigma}_-^{(n)}$. In

the basis $\{|+^{(n)}\rangle, |-^{(n)}\rangle\}$ these operators are represented by the following matrices

$$\hat{\sigma}_z^{(n)} = \begin{bmatrix} 1 & 0 \\ 0 & -1 \end{bmatrix}, \hat{\sigma}_x^{(n)} = \begin{bmatrix} 0 & 1 \\ 1 & 0 \end{bmatrix}, \hat{\sigma}_y^{(n)} = \begin{bmatrix} 0 & -i \\ i & 0 \end{bmatrix}, \hat{\sigma}_+^{(n)} = \begin{bmatrix} 0 & 1 \\ 0 & 0 \end{bmatrix}, \hat{\sigma}_-^{(n)} = \begin{bmatrix} 0 & 0 \\ 1 & 0 \end{bmatrix}. \tag{IV.12}$$

The total Hamiltonian can thus be written $\hat{H} = \sum_{n\in\mathbb{N}} \hat{H}^{(n)}$, where the Hamiltonian projection to $\mathcal{H}_n$, $\hat{H}^{(n)}$, is given by :

$$\begin{aligned} \hat{H}^{(n)} =& (n-1/2)\omega_c \mathbb{1}^{(n)} + \frac{\Omega^{(n)}}{2}\hat{\sigma}_z^{(n)} \\ & - g_{cm}\left(\frac{1}{2}\hat{\sigma}_x^{(n)} + (n-\frac{1}{2})\mathbb{1}^{(n)}\right)\left(\hat{b}+\hat{b}^\dagger\right) + \omega_m \hat{b}^\dagger\hat{b}, \end{aligned} \tag{IV.13}$$

with $\mathbb{1}^{(n)}$ the identity matrix in the subspace spanned by the set $\{|+^{(n)}\rangle, |-^{(n)}\rangle\}$. The first two terms correspond to the projection of $\hat{H}_{JC}$ in this new basis. The third term is the projection of the optomechanical coupling term. This coupling, proportional to $\hat{a}^\dagger\hat{a}$, results in two different effects. An exchange term $\hat{\sigma}_x^{(n)}$ and a static shift of the mechanical resonator position $(n-1/2)\mathbb{1}^{(n)}$. Indeed, the subspace $\mathcal{H}_n$ holds n excitations of which in average $n-1/2$ are stored as photons. This average number of photons shifts statically the mechanical resonator equilibrium position. The term $\propto \mathbb{1}^{(n)}(\hat{b}+\hat{b}^\dagger)$ describes this effect. The other half excitation is exchanged between the states, being half the time a photon and the other half an atomic excitation. This exchange of polaritonic excitations is coupled to the position of the mechanical resonator. The "1/2" proportion is changed if the artificial atom and the cavity mode are no longer in resonance. Nevertheless the overall picture remains valid. The last term in Eq. IV.13 is the mechanical resonator energy, reminding us that we are still working in the basis $\{|\pm^{(n)}\rangle \otimes |l\rangle\}_{n,l\in\mathbb{N}}$. From here we move to the second part of the diagonalization, which takes us to the polaron eigenstates of the full Hamiltonian.

The term $-g_{cm}(n-1/2)\mathbb{1}^{(n)}(\hat{b}+\hat{b}^\dagger)$ can be understood as an additional energy potential linear in the position. In the Heisenberg picture this potential results in a constant force applied on the mechanical resonator. We apply a translation to the position operator in order to absorb this term. We thus set the new equilibrium position of the mechanical resonator to $q_0^{(n)} = \sqrt{2}g_{cm}/\omega_m(n-1/2)$. This is done

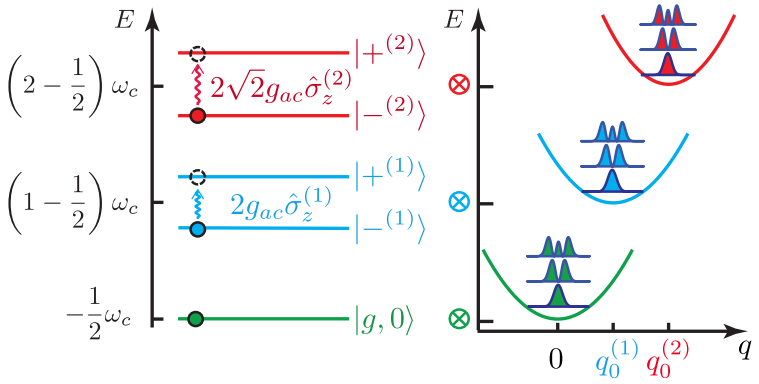

FIGURE IV.4: Description of the system in the polariton-phonon basis. The mechanical resonator couples independently to each polariton doublet.

by making the following transformation to the mechanical resonator operators:

$$\begin{aligned}\hat{b} &= \hat{b}_n + \frac{q_0^{(n)}}{\sqrt{2}} = \hat{b}_n + \frac{g_{cm}}{\omega_m}\left(n-\frac{1}{2}\right),\\ \hat{b}^\dagger &= \hat{b}_n^\dagger + \frac{q_0^{(n)}}{\sqrt{2}}.\end{aligned} \tag{IV.14}$$

The transformation IV.14 introduces annihilation and creation operators[1] $\hat{b}_n$ and $\hat{b}_n^\dagger$ in a new translated basis of $\mathcal{H}_n$. This new basis of Fock states is noted $\{|m^{(n)}\rangle\}_{m^{(n)}\in\mathbb{N}}$, $|m^{(n)}\rangle$ being the Fock state with $m^{(n)}$ phonons[2] of a mechanical resonator centered on $q_0^{(n)}$. One should bear in mind that the mean value of any operator $\langle\hat{O}\rangle$ will depend on the basis used to calculate this mean value. Rewriting the Hamiltonian IV.13 in terms of the new operators we get the following expression:

$$\begin{aligned}\hat{H}^{(n)} = &\left(n-\frac{1}{2}\right)\omega_c - \frac{g_{cm}^2}{\omega_m}\left(n-\frac{1}{2}\right)^2\\ &+\omega_m \hat{b_n}^\dagger \hat{b}_n + \frac{\Omega^{(n)}}{2}\hat{\sigma}_z^{(n)} - \frac{g_{cm}}{2}\sigma_x^{(n)}\left(\hat{b}_n^\dagger + \hat{b}_n\right)\\ &-\frac{g_{cm}^2}{\omega_m}\left(n-\frac{1}{2}\right)\hat{\sigma}_x^{(n)}.\end{aligned} \tag{IV.15}$$

[1] The new operators follow the same commutation relation as the original ones, $[\hat{b}_n, \hat{b}_n^\dagger] = [\hat{b}, \hat{b}^\dagger] = \mathbb{1}$.

[2] $m^{(n)}$ is an integer. The superscript (n) is superfluous but we decided to keep it to remind the reader that this new Fock basis refers to the displaced annihilation and creation operators $\hat{b}_n, \hat{b}_n^\dagger$.

$(n-1/2)\omega_c$ is the reference energy of the n-polariton subspace $\mathcal{H}_n$. $g_{cm}^2/\omega_m(n-1/2)^2$ is the energy shift due to the static displacement of the mechanical resonator in this subspace. The third line of Eq.IV.15 results from the translation transformation. In the displaced frame the static shift of the mechanical resonator leads to a perturbative effect $\propto \hat{\sigma}_x^{(n)}$ which induces a Stark-like shift in the eigenenergies. The effects of this term could be accounted for with usual perturbation theory [66] or they can be dealt with analytically at the expense of losing explicit expressions for the eigenvectors and eigenvalues of the system [117]. We neglect this term in the following. Its second order effects lead to a modification of the eigenenergies of the system of the order $\sim g_{cm}(g_{cm}/\omega_m)^2$. Since in current experimental implementations we have $g_{cm}/\omega_m \ll 1$ the approximation is valid. Nevertheless this ratio may change in future systems, which would require more careful considerations of the energy hierarchies at play in the system.

The central line in Eq.IV.15 is the one responsible for the main coupling between the polariton and the mechanical resonator. It is formally identical to a Jaynes-Cummings Hamiltonian [116] for which we have kept the anti-resonant terms. Using a rotating wave approximation (thus assuming implicetly $|\omega_m - \Omega^{(n)}| \ll \omega_m + \Omega^{(n)}$ for the approximation to be valid) we get to the same Hamiltonian that coupled originally the two level atom to the cavity:

$$\hat{H}^{(n)} \simeq \omega_m \hat{b_n}^\dagger \hat{b}_n + \frac{\Omega^{(n)}}{2}\hat{\sigma}_z^{(n)} - \frac{g_{cm}}{2}\left(\hat{b}_n^\dagger \hat{\sigma}_-^{(n)} + \hat{b}_n \hat{\sigma}_+^{(n)}\right). \tag{IV.16}$$

We can now introduce a polaron number operator (acting on the subspace $\mathcal{H}_n$)

$$\hat{N}_{polaron}^{(n)} = \hat{b}_n^\dagger \hat{b}_n + \hat{\sigma}_+^{(n)}\hat{\sigma}_-^{(n)}$$

that commutes with the projected Hamiltonian, $[\hat{H}^{(n)}, \hat{N}_{polaron}^{(n)}] = 0$. From here, if $\omega_m = \Omega^{(n)}$ the diagonalization is identical to the one performed on the atom-cavity Hamiltonian and we obtain the polaron basis $\{|\pm^{n,m^{(n)}}\rangle\}_{n,m^{(n)}\in\mathbb{N}}$, which diagonalizes the Hamiltonian IV.16.

$$\begin{aligned}
&\forall m^{(n)} \neq 0 : \\
|\pm^{n,m^{(n)}}\rangle &= \frac{1}{\sqrt{2}}\left(|+^{(n)}\rangle|(m-1)^{(n)}\rangle \mp |-^{(n)}\rangle|m^{(n)}\rangle\right) \\
|\pm^{n,m^{(n)}}\rangle &= \frac{1}{2}\big[|g\rangle|n\rangle|m^{(n)}\rangle \mp |g\rangle|n\rangle|(m+1)^{(n)}\rangle \\
&\qquad -i(|e\rangle|n-1\rangle|m^{(n)}\rangle \mp |e\rangle|n-1\rangle|(m+1)^{(n)}\rangle)\big]
\end{aligned} \tag{IV.17}$$

The "ground" state in subspace $\mathcal{H}_n$ is

$$\begin{aligned} m^{(n)} &= 0 : \\ |G^{n,0^{(n)}}\rangle &= |-^{(n)}\rangle|0^{(n)}\rangle \\ &= \frac{1}{\sqrt{2}}\left(|g\rangle|n\rangle|0^{(n)}\rangle - i|e\rangle|n-1\rangle|0^{(n)}\rangle\right) \end{aligned} \tag{IV.18}$$

From Eq.IV.17 we obtain the projector between a given ket in the final polaron-diagonalizing basis $|\pm^{n,m^{(n)}}\rangle$ and a ket from the original atom-cavity-mechanical resonator basis, $|e,g\rangle \otimes |k\rangle \otimes |l\rangle$:

$$\langle \pm^{n,m^{(n)}}|e,k,l\rangle = \frac{i}{2}\delta_{k,n-1}\left(\langle m^{(n)}|l\rangle \mp \langle (m+1)^{(n)}|l\rangle\right) \tag{IV.19}$$

$$\langle \pm^{n,m^{(n)}}|g,k,l\rangle = \frac{1}{2}\delta_{k,n}\left(\langle m^{(n)}|l\rangle \mp \langle (m+1)^{(n)}|l\rangle\ \right) \tag{IV.20}$$

The scalar products $\{\langle m^{(n)}|l\rangle\}_{m^{(n)}\in\mathbb{N}}$ do not assume the simple form of Kroenecker deltas over two indices. Depending on the new equilibrium position $q_0^{(n)}$ the overlap between Fock states of the original and displaced basis varies according to [118] :

$$\forall m^{(n)}, l \in \mathbb{N},\ \langle l|m^{(n)}\rangle = \sqrt{\frac{m^{(n)}!}{l!}}\left(\frac{q_0^{(n)}}{\sqrt{2}}\right)^{l-m^{(n)}} L_{m^{(n)}}^{l-m^{(n)}}\left((q_0^{(n)}/\sqrt{2})^2\right) e^{-(q_0^{(n)}/\sqrt{2})^2}, \tag{IV.21}$$

where $x \mapsto L_{m^{(n)}}^{l-m^{(n)}}(x)$ is the generalized Laguerre polynomial of degree $m^{(n)}$ and index $l - m^{(n)}$.

In the most general case $\Omega^{(n)} \neq \omega_m$ the polaron eigenvectors are given by

$$|+^{n,m^{(n)}}\rangle = \cos\frac{\theta^{n,m^{(n)}}}{2}|+^{(n)}\rangle|(m-1)^{(n)}\rangle + \sin\frac{\theta^{n,m^{(n)}}}{2}|-^{(n)}\rangle|m^{(n)}\rangle, \tag{IV.22}$$

$$|-^{n,m^{(n)}}\rangle = \sin\frac{\theta^{n,m^{(n)}}}{2}|+^{(n)}\rangle|(m-1)^{(n)}\rangle - \cos\frac{\theta^{n,m^{(n)}}}{2}|-^{(n)}\rangle|m^{(n)}\rangle, \tag{IV.23}$$

where

$$\tan[\theta^{n,m^{(n)}}] = -\frac{\sqrt{m^{(n)}}g_{cm}}{\sqrt{(\Omega^{(n)}-\omega_m)^2 + m^{(n)}g_{cm}^2}},\ \theta^{n,m^{(n)}} \in \left]-\frac{\pi}{2}, 0\right]. \tag{IV.24}$$

The associated eigenenergies are

$$\langle \pm^{n,m^{(n)}} | \hat{H}^{(n)} | \pm^{n,m^{(n)}} \rangle = \omega_0^{(n)} + \left(m^{(n)} - \frac{1}{2} \right) \omega_m \pm \sqrt{\frac{(\Omega^{(n)} - \omega_m)^2}{4} + m^{(n)} \frac{g_{cm}^2}{4}}. \tag{IV.25}$$

IV.2.3. Anharmonic energy structure

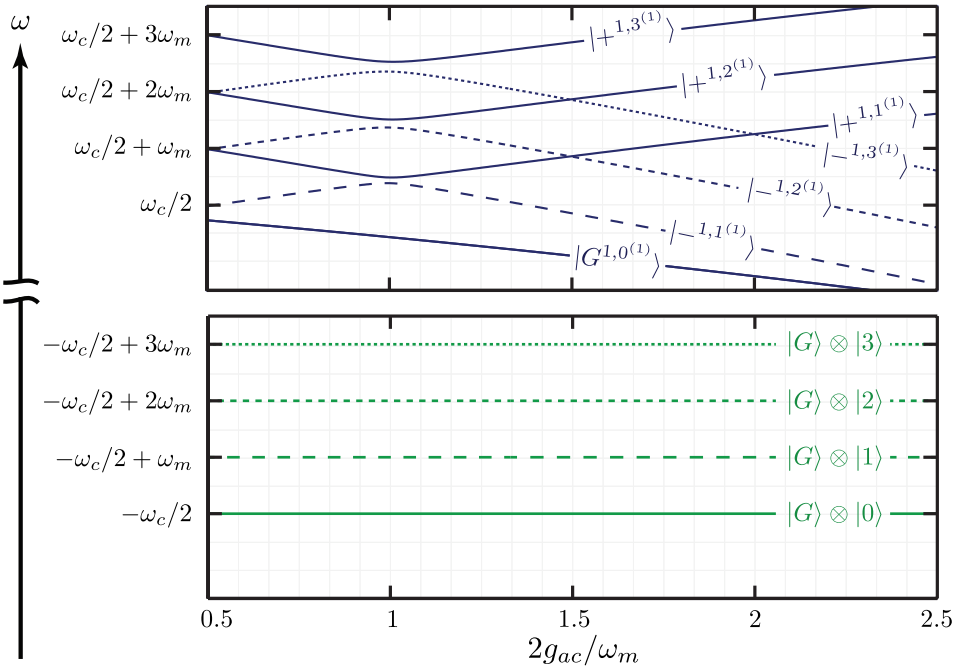

FIGURE IV.5: Energy levels in the subspaces $\mathcal{H}_n, n \leq 1$ as a function of the Jaynes-Cummings coupling g_{ac}. **Top half:** Energy levels in the $n = 1$ subspace for states with a number of polarons verifying $\langle \hat{N}_{polarons} \rangle \leq 3$. **Lower half:** Energy levels in the uncoupled $n = 0$ subspace.

Fig. IV.5 presents the energy levels for a number of polaritons $n = 0, 1$ as a function of the atom-cavity coupling. The $n = 0$ subspace corresponds to states with 0 photons. When the system state is in this subspace the mechanical resonator is uncoupled from the cavity and the two-level atom. The energy levels follow the usual harmonic structure without any dependance on g_{ac}. The picture is radically different in the subspace $\mathcal{H}_1$. The finite number of photons leads to a coupling between the mechanical resonator and the non-linear 1-polariton doublet as was previously discussed. In this subspace the energy levels present an anharmonic structure resulting from the polaron splitting described by Eq. IV.25. Changing the coupling between the cavity and the artificial atom ultimately modifies the polariton splitting $\Omega^{(n)}$. As can be seen in Fig.IV.5, bringing in and out of

resonance the atom-cavity and mechanical parts modifies the splitting between polaron states eventually leading to crossing and anti-crossing of energy levels.

These considerations on the energy structure of the final polaron basis of the total Hilbert space end our presentation of the analytical diagonalization of the problem. To obtain these analytical expressions we had to make a certain number of approximations. First, we neglected the antiresonant terms in the polariton-mechanics coupling. We neglected as well the effects of the term $\propto \hat{\sigma}_x^{(n)}$. Also, we relied on the block diagonal structure of the Hilbert space in order to treat independently each subspace $\mathcal{H}_n$. From now on we take into account a coherent pump on the cavity and the dissipative processes acting both on the cavity, the artificial two-level atom and the mechanical system. The presence of the environment leads to a coupling between the different polariton subspaces. Nevertheless the picture presented in this section establishes a good basis from which to interpret the results presented in the following.

IV.3. Coupling to the environment

From here on we take into account the effects of the environment on the total system. In order to describe the coupling between the cavity photons and an external laser drive at frequency ω_p we add the following time-dependent term to the Hamiltonian of the system:

$$\hat{V}_p(t) = iF_p(\hat{a}^\dagger e^{-i\omega_p t} - \hat{a}e^{+i\omega_p t}). \tag{IV.26}$$

The dissipative processes are described by Lindbladian terms of the form $\gamma_s D[\hat{O}_s]\hat{\rho}$, where γ_s is the decoherence rate associated to the jump operator $\hat{O}_s$ acting on the system. In the previous chapters of this manuscript we introduced and described the noise terms acting on the cavity and the mechanical resonator. We now introduce the dissipative processes experienced by the artificial two-level atom.

IV.3.1. Noise on the atom

In the following we assume that due to its coupling to the electromagnetic field outside the cavity the two-level atom is subject to spontaneous emission. By considering a coupling between the atom and the electromagnetic field of the form $\hat{H}_{int} = \int dq \kappa_q^a \hat{\alpha_q}^\dagger \hat{\sigma}_- + \kappa_q^{a*} \hat{\alpha}_q \hat{\sigma}_+$, it is possible [119] to derive a master equation

involving the operators $\hat{\sigma}_-$ and $\hat{\sigma}_+$ as jump operators. Just as we did for the cavity, we assume that the ratio between the atomic frequency and the temperature is big enough so that the effects of transitions stimulated by thermal photons can be neglected. We thus only add the Lindbladian term $\gamma_a D[\hat{\sigma}_-]\hat{\rho}$ to the master equation. This term accounts for the irreversible loss of an atomic excitation to the electromagnetic environment. The two-level atom could also be subject to other forms of dissipative processes such as non-radiative dephasing (described by a term $\propto D[\hat{\sigma}_z]\hat{\rho}$), but we restrict the discussion in this manuscript to the spontaneous emission of the atom.

IV.3.2. Final form of the master equation

We thus work with the following form of the master equation :

$$\begin{aligned}\frac{d\hat{\rho}(t)}{dt} =& -i[\hat{H}_{tot} + \hat{V}_p(t), \hat{\rho}] \\ &+ \gamma_c L[\hat{a}]\hat{\rho} + \gamma_a L[\hat{\sigma}_-]\hat{\rho} \\ &+ n_{th}\gamma_m L[\hat{b}^\dagger]\hat{\rho} + (n_{th}+1)\gamma_m L[\hat{b}]\hat{\rho}.\end{aligned} \tag{IV.27}$$

In the following we assume that both the atomic excitations and cavity photons decay with the same rate and thus set $\gamma_a = \gamma_c = \gamma_{ac}$. We define polariton and mechanical quality factors as follows: $Q_{ac} = \omega_c/\gamma_{ac} = \omega_a/\gamma_{ac}$ and $Q_m = \omega_m/\gamma_m$.

IV.4. Coherently pumped single polariton optomechanics

From now on we restrict the discussion to the subspaces $\mathcal{H}_n$ with $n \leq 1$. This truncation of the polariton Hilbert space is allowed by a well-known phenomenon in cavity and circuit quantum electrodynamics, the photon blockade effect. It is a consequence of the strong Jaynes-Cummings coupling between the cavity mode and the intrinsically non-linear two-level artificial atom. We first briefly discuss the physics behind photon blockade effects and present the main consequences of the Hilbert space truncation on the formalism.

IV.4.1. Photon blockade effect in a coherently pumped scenario

A bare cavity, one that is not coupled to any other system, has an harmonic ladder of equidistant energy levels separated by an energy $\hbar\omega_c$. The equidistant Fock states can be adressed by an external coherent drive at frequency ω_c leading to the excitation of a coherent state $|\alpha\rangle = \sum_k \exp(-|\alpha|^2/2)\alpha^k/\sqrt{k!}|k\rangle$ overlapping all the Fock states $|k\rangle$ of the Hilbert space.
It has been shown that a cavity coupled to an atom having a small number of states, and thus highly non-linear, can present photon blockade effects [120–122]. Due to the resulting anharmonicity of the spectrum, a pump tuned to excite the first photon will be off-resonance with respect to transitions exciting further the system. Once the first photon is excited the injection of a second one is blocked. It is important to note that in real life experiments the levels have a finite linewidth and levels non-resonant with the pump could actually be excited. The appearance of the photon blockade effects requires a spacing between levels larger than the linewidths. For the Jaynes-Cummings Hamiltonian the photon blockade rises if one is in the so-called strong coupling regime, $g_{ac}/\gamma_{ac} \gg 1$. The pump intensity has to be small enough as to avoid excitation of non resonant transitions. Here we assume that the system parameters ensure photon blockade thus allowing us to project the problem into the subspaces $\mathcal{H}_0$ and $\mathcal{H}_1$.

IV.4.2. Dimension 3 polariton Hilbert space

The atom-cavity degrees of freedom are thus described in a Hilbert space spanned by the vectors $|g, k=0\rangle$, $|-^{(1)}\rangle$ and $|+^{(1)}\rangle$. In this dimension-3 subspace the operators of interest are thus represented by 3×3 matrices in the basis $\{|G\rangle, |-^{(1)}\rangle, |+^{(1)}\rangle\}$. The projection of the cavity photon annihilation and creation operators are represented by the following matrices:

$$\hat{a} \equiv \frac{1}{\sqrt{2}} \begin{bmatrix} 0 & 1 & 1 \\ 0 & 0 & 0 \\ 0 & 0 & 0 \end{bmatrix}, \hat{a}^\dagger \equiv \frac{1}{\sqrt{2}} \begin{bmatrix} 0 & 0 & 0 \\ 1 & 0 & 0 \\ 1 & 0 & 0 \end{bmatrix}. \tag{IV.28}$$

For the atomic lowering and raising operators we get:

$$\hat{\sigma}_- \equiv \frac{1}{\sqrt{2}} \begin{bmatrix} 0 & -i & i \\ 0 & 0 & 0 \\ 0 & 0 & 0 \end{bmatrix}, \hat{\sigma}_+ \equiv \frac{1}{\sqrt{2}} \begin{bmatrix} 0 & 0 & 0 \\ i & 0 & 0 \\ -i & 0 & 0 \end{bmatrix}. \tag{IV.29}$$

In the simple case of a resonant Jaynes-Cummings system ($\omega_c = \omega_a$) for which the atomic and photonic decay rates are strictly identical ($\gamma_c = \gamma_a$) the dissipative processes on both the atom and the photon are easily described in this new reduced picture. The lower and upper polariton states decay indepently at a rate $\gamma_{ac} = \gamma_a = \gamma_c$ towards the ground state. We introduce the jump operators:

$$\hat{c}_- \equiv \begin{bmatrix} 0 & 1 & 0 \\ 0 & 0 & 0 \\ 0 & 0 & 0 \end{bmatrix}, \hat{c}_+ \equiv \begin{bmatrix} 0 & 0 & 1 \\ 0 & 0 & 0 \\ 0 & 0 & 0 \end{bmatrix}, \tag{IV.30}$$

responsible for the decay channels of the lower and upper polariton respectively. The atom and photon Lindbladian terms then become $\gamma_c L[\hat{a}]\hat{\rho} + \gamma_a L[\hat{\sigma}_-]\hat{\rho} \mapsto \gamma_{ac} L[\hat{c}_-]\hat{\rho} + \gamma_{ac} L[\hat{c}_+]\hat{\rho}$.

The corresponding density matrix of this reduced system is noted and represented as follows:

$$\hat{\rho}^{(1)}_{JC} \equiv \begin{bmatrix} \rho_{GG} & \rho_{G-^{(1)}} & \rho_{G+^{(1)}} \\ \rho_{-^{(1)}G} & \rho_{-^{(1)}-^{(1)}} & \rho_{-^{(1)}+^{(1)}} \\ \rho_{+^{(1)}G} & \rho_{+^{(1)}-^{(1)}} & \rho_{+^{(1)}+^{(1)}} \end{bmatrix}. \tag{IV.31}$$

IV.4.3. Joint spectral density of states

Let us consider that the system is initially in a generic uncoupled state of the form $|G\rangle\langle G| \otimes \hat{\rho}_m$, which corresponds to a state with no photons in the cavity, the artificial atom in its ground state and an arbitrary state for the mechanical resonator. By applying a coherent pump to the cavity the initial state previously defined gets coupled to states in subspace $\mathcal{H}_1$ in which the distinction between photons, atomic excitations and phonons no longer holds and the tripartite polarons are the relevant elementary excitations.

Fig.IV.6 presents the transitions excited by the coherent pump between states in $\mathcal{H}_0$ and states in $\mathcal{H}_1$. The pump links the initial atom-cavity-mechanics states to polaron states containing a different number of phonons. Using the diagonalized basis defined in Eqs.IV.22 and IV.23 we introduce a joint spectral density of states that is useful to understand the possible transitions excited by the pump as a function of the frequency pump. The joint spectral density of states, $D[\omega]$, is defined as follows :

$$D[\omega] = \sum_{\substack{s=\pm \\ m,l\in\mathbb{N}}} |\langle s^{1,m}|\hat{V}_p|G,l\rangle|^2 \delta[\omega - (\omega_{s^{1,m}} - \omega_{G,l})]. \tag{IV.32}$$

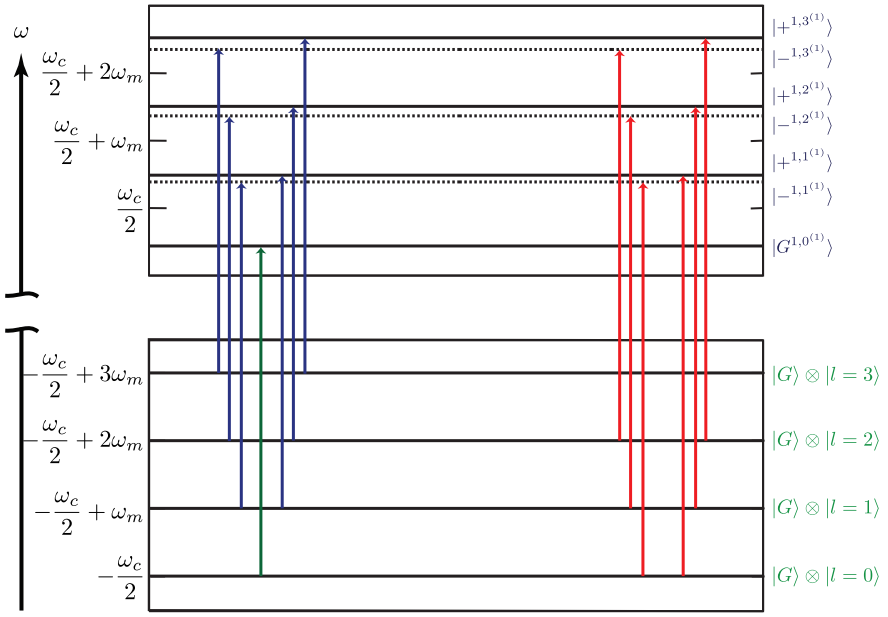

FIGURE IV.6: Energy levels in the subspaces $\mathcal{H}_0$ and $\mathcal{H}_1$ and the transitions induced by the coherent pump. In the upper half solid lines correspond to upper polaron states ($|+^{1,m^{(1)}}\rangle$) while dashed lines correspond to lower polaron states ($|-^{1,m^{(1)}}\rangle$). Green, blue and red arrows correspond to transitions conserving, reducing and increasing the average number of phonons respectively. The atom-cavity coupling is set to give a resonant single polariton-mechanics scenario, $\Omega^{(1)}=\omega_m$. The optomechanical coupling is given by $g_{cm}/\omega_m=10^{-1}$.

Where $\omega_{\pm^{n,m^{(n)}}}$ is the eigenenergy of the state $|\pm^{n,m^{(n)}}\rangle$ and $\omega_{G,l}$ is the energy of the state $|G,l\rangle=|G\rangle\otimes|l\rangle$. $D[\omega]$ explores the optically induced transitions between states in $\mathcal{H}_0$ to states in $\mathcal{H}_1$. The generalization to transitions between other subspaces is straightforward but here we are only exploring transitions exciting at most one polaritonic excitation. The function $w\mapsto D[\omega]$ presents a series of delta peaks centered on the frequency (energy) difference between two coupled states, each delta peak being weighted by the squared of the corresponding coupling matrix element.

Fig. IV.7 presents $D[\omega]$ as a function of ω for two different sets of parameters. For clarity the delta peaks have been convoluted by a Lorenzian[3] of width γ_{ac}. The main panel shows $D[\omega]$ for $g_{cm}/\omega_m=10^{-1}$. It displays two spectral structures centered on the lower (upper) polariton energy $\omega_-^{(1)}$ ($\omega_+^{(1)}$). Each structure is itself split into a doublet with a splitting $\sim g_{cm}$. The inset of Fig.IV.7 presents $D[\omega]$ for a weaker optomechanical coupling $g_{cm}/\omega_m=10^{-3}$. In this case the polaron fine

[3] The main contribution to the dissipative processes undergone by the polaron states comes from the Lindbladian term with the fastest rate, in usual experiments this corresponds to the atomic-photonic decay.

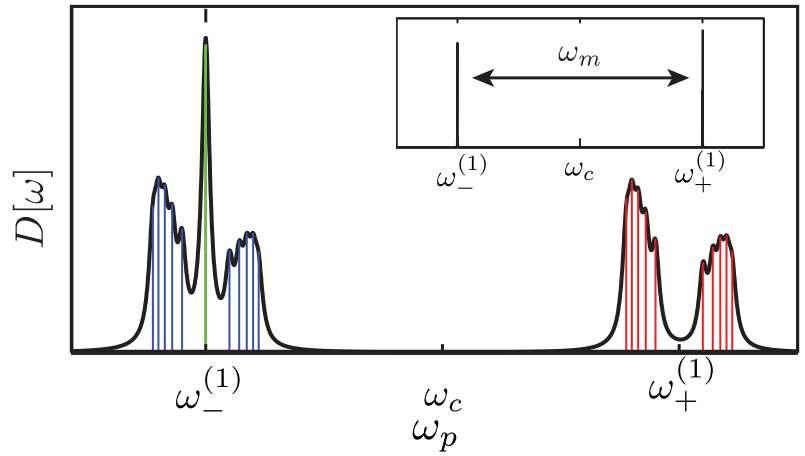

FIGURE IV.7: Optical joint spectral density of polaron states describing transitions between the states with 0 and 1 polaritons. Main panel: $g_{cm}/\omega_m = 10^{-1}$, $Q_{ac} = 10^4$. Insight: $g_{cm}/\omega_m = 10^{-3}$, $Q_{ac} = 10^6$. For clarity, we only present transitions between states with $m^{(n)} \leq 5$ polarons. Blue, green and red peaks represent transitions reducing, conserving and increasing the number of phonons respectively.

structure splitting $\sim g_{cm}$ is no longer visible at a scale $\sim \omega_m$ and $D[\omega]$ presents only two resonances at $\omega_\pm^{(1)}$.

The structure of $D[\omega]$ is best understood by looking closely at the possible transitions from subspace $\mathcal{H}_0$ to subspace $\mathcal{H}_1$ as depicted in Fig.IV.6. The form of $D[\omega]$ arises from the fact that under the coherent pump the system can undergo three different kinds of transitions. Let us assume that the system is initially in a state of the form $|G\rangle \otimes |m\rangle$ with $m \neq 0$.
If the pump is set as to excite the lower polariton ($\omega_p \sim \omega_-^{(1)}$) then the system is roughly taken to the state $|-^{(1)}\rangle \otimes |m\rangle$, which is in the m-polarons subspace $\mathcal{H}_m^{(1)}$. The two eigenstates of the Hamiltonian that are actually excited are $|\pm^{1,m^{(1)}}\rangle$. The corresponding transitions (shown as green arrows in Fig.IV.6 and green peaks in Fig.IV.7) are split with respect to $\omega_-^{(1)}$ by an amount proportional to $\sqrt{m}g_{cm}$.
Now, if the pump frequency is tuned to $\omega_p \sim \omega_+^{(1)}$ then the system is roughly taken to the state $|+^{(1)}\rangle \otimes |m\rangle$, which is in the $(m+1)$-polarons subspace $\mathcal{H}_{m+1}^{(1)}$. The two excited states are in this case $|\pm^{1,(m+1)^{(1)}}\rangle$ and the corresponding transitions (depicted in red in Figs. IV.6 and IV.7) are split with respect to $\omega_+^{(1)}$ by an amount proportional to $\sqrt{m+1}g_{cm}$.
Finally, the third kind of possible transitions (depicted in green) corresponds to the transition $|G\rangle|0\rangle \mapsto |G^{1,0^{(1)}}\rangle$. Here one starts from a state with 0 phonons and excites a state with 0 polarons. Having no polaronic excitation in the final state there is no energy splitting and this particular transition sits at $\omega_p = \omega_-^{(1)}$.

In Fig.IV.7 the peak at $\omega = \omega_-^{(1)}$ (green peak) corresponds to the only transition linking two states with the same number of phonons $|G\rangle|0\rangle \mapsto |G^{1,0^{(1)}}\rangle$. The resonances around $\omega_-^{(1)}$ (blue peaks) correspond to transitions linking a state with m phonons to a state with m polarons. Since the m-polarons states are superpositions of the states $|-^{(1)}\rangle \otimes |m\rangle$ and $|+^{(1)}\rangle \otimes |m-1\rangle$ these transitions lead to an average reduction of the number of phonons. On the other hand the transitions around $\omega_+^{(1)}$ (red peaks) couple states with m phonons to states with $m+1$ polarons. These transitions increase the number of phonons (the final state is a superposition of the states $|-^{(1)}\rangle \otimes |m+1\rangle$ and $|+^{(1)}\rangle \otimes |m\rangle$). Carefully tuning the pump frequency to any one of these transitions will lead to cooling or amplification of mechanical motion.

Here we have discussed the doublet structures in $D[\omega]$ in terms of the possible transitions excited in the system by the coherent pump. In section IV.5.2 we show that the Jaynes-Cummings coupling of the cavity to the two-level atom results in a splitting of the standard optomechanical sidebands. These split sidebands anti-cross when the hybrid system considered here is at resonance ($\Omega^{(1)} = \omega_m$), which leads to the doublet structures we just discussed.

IV.5. Coherently pumped stationary statistics

Using the numerical methods presented in chapter II we study the properties of the stationary state of the master equation IV.27. We discuss cooling and amplification of mechanical motion. We also discuss the ability of the hybrid system to reach non-classical "trajectories" of mechanical motion. Finally, we discuss such features as a function of different parameters of the system.

IV.5.1. Stationary phonon statistics

As discussed before, by tuning the pump frequency to either one of the polariton structures in the joint spectral density of states it is possible to cool or amplify mechanical motion. In what follows we discuss the phonon stationary statistics as a function of the pump frequency[4]. We do so by numerically diagonalizing the Liouvillian superoperator for each value of ω_p.

[4] The time dependance of the additional pump terms in the Hamiltonian can be removed by moving to the rotating frame via the unitary operator $\hat{U}(t) = \exp(-i\omega_p t(\hat{a}^\dagger\hat{a} + \hat{\sigma}_z/2)$.

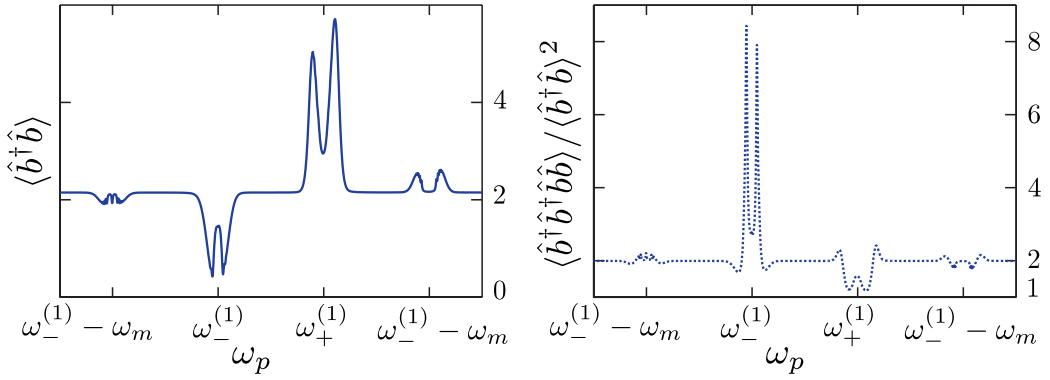

FIGURE IV.8: Stationary phonon statistics as a function of the pump frequency ω_p. Left panel (solid line): Stationary number of phonons. Right panel (dotted line): Stationary second order autocorrelation function. $Q_{ac} = Q_m = 10^4,\ 2g_{ac} = \Omega^{(1)} = \omega_m,\ g_{cm}/\omega_m = 10^{-1},\ n_{th} = 2.15.$

Fig.IV.8 presents the mechanical resonator stationary number of phonons and second order autocorrelation function as a function of the pump frequency ω_p. We consider a finite temperature environment and a strong enough optomechanical coupling (compared to the loss rates) as to clearly separate the polaron resonances previously discussed. When the pump is tuned far from the system resonances the mechanical resonator statistics follow those dictated by the thermal environment. The average phonon number is equal to the mean thermal occupancy $\langle \hat{b}^\dagger \hat{b} \rangle = n_{th}$ and the second order autocorrelation function has the value corresponding to a thermal state $\langle \hat{b}^\dagger \hat{b}^\dagger \hat{b} \hat{b} \rangle / \langle \hat{b}^\dagger \hat{b} \rangle^2 = 2$. On the other hand, if the pump frequency is tuned to excite the transitions described in Fig.IV.6 it is possible to drastically change the mechanical resonator statistics. A pump tuned to match the lower polariton energy will induce a decrease of the mechanical resonator occupation number. This cooling is accompanied by strong bunching of phonons in comparison to the statistics of a thermal state. If the pump is tuned to the upper polariton energy the number of phonons in the stationary state is amplified leading to values of the autocorrelation function closer to those of a coherent state $\langle \hat{b}^\dagger \hat{b}^\dagger \hat{b} \hat{b} \rangle / \langle \hat{b}^\dagger \hat{b} \rangle^2 = 1$.

Fig.IV.9 presents the stationary number of photons as a function of ω_p for the same set of parameters. It should be noticed that around the lower polariton energy ($\omega_p \sim \omega_-^{(1)}$) the number of photons does present the triple-peak structure predicted by the joint spectral density of states of Eq.IV.32. As was previously discussed this central peak corresponds to a transition linking two states with the same number of phonons and does not lead to any modification of mechanical motion. As expected the phonon statistics of Fig.IV.8 only present two split peaks around this frequency.

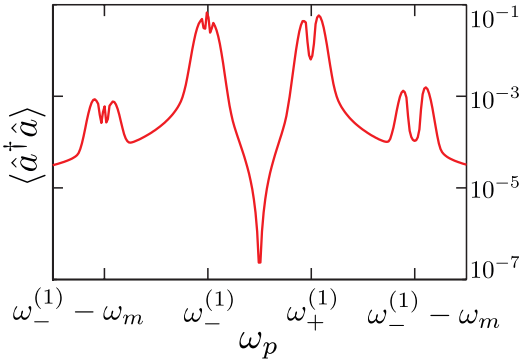

FIGURE IV.9: Stationary number of photons as a function of the pump frequency ω_p.
$Q_{ac} = Q_m = 10^4,\ 2g_{ac} = \Omega^{(1)} = \omega_m,\ g_{cm}/\omega_m = 10^{-1},\ n_{th} = 2.15.$

IV.5.1.1. Resonant optomechanical effects on mechanical motion

In usual optomechanics (i.e for $g_{ac} = 0$) cooling or amplification of mechanical motion are obtained by pumping the cavity on either its red or blue optomechanical sideband. The off-resonant pumping of photons leads to second order transitions modifying the mechanical properties. The hybrid system we study here has a radically different behavior. By introducing the non-linear artificial atom in the cavity we are able to modify the mechanical resonator statistics by resonantly pumping the dressed photon states. Now cooling or amplification arise from first order transitions between system states. Fig.IV.8 also presents the resonances corresponding to the second order transitions which are off-resonance with respect to the optical response. As can be seen in Fig.IV.9, when exciting these transitions the number of photons actually injected into the system is much less leading to smaller effects on the mechanics.

In our hybrid scheme the optical transitions inducing cooling of mechanical motion become aligned with the Jaynes-Cummings resonances. Fig.IV.10 presents a comparison between the cooling capabilities of our scheme and the usual optomechanical setup for moderate optomechanical couplings, $g_{cm}/\omega_m = 10^{-3}$. In the atom-less scenario, the number of photons that can be injected into the cavity by pumping the red sideband is hindered by the very narrow optical response, and the phonon number barely deviates from the thermal occupation (solid line). Whereas in a hybrid system coupled to a two-level artificial atom the possibility to reduce the number of phonons by resonantly injecting photons into the system leads to a much more efficient cooling of mechanical motion (dashed line).

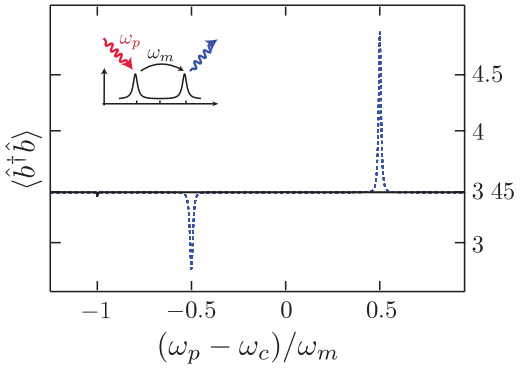

FIGURE IV.10: Stationary number of phonons as a function of ω_p for $Q_m = 10^6$, $Q_{ac} = 10^6$, $g_{cm}/\omega_m = 10^{-3}$, $F_p/\gamma_{ac} = 100$. The dashed blue line represents the hybrid QED-optomechanics case with an atom ($g_{ac} \neq 0$) while the black solid line corresponds to the usual atomless scenario($g_{ac} = 0$). The inset depicts schematically the doubly-resonant polariton cooling of motion.

IV.5.1.2. Amplification of mechanical motion and non-classical "trajectories"

So far we have discussed the cooling capabilities of the system under consideration. Let us now choose a pump frequency tuned to the resonances around the energy of the upper polariton $\omega_+^{(1)}$. The transitions corresponding to these resonances increase the number of phonons excited in the mechanical resonator thus leading to amplification of mechanical motion. Optomechanically induced amplification and instability of mechanical motion have already been discussed in the semi-classical regime [6] and in the quantum regime [46, 67]. Here we revisit this concept with our hybrid system and present some of the insight we gained by looking at the phonon number distribution in the stationary state of the system. In the following we set the pump frequency to $\omega_p = \omega_+^{(1)} + g_{cm}$. As shown in Fig.IV.11 for strong enough pump intensities, tuning the coherent pump to this frequency leads to amplified statistics of mechanical motion.

In a pump-less scenario ($F_p = 0$, inset *a* in Fig.IV.11) the mechanical resonator is only subject to the effects of its thermal environment. Its Wigner distribution is given by a gaussian centered around 0. Without any optomechanical modification the stationary probability distribution over the Fock states of the mechanical resonator, $T[l] = Tr[|l\rangle\langle l|\hat{\rho}]$, is given by the usual thermal distribution with an average number of phonons equal to n_{th}:

$$T_{th}[l] = \frac{(n_{th})^l}{(n_{th}+1)^{l+1}}. \tag{IV.33}$$

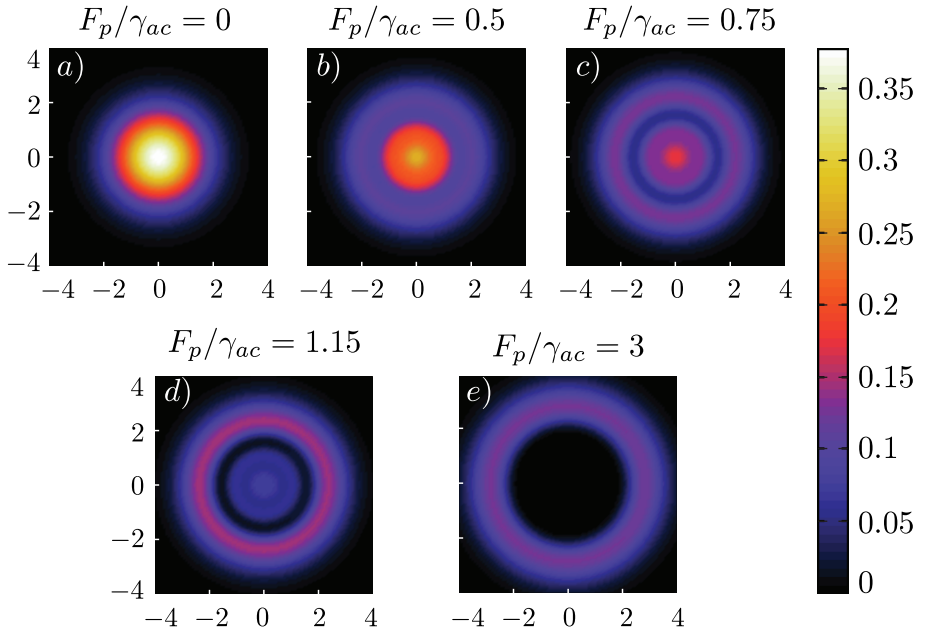

FIGURE IV.11: Stationary state Wigner distribution of the mechanical resonator in the $\mathbb{C}$-plane of the scalar field β (as discussed in chapter II) for increasing values of the pump intensity F_p. In all the figures we have set : $g_{ac} = \omega_m/2,\ g_{cm} = \omega_m/10,\ Q_{ac} = Q_m = 10^4,\ \omega_p = \omega_+^{(1)} + g_{cm}$. The system is coupled to a finite temperature environment exciting an average number of thermal phonons $n_{th} = 2.15$.

As can be seen in Fig.IV.11 increasing the pump intensity leads to the appearance of non gaussian statistics for the mechanical resonator. Inset e) of the figure presents the form of the Wigner distribution for values of F_p beyond threshold for which the thermal-gaussian lobe centered in zero completely disappears giving place to a ring-like shape of the Wigner distirbution. This kind of Wigner distributions has been discussed in the literature as corresponding to " a coherent state undergoing circular motion in phase space but with an undetermined phase" [67]. Here we are interested on the effects of a finite temperature environment and we have observed that the phonon statistics are best described by the so-called cothermal distribution [123] which corresponds to a state having in average n_{coh} coherent phonons and n_{th} thermal phonons. The cothermal distribution is given by the following formula:

$$\begin{aligned} T_{coth}[l] &= e^{-n_{coh}/(n_{th})} \frac{(n_{th})^l}{(n_{th}+1)^{l+1}} L_l\left[\frac{-n_{coh}}{n_{th}(n_{th}+1)}\right] \\ &= e^{-n_{coh}/(n_{th})} T_{th}[l] L_l\left[\frac{-n_{coh}}{n_{th}(n_{th}+1)}\right], \end{aligned} \tag{IV.34}$$

where $x \mapsto L_l[x]$ is the l-th Laguerre polynomial. The total number of phonons

in such a state is $\langle \hat{b}^\dagger \hat{b} \rangle = n_b = n_{coh} + n_{th}$ and the second order autocorrelation function is given by

$$\frac{\langle \hat{b}^\dagger \hat{b}^\dagger \hat{b} \hat{b} \rangle}{\langle \hat{b}^\dagger \hat{b} \rangle^2} = 2 - \left(\frac{n_{coh}}{n_b} \right)^2 . \tag{IV.35}$$

As the coherent fraction of the stationary states becomes predominant the autocorrelation function of the mechanical resonator approaches 1 corresponding to the usual statistics of a coherent state. The stationary state of Fig.IV.11e is well fitted by a cothermal distribution with $n_{th} = 0.095$ thermal phonons and $n_{coh} = 9.043$ coherent phonons.

The different insets in Fig.IV.11 present how the mechanical resonator goes from a pure thermal state to the "cothermal" state previously discussed. From the thermal state (Fig.IV.11a), as the pump intensity F_p increases one first observes the appearance of the ring like shape additional to the thermal lobe (Fig.IV.11b). Then the thermal lobe starts fading away (Fig.IV.11d) until it completely disappears giving rise to the cothermal distribution (Fig.IV.11e). Both the initial and final states can be described in terms of an analytical description of the phonon distribution. Nevertheless for those intermediate values for which the thermal lobe and the cothermal ring coexist (Fig.IV.11c) we have not been able to find an analytical description of the interplay between the polariton and the mechanics leading to these "superpositions". We remain confident though that the analytical treatment that is presented in the following sections will shed new light into the problem.

The state shown in Fig.IV.11e) does not result from a gaussian Wigner distribution. But it can be interpreted as a gaussian state having lost all information on its phase (a coherent state undergoing circular motion in phase space). From this point of view could it be called non-classical? Defining a non-classical state for a harmonic oscillator is in itself a difficult question. A squeezed state for which the noise on one of its quadratures is below the standard quantum limit is a gaussian non-classical state. Entangled states are also non-classical states but defining a good measure of entanglement for the kind of open systems considered here is not a simple task. Here we loosely define a non-classical state as a state presenting negative values on its Wigner distribution[5].

As shown in Fig.IV.12 when pumped at the right frequency our system offers the possibility to reach stationary non-classical statistics for the mechanical resonator. The figure depicts the stationary statistics for a zero temperature environment. We have checked that for small enough finite temperatures this negative values for

[5] Ref.[43] gives an insightful discussion on other signatures of non-classicality for mechanical resonators.

the Wigner distribution can be reached by increasing slightly the pump frequency. With the set of parameters in Fig.IV.12 a pump intensity of the order $F_p = 10\gamma_{ac}$ leads to non-classical statistics for dilution cryostat temperatures $\sim$ 4mK. Evidently as the temperature rises the non-classicality succumbs under thermal noise and the negative values dissapear as can be seen in the Wigner distributions depicted in Fig.IV.11

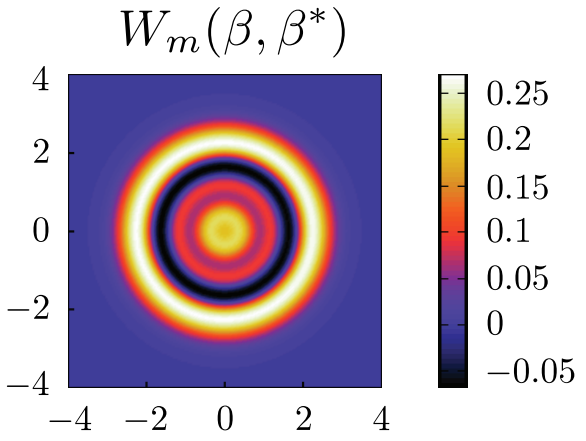

FIGURE IV.12: Non classical Wigner distribution of a mechanical resonator. Zero temperature environment, pump intensity below threshold. $F_p/\gamma_{ac} = 1.15,\ g_{ac} = \omega_m/2,\ g_{cm} = \omega_m/10,\ Q_{ac} = Q_m = 10^4,\ \omega_p = \omega_+^{(1)} + g_{cm}$.

IV.5.2. Polaritonically split optomechanical sidebands

We studied the behavior of the system when the polariton splitting varies. The polariton splitting is tailored by the Jaynes-Cummings coupling $\Omega^{(1)} = 2g_{ac}$. By changing this parameter it is then possible to bring in and out of resonance the polariton doublet and the mechanical resonator. This polariton-splitting-wise study allowed us to better understand the doublet structures appearing in Fig.IV.7. The density plot in Fig.IV.13 depicts the behaviour of the stationary number of phonons as a function of the polariton splitting and the coherent pump frequency. For zero coupling between the artificial atom and the cavity ($g_{ac} = 0 = \Omega^{(1)}$) we get the picture of standard optomechanics. The mechanical resonator properties are essentially modified when the cavity is pumped at its two optomechanical sidebands ($\omega_p = \omega_c \pm \omega_m$). For increasing values of the Jaynes-Cummings coupling a splitting of the two optomechanical sidebands occurs. Eventually, when $\Omega^{(1)} = \omega_m$, these split sidebands can cross or anticross depending on the observable under consideration thus leading to the doublet structures appearing in the joint spectral density of states.

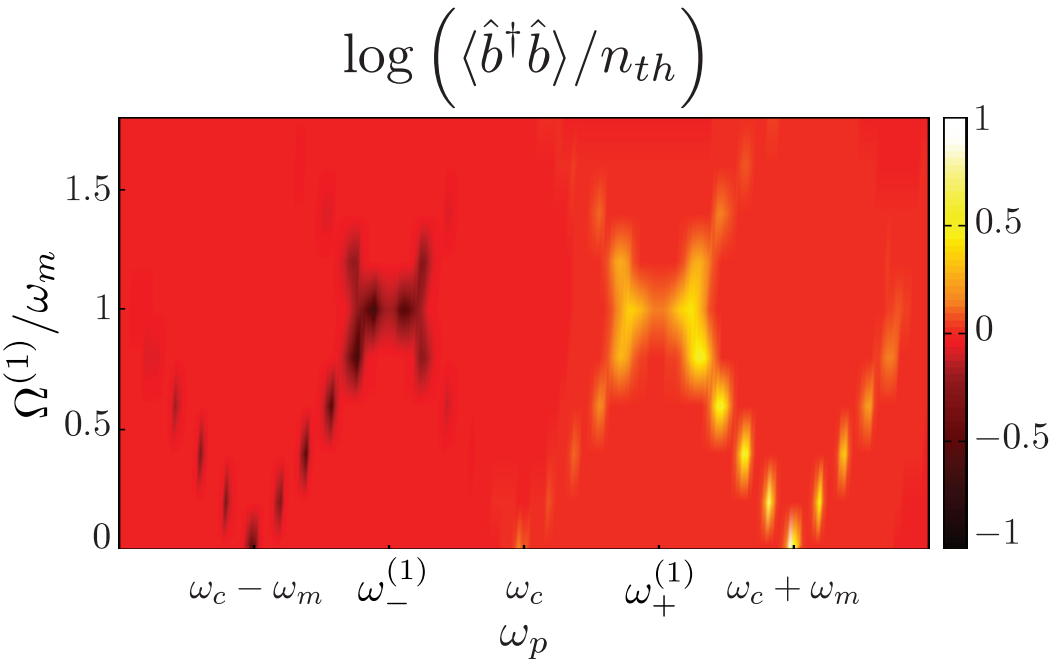

FIGURE IV.13: Logarithm of the stationary number of phonons as a function of the pump frequency ω_p and of the vacuum Rabi splitting $\Omega^{(1)}$. $F_p/\gamma_{ac}=1,\ g_{cm}=\omega_m/10,\ Q_{ac}=Q_m=10^4$.

IV.5.3. Dependance on the decay rates

We also studied the influence of the polariton and mechanical quality factors. Cooling and amplification of mechanical motion arise from the exchange of excitations between the 1-polariton level structure and the mechanical resonator. When exciting resonantly the lower polariton, the annihilation of a mechanical phonon excites the Jaynes-Cummings system from the lower to the upper polariton level. If the polaritonic excitation is rapidly lost (through non-radiative or radiative loss mechanisms) and rapidly re-excited (by means of the optical pump) one can gradually depopulate the mechanical oscillator thus leading to cooling of its motion. This explains why worsening the cavity (smaller quality factor) in a certain range enhances the cooling mechanism. A polariton quality factor of 10^3 leads to a stationary phononic occupation $\sim 10^{-2}$ for a pump still obeying $F_p/\gamma_c=1$. For $Q_{ac}=10^4$ we obtain a cooled phononic occupancy $\sim 4.10^{-1}$. Similarly, increasing the polariton losses mechanisms leads to stronger amplification of mechanical motion. One has to be careful though with the value of the quality factors. If the atomic spontaneous emission and cavity photon leakages become too important the polaritonic fine structure is no longer resolved and no cooling or amplification is possible.

The situation instead is radically different for the mechanical resonator. A reduction of the mechanical quality factor decreases the cooling and amplification efficiencies in all cases. As the mechanical quality factor goes down much more intense optomechanical effects are needed in order to counteract the thermalization induced by the environment. This intensification could be achieved by either increasing the optomechanical coupling or increasing the number of photons excited in the cavity by considering stronger pump intensities.

IV.5.4. Time resolved thermalization of a Fock state

Fig.IV.14 presents the time evolution of the number of photons and phonons for a coherently pumped system. Initially the state is in a state of the form $|G\rangle \otimes |l = 2\rangle$ with the mechanical resonator in a Fock state with 2 phonons and no polaritons. At a time $t > 0$ the pump, whose frequency has been set to $\omega_p = \omega_-^{(1)}$, is turned on with a heaviside profile. The discontinous profile of the pump enriches with high frequencies the pump spectrum thus leading to an involved early transient regime. As the stationary number of photons approaches a stationary state the number of phonons exponentially decreases with an effective dissipation constant $\gamma_{eff} \cong 18\gamma_m$ towards a state containing $n_{min} \sim 1/10$ phonons.

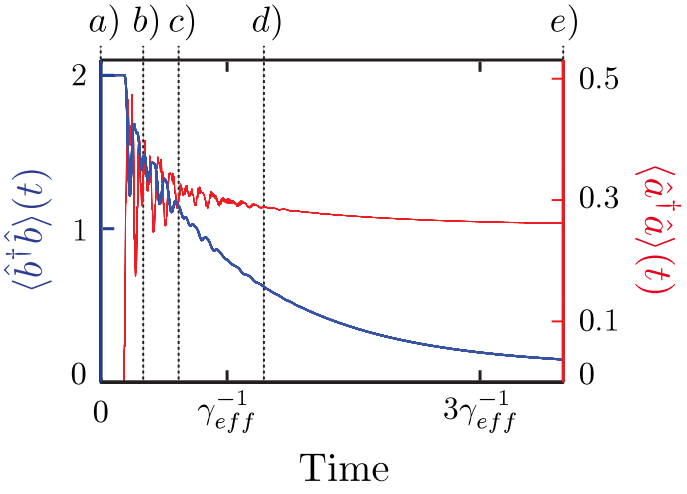

FIGURE IV.14: Time evolution of the number of photons (red) and phonons (blue) for an initial state of the form $|G\rangle \otimes |l = 2\rangle$. The coherent pump, with frequency $\omega_p = \omega_-^{(1)}$, is turned on at a time $t > 0$ with a heaviside profile. $Q_m = Q_{ac} = 10^4,\ g_{ac} = \omega_m/2,\ g_{cm} = \omega_m/10,\ F_p = 10\sqrt{2}\gamma_{ac}$.

In this scenario, the mechanical resonator starts in a highly non-classical Fock state and ends up in a gaussian state, close to the ground state but having slightly different statistics since its correlation function presents (in good agreement with

Fig.IV.8) a bunched value in comparison to a thermal state. With the set of parameters of Fig.IV.14 we obtain $\langle \hat{b}^\dagger \hat{b}^\dagger \hat{b}\hat{b} \rangle / \langle \hat{b}^\dagger \hat{b} \rangle^2 = 3.36$.

Fig.IV.15 presents the Wigner distribution of the mechanical resonator at five different times marked by the vertical dashed lines in Fig.IV.14. Panel *a*) shows the Wigner distribution for the 2 phonons Fock state with its negative values. As time advances the system enters its transient regime (panels *b* and *c*) where first the negatives values are lost and it starts converging to a gaussian state. From the point *d*) until the end the state remains in a gaussian state and the phonon population exponentially decays leading to a state near the ground state as previously discussed.

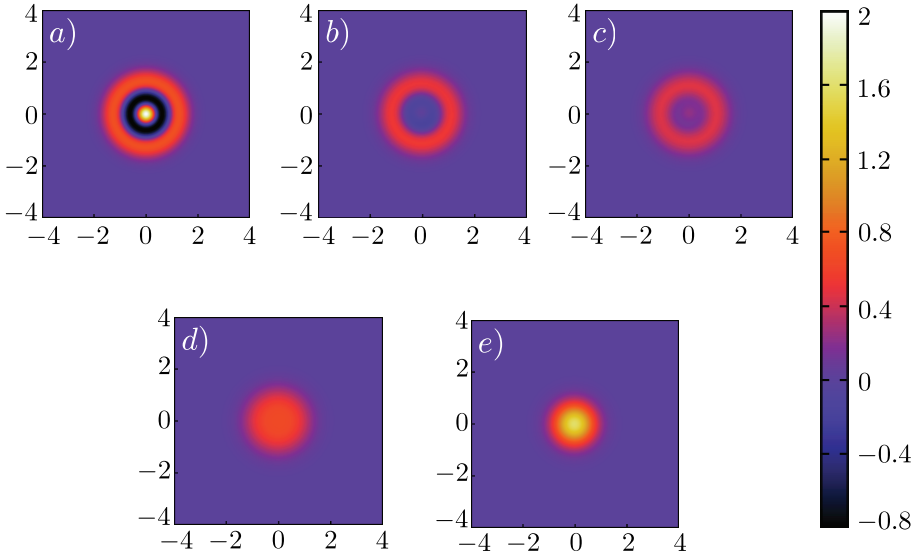

FIGURE IV.15: Mechanical resonator Wigner function at different times for a system pumped as to induce cooling of mechanical motion. The different panels correspond to snapshots taken at different times marked by the vertical dashed lines in Fig.IV.14. The set of parameters considered is the same as in Fig.IV.14.

Given the non-linear couplings and the dimension of the Hilbert spaces it is not necessarily straightforward to get analytical insight into the dynamical (time-dependent) behavior of such systems. The kind of numerical resolution employed here appears thus a good tool to obtain insights into how the decoherence processes at play manifest themselves within the considered formalism.

IV.6. Incoherently pumped single-polariton optomechanics

Given the form of the considered optomechanical coupling it is essential to inject energy from the "outside world" to excite photons and obtain optomechanical effects. This far we have only considered a coherent pump at a given frequency in order to excite the polariton system from the ground state $|G\rangle$ to either one of the two 1-polariton states $|\pm^{(1)}\rangle$. Now we discuss incoherent pumping of the 1-polariton subspace. While the coherent pump couples the coherences of the density matrix, the incoherent one only couples the populations. We explore this new experimental configuration with analytical tools that yield insight into the stationary statistics of our tripartite system. We first briefly discuss the physical process behind this so-called incoherent pumping and the master equation we used to describe it. Then we present the analitycal method used to describe the problem. This method is greatly inspired by a theoretical work studying the strong light-matter coupling between a two-level system and a cavity mode [123]. Here we generalize the method to our effective three level structure (the polariton system spanned by the states $\{|G\rangle,\ |-^{(1)}\rangle,\ |+^{(1)}\rangle\}$) coupled to the mechanical resonator. Finally we discuss the emission of strongly antibunched phonons under incoherent pumping.

IV.6.1. Incoherent pumping

Up to this point the dynamics of the system have been described by the master equation IV.27:

$$\begin{aligned}\frac{d\hat{\rho}(t)}{dt} =& -i[\hat{H}_{tot} + \hat{V}_p(t), \hat{\rho}] \\ &+ \gamma_c L[\hat{a}]\hat{\rho} + \gamma_a L[\hat{\sigma}_-]\hat{\rho} \\ &+ n_{th}\gamma_m L[\hat{b}^\dagger]\hat{\rho} + (n_{th}+1)\gamma_m L[\hat{b}]\hat{\rho}.\end{aligned} \tag{IV.36}$$

The terms in the second line of this master equation rule the dissipative processes undergone by the cavity and the two-level artificial atom. These dissipative processes are characterized by two loss rates (γ_c and γ_a) measuring the rate at which photonic and atomic excitations are lost to the environment and two jump operators ($\hat{a}$ and $\hat{\sigma}_-$) determining how this information is lost. A photon can be annihilated from the cavity and/or the atom can be deexcited from its excited to its ground state.

The incoherent pumping under consideration corresponds to a similar process but performed in the opposite direction. The environment randomly excites the 1-polariton states from the ground state $|G\rangle$. This excitation is described by a similar Master Equation which now contains jump operators increasing the number of photonic and/or atomic excitations. From an experimental point of view, this incoherent pumping can be achieved by coherently pumping higher energy levels in the Jaynes-cummings ladder ($n \geq 2$) and waiting for the decoherence to kick-in and incoherently take the polariton excitations to the desired $n = 1$ subspace. We would like to add that incoherent pumping is an important method in experimental quantum optics toolboxes. As an example, first proofs of strong light-matter coupling between a quantum dot and a semiconductor microcavity were first achieved with this configuration [107].

For the sake of simplicity we still continue restricting ourselves to the problem projected to the subspace containing 1 polariton. We assume that the atom and the cavity are resonant ($\omega_c = \omega_a$) and that the photonic and atomic loss rates are identical ($\gamma_a = \gamma_c = \gamma_{ac}$). Since the Jaynes-Cummings part of the problem is symmetrical with respect to photon and atomic excitations, it will be clearer to discuss the photonic and atomic properties of the system using the basis of states $\{|G\rangle,\ |-^{(1)}\rangle,\ |+^{(1)}\rangle\}$. From now on the considered master equation for the system is:

$$\begin{aligned}\frac{d\hat{\rho}(t)}{dt} =& -i[\hat{H}_{tot}+,\hat{\rho}] \\ &+ \gamma_{ac}L[\hat{c}_-]\hat{\rho} + \gamma_{ac}L[\hat{c}_+]\hat{\rho} \\ &+ \gamma^-_{inc}L[\hat{c}^\dagger_-]\hat{\rho} + \gamma^+_{inc}L[\hat{c}^\dagger_+]\hat{\rho} \\ &+ n_{th}\gamma_m L[\hat{b}^\dagger]\hat{\rho} + (n_{th}+1)\gamma_m L[\hat{b}]\hat{\rho},\end{aligned} \tag{IV.37}$$

where $\hat{c}_- = |G\rangle\langle -^{(1)}|$ and $\hat{c}_+ = |G\rangle\langle +^{(1)}|$ are the jump operators describing the de-excitation of the lower and upper polariton respectively to the ground state. The state $|\pm^{(1)}\rangle$ is incoherently pumped with a rate $\gamma^\pm_{inc}$ from the ground state, this process being described by the corresponding jump operator $\hat{c}^\dagger_\pm$. In this new configuration we omit the coherent photon pump. Here $\hat{H}_{tot}$ is the effective Hamiltonian for the projected system for which we have neglected the anti-resonant terms in the effective polariton-mechanics coupling.

IV.6.2. "One-atom laser approach"

In order to follow the dynamics of the system we study the correlations between the mechanical resonator and the three-level polariton system. Let us introduce a series of operators measuring such correlations:

$$\begin{aligned}\forall m \in \mathbb{N}: \quad & N_b[m] = \langle \hat{b}^{\dagger m} \hat{b}^m \rangle, \\ & N_+[m] = \langle \hat{b}^{\dagger m-1} \hat{b}^{m-1} \hat{\sigma}_+^{(1)} \hat{\sigma}_-^{(1)} \rangle, \\ & N_-[m] = \langle \hat{b}^{\dagger m-1} \hat{b}^{m-1} \hat{\sigma}_-^{(1)} \hat{\sigma}_+^{(1)} \rangle, \\ & N_G[k] = \langle \hat{b}^{\dagger m-1} \hat{b}^{m-1} |G\rangle\langle G| \rangle, \\ & N_{b\sigma}[m] = \langle \hat{b}^{\dagger m} \hat{b}^{m-1} \hat{\sigma}_-^{(1)} \rangle, \\ & N_{b^\dagger \sigma_+}[m] = \langle \hat{b}^{\dagger m-1} \hat{b}^m \hat{\sigma}_+^{(1)} \rangle.\end{aligned} \tag{IV.38}$$

The master equation IV.37 rules the evolution of the previously discussed correlators. We do not present here the complete derivation of the equations but rather present a simplified version by assuming that the environment is at zero temperature, $n_{th} = 0$, and that the incoherent pumping rates for both polariton states are identical, $\gamma_{inc}^+ = \gamma_{inc}^- = \gamma_{inc}$. With these hypotheses the master equation now reads

$$\begin{aligned}\frac{d\hat{\rho}(t)}{dt} = & -i[\hat{H}_{tot}+, \hat{\rho}] + \gamma_{ac}(L[\hat{c}_-]\hat{\rho} + L[\hat{c}_+]\hat{\rho}) \\ & + \gamma_{inc}(L[\hat{c}_-^\dagger]\hat{\rho} + L[\hat{c}_+^\dagger]\hat{\rho}) + \gamma_m L[\hat{b}]\hat{\rho}.\end{aligned} \tag{IV.39}$$

By tracing out the mechanical resonator degrees of freedom we obtain a reduced density matrix on the polariton sub-system. This reduced density matrix being unitary we have:

$$\left\langle |G\rangle\langle G| + |-^{(1)}\rangle\langle -^{(1)}| + |+^{(1)}\rangle\langle +^{(1)}| \right\rangle = 1. \tag{IV.40}$$

From Eq.IV.40 it follows that $N_+[m] + N_-[m] + N_G[m] = N_b[m-1]$. This allows us to reduce the number of equations at play. We also introduce the following notation:

$$\begin{aligned}N_{b\sigma}[m] &= N_{b\sigma}^r[m] + iN_{b\sigma}^i[m] \\ N_{b^\dagger\sigma_+}[m] &= N_{b\sigma}^r[m] - iN_{b\sigma}^i[m]\end{aligned} \tag{IV.41}$$

With this notations the set of first order differential equations for the mean values of the system correlators is:

$$\begin{aligned}
\forall m \in \mathbb{N}: \quad \dot{N}_b[m] &= -2mg_{cm}N^i_{b\sigma}[m] - m\gamma_m N_b[m] \\
\dot{N}_+[m] &= 2g_{cm}N^i_{b\sigma}[m] + \gamma_{inc}N_G[m] - \gamma_{ac}N_+[m] - (m-1)\gamma_m N_+[m] \\
\dot{N}_G[m] &= \gamma_{ac}\left(N_+[m] + N_-[m]\right) - \left(2\gamma_{inc} + (m-1)\gamma_m\right)N_G[m] \\
\dot{N}^r_{b\sigma}[m] &= -(\omega_m - \Omega^{(1)})N^i_{b\sigma}[m] - \left(\gamma_{ac} + (m-1/2)\gamma_m\right)N^r_{b\sigma}[m] \\
\dot{N}^i_{b\sigma}[m] &= (\omega_m - \Omega^{(1)})N^r_{b\sigma}[m] - (\gamma_{ac} + (m-1/2)\gamma_m)N^i_{b\sigma}[m] \\
&\quad -g_{cm}\left(2N_+[m+1] + mN_+[m] + N_G[m+1] - N_b[m]\right).
\end{aligned} \tag{IV.42}$$

We are only interested in the stationary state properties of the system. We thus set the time derivatives in the set of equations IV.42 to zero. It is then possible to write all the correlators in terms of the phonon correlators $N_b[m]$ as follows:

$$\begin{aligned}
N_G[m] =& \frac{\gamma_{ac}}{\gamma_{ac} + 2\gamma_{inc} + (m-1)\gamma_m}N_b[m-1] \\
N^r_{b\sigma}[m] =& \frac{(\omega_m - \Omega^{(1)})\gamma_m}{g\Gamma_T[m]}N_b[m] \\
N^i_{b\sigma}[m] =& -\frac{\gamma_m}{2g_{cm}}N_b[m] \\
N_+[m] =& \frac{\gamma_{ac}\gamma_{inc}}{(\gamma_{ac} + 2\gamma_{inc} + (m-1)\gamma_m)(\gamma_{ac} + (m-1)\gamma_m)}N_b[m-1] \\
& - \frac{\gamma_m}{\gamma_{ac} + (m-1)\gamma_m}N_b[m],
\end{aligned} \tag{IV.43}$$

where we have introduced the total decoherence on states of the subspace with m polarons

$$\Gamma_T[m] = 2\gamma_{ac} + (2m-1)\gamma_m. \tag{IV.44}$$

The stationary statistics are fully determined by the set of equations IV.43 and the following second order recurrence relation on $\{N_b[m]\}_{m\in\mathbb{N}}$

$$A(m)N_b[m-1] + B(m)N_b[m] + C(m)N_b[m+1] = 0. \tag{IV.45}$$

The coefficients of the recurrence relation are given by:

$$\begin{aligned}
A(m) =& -m\frac{\gamma_{ac}\gamma_{inc}}{(\gamma_{ac} + 2\gamma_{inc} + (m-1)\gamma_m)(\gamma_{ac} + (m-1)\gamma_m} \\
B(m) =& m\frac{\gamma_m}{\gamma_{ac} + (m-1)\gamma_m} + m\frac{\gamma_m}{\gamma_{ac} + m\gamma_m} + C_{eff}[m]^{-1} \\
C(m) =& \frac{2\gamma_m}{\gamma_{ac} + m\gamma_m},
\end{aligned} \tag{IV.46}$$

where we introduced the effective coupling and cooperativity

$$\begin{aligned} g_{eff}[m] =& \frac{g_{cm}}{\sqrt{1+\left(\frac{2(\omega_m-\Omega^{(1)})}{\Gamma_T[m]}\right)^2}} \\ C_{eff}[m] =& \frac{4g_{eff}^2[m]}{\gamma_m\Gamma_T[m]}. \end{aligned} \tag{IV.47}$$

By definition $N_b[0] = 1$ and $N_b[1] = n_b$ is the number of phonons in the stationary state. The previous equations tell us that if one is able to obtain the stationary number of phonons it is possible to calculate all the correlators of the system to any order. As an example the stationary populations of the ground state $|G\rangle$ and of the upper polariton $|+^{(1)}\rangle$ are given by:

$$\begin{aligned} P_g =& \langle|G\rangle\langle G|\rangle = \frac{\gamma_{ac}}{\gamma_{ac}+2\gamma_{inc}} \\ P_+ =& \langle|+^{(1)}\rangle\langle+^{(1)}|\rangle = \frac{\gamma_{inc}}{\gamma_{ac}+2\gamma_{inc}} - \frac{\gamma_m}{\gamma_{ac}}n_b, \end{aligned} \tag{IV.48}$$

and the mechanical resonator second order auto-correlation function is given by :

$$G_2 = \frac{\langle\hat{b}^{\dagger 2}\hat{b}^2\rangle}{\langle\hat{b}^\dagger\hat{b}\rangle^2} = \frac{1}{n_b^2}\frac{\gamma_{ac}+\gamma_m}{2\gamma_m}\left[\frac{\gamma_{inc}}{\gamma_{ac}+2\gamma_{inc}} - \left(\frac{\gamma_m}{\gamma_{ac}} + \frac{\gamma_m}{\gamma_p+\gamma_m} + C_{eff}[1]^{-1}\right)n_b\right]. \tag{IV.49}$$

IV.6.3. Emission of strongly anti-bunched phonons

As shown in Fig.IV.16 the incoherent pump populates the excited polaritonic states that, in the eigenbasis of the Hamiltonian, leads to excitation of polarons and then emission of phonons. By looking at the statistics of the emitted phonons we have seen that for weak enough values of γ_{ac} (the broadening of the polaritonic levels) the system exhibits emission of phonons with sub-poissonian, antibunched statistics (second-order correlation function $G_2 \ll 1$). In this regime, the system acts as a single-phonon emitter under incoherent pumping. Hence, phonon blockade type effects arise from the non-linearity introduced into our hybrid system by the artificial two-level atom.

In Fig.IV.16 we also present the analitycal results from the previously discussed treatment. The stationary number of phonons is obtained from the numerical resolution of the master equation. It is then injected into equation IV.49 and compared to the numerical value. The analytical results (circles) and numerical solutions of the master equation (continuous lines) are in excellent agreement.

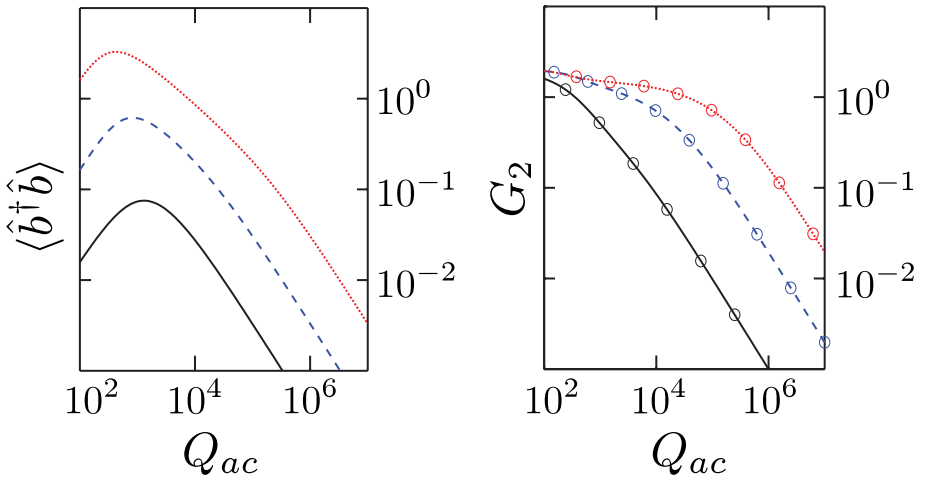

FIGURE IV.16: Phonon occupation number and second-order auto correlation function G_2 as a function of the polariton quality factor Q_{ac}. The incoherent pump rate is set to $\gamma_{inc} = \gamma_{ac}$. Black-solid, blue-dashed and red-dotted lines correspond to numerical results obtained for mechanical quality factors $Q_m = 10^3,\ 10^2$ and 10^1 respectively. The corresponding analytical values for G_2 are represented by circles and are in excellent agreement with the fully numerical calculations.

The formalism introduced in this part of the manuscript allows us to compute the stationary correlations of the system at all orders. Here we have only included the calculations for a zero temperature environment and for an incoherent pump populating at the same rate both polaritonic states. The generalization to finite temperature and differential pumping can be found in Appendix D.

The set of correlators introduced in Eq.IV.38 respects the symmetries of the Hamiltonian considered in this part. We remind that we have neglected the counter-rotating terms in the effective polariton-mechanics coupling and thus the number of polarons (represented by the operator $\hat{N}^{(1)}_{polaron} = \hat{b}^\dagger \hat{b} + \sigma^{(1)}_+ \sigma^{(1)}_-$) is a constant of motion. Generalizing the method should allow us to study the effects of this counter-rotating terms as well as to analytically study the statistics in a scenario with a coherent pump. Finally, during this thesis we only considered the final phonon statistics but understanding the signatures of these effects on the photon statistics constitutes an important step for the experimental observation of these non-classical states of mechanical motion.

Conclusion and perspectives

In this thesis, we have presented theoretical results for quantum optomechanical systems with non-conventional nonlinear coupling schemes. In chapter I we introduced the field of optomechanics and we set the theoretical framework of our work. In chapter II we described the numerical methods used during this research project. Chapters III and IV presented the original results of this thesis.

In Chapter III, we described our quantum theory of photothermal cavity cooling. While in usual radiation-pressure optomechanics the main time scale at play in the cooling mechanism is the photons lifetime $1/\gamma_c$, in photothermal based systems this role is played by the thermal relaxation time τ_{th}. The possibility to have $\tau_{th}\gamma_c \gg 1$ and since photothermal forces can overcome radiation pressure by several orders of magnitude it is possible to cool mechanical motion close to the ground state even in the so-called "bad cavity" regime. Photothermal optomechanics could be relevant for integrated solid-state optomechanical systems such as those based on semiconductor microstructures.

In Chapter 4, we presented a theory for a cavity quantum optomechanical system coupled to a single quantum emitter (two-level system artificial atom). We showed that this tripartite configuration (cavity field, atom, mechanical oscillator) provides a way to explore single-photon optomechanics thanks to the large nonlinearity provided by the two-level system. We investigated in detail single-polariton resonant cooling and amplification of mechanical motion as well as the peculiar quantum phonon statistics obtainable in this regime. This kind of system could be obtained by using quantum dots in semiconductor microresonators or by using circuit QED architectures with superconducting resonators and Josephson junctions.

Appendix A

Kraus sum representation of the master equation

When describing a system A coupled to some environment E one should in principle work with the density matrix $\hat{\rho}_{A+E}$ of the total system. Nevertheless we are only interested in the system density matrix $\hat{\rho}_A$ which is obtained by tracing out the environment degrees of freedom by means of a partial trace $\hat{\rho}_A = Tr_E[\hat{\rho}_{A+E}]$. In the case of weak coupling to a memory-less environment (a Markovian environment) the evolution of the reduced density matrix of the system is ruled by a Master Equation which is a first order differential equation on $\hat{\rho}_A$. Such an equation can be obtained from the microscopic description of the coupling to the environment, the derivation is carried through for the mechanical resonator in Appendix B. Here we present a different derivation relying on very general considerations on the algebraic structure and physical meaning of the variables under consideration. We only give the main lines of an insightful derivation for which a more thorough discussion can be found in [69].

When considering the evolution of a density matrix we are basically wondering how the density matrix at any given time t, $\hat{\rho}_A(t)$, is mapped at a later time $t + \tau > t$ into a different density matrix $\hat{\rho}_A(t + \tau)$. We thus have to consider a quantum process transforming a density matrix into another. We will note $\hat{\rho}_A$ the initial density matrix and $L_A(\hat{\rho}_A)$ the transformed density operator. L_A is called a quantum map described as a linear super-operator acting in the Hilbert space of operators. In order to preserve the necessary physical (and algebraic) properties of the density matrix the quantum map L_A has to be a linear operation preserving

the hermiticity, the trace and the positivity of $\hat{\rho}_A$,

$$\begin{aligned} L_A(p\hat{\rho}_A + q\hat{\rho}'_A) &= pL_A(\hat{\rho}_A) + qL_A(\hat{\rho}'_A), \text{ where } p+q=1 \\ (L_A(\hat{\rho}_A))^\dagger &= L_A(\hat{\rho}_A) \\ Tr\left[L_A(\hat{\rho}_A)\right] &= 1 \\ \langle\psi|L_A(\hat{\rho}_A)|\psi\rangle &\geq 0, \ \forall|\psi\rangle. \end{aligned} \tag{A.1}$$

Additionally the quantum map has to be completely positive, which is to say that it has to be an acceptable physical process even if the system A were to be entangled to some system B.

It can be shown [69] that if the system A is not initially entangled with any other system (and this is a crucial hypothesis) then any quantum map can be cast in the following Kraus sum form

$$L_A(\hat{\rho}_A) = \sum_\mu \hat{M}_\mu \hat{\rho}_A \hat{M}_\mu^\dagger, \tag{A.2}$$

where the Kraus sum in Eq.A.2 has at most $N_K \leq N_A^2$ terms, N_A being the dimension of system A Hilbert space. In order to ensure the preservation of the density matrix trace the set of Kraus operators $\{\hat{M}_\mu\}_\mu$ has to obey the normalization condition

$$\sum_\mu \hat{M}_\mu^\dagger \hat{M}_\mu = \mathbb{1}. \tag{A.3}$$

We now use the Kraus sum representation in order to describe the dynamics of system A when coupled to an environment E. Our aim is to derive a first order differential equation with constant coefficients on $\hat{\rho}_A(t)$. To do so let us assume that the time interval τ is small enough for $\hat{\rho}_A(t+\tau) - \hat{\rho}_A(t)$ to be a first-order quantity in τ, which can be identified with $\tau d\hat{\rho}_A/dt$. These identification holds if τ is small compared to the characteristic evolution time T_r of $\hat{\rho}_A$. In usual analysis the identification becomes an equality by taking the limit $\tau \mapsto 0$ but we will see that physically the equation of motion of our system coupled to an environment can not be taken to this limit. The time slicing has to be coarse-grained, small enough to allow a quasi-continuous following of the system evolution and long enough to allow us to neglect the correlations building up between the system and the environment.

We want to use the Kraus sum representation previously discussed in order to describe the increment $\hat{\rho}_A(t+\tau) - \hat{\rho}_A(t)$. To do so we assume that at time t the environment is in a steady state described by the density operator $\bar{\rho}_E$ and that

the total density operator is given by

$$\hat{\rho}_{A+E}(t) = \hat{\rho}_A(t) \otimes \bar{\rho}_E. \tag{A.4}$$

Since there is no entanglement between the system and the environment we can apply the previous results and we thus can write

$$\hat{\rho}_A(t+\tau) = L_\tau \left[\hat{\rho}_A(t)\right] = \sum_{\mu=0}^{N_k-1} \hat{M}_\mu(\tau)\hat{\rho}_A(t)\hat{M}_\mu^\dagger(\tau). \tag{A.5}$$

Eq.A.5 holds as long as Eq.A.4 describes correctly the initial state of the total system. But to be precise this initial state should actually be written under the form

$$\hat{\rho}_{A+E}(t) = \hat{\rho}_A(t) \otimes (\bar{\rho}_E + \delta\hat{\rho}_E(t)) + \delta\hat{\rho}_{A+E}(t), \tag{A.6}$$

where we have included the fluctuations of the environment around its steady state, $\delta\hat{\rho}_E(t)$, and the entanglement between A and E, $\delta\hat{\rho}_{A+E}(t)$. These two additional terms rise from the past interactions between the two parts of the total system. Keeping these terms could forbid the use of the Kraus sum representation (since A would be initially entangled with E), and even if it could be applied the operators $\hat{M}_\mu(\tau)$ would have to be functions of t in order to take into account the history of the interaction between environment and system. Nevertheless if the environment is large enough one can make a Markov approximation in which the environment is memory-less, in this case the incremental evolution of $\hat{\rho}_A$ over a time interval τ takes place as if $A+E$ was initially described by Eq.A.4. The "big enough" environment has energy levels spanning over a wide range of energies $\hbar\Delta\omega$, the typical correlation time of the environment observables τ_c is loosely given by $\tau_c \sim \hbar/\Delta\omega$. The environment fluctuation and the entanglement between A and E quickly wash away for times longer than τ_c. For $\tau \gg \tau_c$ the environment will thus be Markovian and we can safely neglect the correlations between A and E.

The system, coupled to an amnesiac environment, undergoes random walks that have a duration $\sim \tau_c$. Each step induces a phase change of the order $V\tau_c/\hbar$, where V is the order of magnitude of the coupling between A and E. After a time t the system accumulates a phase dispersion $\Delta\phi(t)$ that is related to T_r by

$$\Delta\phi(t)^2 = \frac{V^2{\tau_c^2}^2}{\hbar}\frac{t}{\tau_c} = \frac{t}{T_r}. \tag{A.7}$$

The Markov condition of a very short environment memory time, $\tau_c \ll T_r$, is thus satisfied when $V\tau_c \ll \hbar$. The Markov approximation and the quasi-continuous

following of the evolution of A will be ensured as long as

$$\tau_c \ll \tau \ll T_r. \tag{A.8}$$

Then it is safe to assume the increment given by Eq.A.4 and we are able to obtain the Master Equation from Eq.A.5.

By definition $L_\tau[\hat{\rho}_A(t)] = \hat{\rho}_A(t+\tau) = \hat{\rho}_A(t) + O(\tau)$, among the Kraus operators there is at least one of order unity (in order to obtain the equality when $\tau = 0$) which we assume to be $\hat{M}_0$. Without loss of generality we write it as

$$\hat{M}_0 = \mathbb{1} - i\hat{K}\tau + O(\tau^2). \tag{A.9}$$

Let us introduce the hermitian and anti-hermitian parts of the τ-independent operator $\hat{K}$.

$$\hat{H} = \hbar\frac{\hat{K} + \hat{K}^\dagger}{2} \quad \text{and } \hat{J} = i\frac{\hat{K} - \hat{K}^\dagger}{2}. \tag{A.10}$$

All the other terms of interest in the Kraus sum are of order 1 in τ, we can thus write $\forall \mu \neq 0,\ \hat{M}_\mu = \sqrt{\tau}\hat{L}_\mu$. From the trace preservation condition we can see that

$$\sum_{\mu=0}^{N_K-1} \hat{M}_\mu^\dagger \hat{M}_\mu = \mathbb{1} - 2\hat{J}\tau + \sum_{\mu\neq 0} \tau \hat{L}_\mu^\dagger \hat{L}_\mu = \mathbb{1}, \tag{A.11}$$

which in the end leads to

$$\hat{J} = \frac{1}{2}\sum_{\mu\neq 0} \hat{L}_\mu^\dagger \hat{L}_\mu. \tag{A.12}$$

Finally we get to the master equation for $\hat{\rho}_A(t)$ in the generic Lindblad form

$$\frac{d\hat{\rho}_A}{dt} = -\frac{i}{\hbar}\left[\hat{H}, \hat{\rho}_A\right] + \sum_{\mu\neq 0}\left(\hat{L}_\mu \hat{\rho}_A \hat{L}_\mu^\dagger - \frac{1}{2}\hat{L}_\mu^\dagger \hat{L}_\mu \hat{\rho}_A - \frac{1}{2}\hat{\rho}_A \hat{L}_\mu^\dagger \hat{L}_\mu\right). \tag{A.13}$$

In Eq.A.13 $\hat{H}$ contains two contributions. On the hand the actual Hamiltonian $\hat{H}_A$ of system A, on the other an energy shift induced by the coupling to the environment.

The Kraus sum representation can be interpreted by introducing an environment simulator B which replaces the environment E. In this effective picture the quantum map undergone by $\hat{\rho}_A$ results from entanglement building between A and B and a following unread measurement performed by B. The unread measurement

procedure is then responsible for the statistical mixture ($\hat{\rho}_A$ is then a probability-weighted sum of all the states related to the possible outcomes of B's measurement), it erases the entanglement. The relaxation process undergone by the system can thus be interpreted as an irreversible leakage of information to the environment. The Markovian environment does not keep any track of the information received from A. In this effective picture an operator $\hat{L}_\mu$ can be understood as a jump operator defining the projection undergone by A after a measurement by B with a given result.

The presentation given here of the master equation does not explicitly yield the precise form of the master equation. Nevertheless it is possible to infer the quantum jump operators that affect the system, and an experiment can precise the time constants associated to each quantum jump. In our case of interest we assume that the optomechanical cavity is subject to two noisy channels. First, a photon can leave the cavity and be lost to the electromagnetic vacuum beyond the mirrors. Such channel is described by the jump operator $\hat{a}$ which destroys a photon in the cavity. Second, the mechanical resonator is coupled to a thermal environment at finite temperature T which is able to either excite or absorb one mechanical excitation, this two processes are ruled by the quantum jump operators $\hat{b}^\dagger$ and $\hat{b}$ respectively. The master equation ruling our system is then

$$\frac{d\hat{\rho}}{dt} = -\frac{i}{\hbar}\left[\hat{H}, \hat{\rho}\right] + \gamma_c D[\hat{a}]\hat{\rho} + \gamma_m(n_{th}+1)D[\hat{b}]\hat{\rho} + \gamma_m n_{th} D[\hat{b}^\dagger]\hat{\rho}, \tag{A.14}$$

where $\hat{H}$ is the optomechanics Hamiltonian defined in Eq.I.20, $D[\hat{o}]\hat{\rho} = \hat{o}\hat{\rho}\hat{o}^\dagger - 1/2(\hat{o}^\dagger\hat{o}\hat{\rho} + \hat{\rho}\hat{o}^\dagger\hat{o})$ is the lindbladian super operator with an associated quantum jump operator $\hat{o}$ and n_{th} is the mean thermal occupancy of the mechanical resonator when at equilibrium at temperature T,

$$n_{th} = \frac{1}{e^{\frac{\hbar\omega_m}{k_b T}} - 1}. \tag{A.15}$$

Appendix B

Master equation derivation from a microscopic Hamiltonian

In this appendix we derive the Lindblad master equation from a microscopic Hamiltonian coupling a mechanical resonator to a thermal reservoir at temperature T.

Total system Hamiltonian:

Let us consider a closed system comprising the mechanical resonator and the thermal reservoir. Let us assume the following form for the total Hamiltonian:

$$\hat{H} = \hat{H}_S + \hat{H}_R + \hat{V}_{B_R}, \tag{B.1}$$

where $\hat{H}_S$ is the mechanical resonator Hamiltonian, $\hat{H}_R$ is the reservoir Hamiltonian and $\hat{V}_{B_R}$ is the coupling term between the two of them.

$\hat{H}_S$ is given by:

$$\hat{H}_S = \hbar\omega_m(\hat{b}^\dagger\hat{b} + 1/2), \tag{B.2}$$

where $\hat{b}$ an $\hat{b}^\dagger$ are the usual annihilation and creation operators. We assume that the coupling between the system and the reservoir is of the form:

$$\hat{V}_{B_R} = i\hbar \int dk \left(\kappa_k \hat{\beta}_k \hat{b}^\dagger - \kappa_k^* \hat{\beta}_k^\dagger \hat{b}\right), \tag{B.3}$$

where we have assumed that the mechanical resonator is coupled to the different modes, labeled by the index k, of the reservoir. $\hat{\beta}_k$ and $\hat{\beta}_k^\dagger$ are the annihilation and creation operators of the k-th mode of the reservoir. The form of the Hamiltonian

in Eq.B.3 was discussed in chapter I. Briefly, it can be obtained by assuming that the system position is linearly coupled to the positions of an infinite amount of harmonic oscillators and then neglecting the resulting counter rotating terms.

The reservoir Hamiltonian is on the other hand given by:

$$\hat{H}_R = \int dk \hbar \omega_k \hat{\beta}_k^\dagger \hat{\beta}_k. \tag{B.4}$$

Before moving forward let us introduce the following notation:

$$\hat{H} = \hat{H}_0 + \hat{V}_{SR} = (\hat{H}_S + \hat{H}_R) + (\hat{V}_{B_R}). \tag{B.5}$$

Time evolution of the master equation in the interaction picture:

Let $\hat{\rho}_{S,R}$ be the total system density matrix. Its time evolution is given by the Schrödinger equation:

$$i\hbar \frac{d}{dt}\hat{\rho}_{S,R} = \left[\hat{H}, \hat{\rho}_{S,R}\right] \tag{B.6}$$

In the interaction picture with respect to $\hat{H}_0$ we have:

$$\frac{d}{dt}\tilde{\rho}_{S,R}(t) = \frac{1}{i\hbar}\left[\tilde{V}_{SR}(t), \tilde{\rho}_{S,R}(t)\right] \tag{B.7}$$

$$\tilde{\rho}_{S,R}(t) = e^{i\hat{H}_0 t/\hbar}\hat{\rho}_{S,R}e^{-i\hat{H}_0 t/\hbar} \tag{B.8}$$

$$\tilde{V}_{SR}(t) = e^{i\hat{H}_0 t/\hbar}\hat{V}_{SR}e^{-i\hat{H}_0 t/\hbar} \tag{B.9}$$

By formally integrating Eq.B.7 twice we obtain the following expression for the increment $\Delta\tilde{\rho}_{S,R}(t)$ of the total density matrix between times t and $t + \Delta t$:

$$\Delta\tilde{\rho}_{S,R} = \frac{1}{i\hbar}\int_t^{t+\Delta t} dt_1 \left[\tilde{V}_{SR}(t_1), \tilde{\rho}_{S,R}(t_1)\right] + \left(\frac{1}{i\hbar^2}\right)\int_t^{t+\Delta t} dt_1 \int_t^{t_1} dt_2 \left[\tilde{V}_{SR}(t_1), \left[\tilde{V}_{SR}(t_2), \tilde{\rho}_{S,R}(t_2)\right]\right] \tag{B.10}$$

This far Eq.B.10 is exact. By iterating the formal integration it is possible to obtain higher order terms on $\hat{V}_{SR}$. Nevertheless we assume weak coupling to the reservoir and we thus limit ourselves to second order. The first order term leads to a Lamb-shift renormalization of the system energy, it will be neglected in the following.

Main approximations:

First of all let us assume that the time interval Δt verifies:

$$\tau_{R_b} \ll \Delta t \ll T_S, \tag{B.11}$$

where τ_{R_b} is the typical time scale of the reservoir's thermalization. T_S is the typical time scale of the interaction between the system and the reservoir. The approximation in Eq.B.11 implies a coarse-grained slicing of time, small enough to continuously follow the time evolution of the system dynamics and big enough for the reservoir to "forget" any correlations that could have built between the two parts.

In the following we also assume that the reservoir is sufficiently large to allow us to neglect any initial correlation between the system and the reservoir. For any given time t we write:

$$\tilde{\rho}_{S,R}(t) = \tilde{\rho}_S(t) \otimes \tilde{\rho}_{R_b}(t), \tag{B.12}$$

where $\hat{\rho}_S(t)$ and $\hat{\rho}_{R_b}(t)$ are the system and reservoir density matrices respectively.

Finally, we assume that the reservoir is at thermal equilibrium at temperature T and thus its stationary density matrix is given by:

$$\tilde{\rho}_{R_b}(t) = \hat{\sigma}_R = \exp(-\hat{H}_R/kT) = c^{te}. \tag{B.13}$$

Having made these approximations the increment of the density matrix over a time interval Δt is rewritten:

$$\Delta\tilde{\rho}_{S,R} = \frac{1}{\hbar^2}\int_t^{t=\Delta t} dt_1 \int_t^{t_1} dt_2 \left[\tilde{V}_{SR}(t_1), \left[\tilde{\rho}_S(t_2)\otimes\sigma_R, \tilde{V}_{SR}(t_2)\right]\right] \tag{B.14}$$

General considerations on the coupling Hamiltonian

In the following we work with these notations:

$$\hat{V}_{SR} = \sum_{\gamma\in\{\beta,\beta^*\}} \hat{A}_\gamma \otimes \hat{X}_\gamma, \tag{B.15}$$

where we have introduced operators acting on the system $\{\hat{A}_\gamma\}_\gamma$ and operators acting on the reservoir $\{\hat{X}_\gamma\}_\gamma$:

$$\hat{A}_\beta = \hat{b} \quad , \quad \hat{A}_{\beta^*} = \hat{b}^\dagger \tag{B.16}$$

$$\hat{X}_\beta = -i\hbar \int dk\ \kappa_k^* \hat{\beta}_k \quad , \quad \hat{X}_{\beta^*} = i\hbar \int dk\ \kappa_k \hat{\beta}_k^\dagger = \hat{X}_\beta^\dagger. \tag{B.17}$$

Let $\{|s\rangle\}_s$ be an orthonormal basis of eigenvectors of the system Hamiltonian $\hat{H}_S$ ($\hat{H}_S = \sum_s \hbar\omega_s |s\rangle\langle s|$). We introduce the frequency dependent operators $\hat{A}_\gamma(\Omega)$ defined as follows:

$$\hat{A}_\gamma(\Omega) = \sum_{s,r} \delta(\omega_{s,r} - \Omega)\ |r\rangle\langle r|\hat{A}_\gamma|s\rangle\langle s|, \text{ where } \omega_{s,r} = \omega_s - \omega_r. \tag{B.18}$$

In the interaction picture with respect to $\hat{H}_0$ they are written:

$$\begin{aligned} \tilde{A}_\gamma(\Omega) &= \sum_{s,r} \delta(\omega_{s,r} - \Omega)\ e^{iH_0 t/\hbar}\ |r\rangle\langle r|\hat{A}_\gamma|s\rangle\langle s|e^{-iH_0 t/\hbar} \\ &= e^{-i\Omega t}\hat{A}_\gamma(\Omega). \end{aligned} \tag{B.19}$$

Noting that $\sum_\Omega \hat{A}_\gamma(\Omega) = \hat{A}_\gamma$ the coupling term becomes:

$$\tilde{V}_{SR}(t) = \sum_\Omega \sum_\gamma e^{-i\Omega t}\hat{A}_\gamma(\Omega) \otimes \tilde{X}_\gamma(t) = \sum_\Omega \sum_\gamma e^{i\Omega t}\hat{A}_\gamma^\dagger(\Omega) \otimes \tilde{X}_\gamma^\dagger(t) \tag{B.20}$$

Autocorrelation functions

We now expand the nested commutators in Eq.B.14 and we perform a partial trace over the reservoir degrees of freedom. We obtain:

$$\begin{aligned} \frac{\Delta\tilde{\rho}_S}{\Delta t} = \frac{1}{\hbar^2 \Delta t} \int_{t_1}^{t+\Delta t} dt_1 \int_t^{t_1} dt_2 Tr_R \Big\{ &\tilde{V}_{SR}(t_2)\,(\tilde{\rho}_S \otimes \sigma_R)\,\tilde{V}_{SR}(t_1) - (\tilde{\rho}_S \otimes \sigma_R)\,\tilde{V}_{SR}(t_2)\tilde{V}_{SR}(t_1) \\ &- \tilde{V}_{SR}(t_1)\tilde{V}_{SR}(t_2)\,(\tilde{\rho}_S \otimes \sigma_R) + \tilde{V}_{SR}(t_1)\tilde{V}_{SR}(t_2)\,(\tilde{\rho}_S \otimes \sigma_R) \Big\} \end{aligned} \tag{B.21}$$

Using Eq.B.20 this expression becomes:

$$\begin{aligned}\frac{\Delta\tilde{\rho}_S}{\Delta t} = \frac{1}{\hbar^2\Delta t}\int_{t_1}^{t+\Delta t} dt_1 \int_t^{t_1} dt_2 \sum_{\gamma,\gamma'}\sum_{\Omega,\Omega'} \\ Tr_R\{\, e^{-i\Omega t_2}\hat{A}_\gamma(\Omega)\otimes\tilde{X}_\gamma(t_2)\,(\tilde{\rho}_S(t_2)\otimes\sigma_R)\, e^{i\Omega' t_1}\hat{A}^\dagger_{\gamma'}(\Omega')\otimes\tilde{X}_{\gamma'}(t_1) \\ - e^{i\Omega t_1}\hat{A}^\dagger_{\gamma'}(\Omega')\otimes\tilde{X}^\dagger_{\gamma'}(t_1)e^{-i\Omega t_2}\hat{A}_\gamma(\Omega)\otimes\tilde{X}_\gamma(t_2)\,(\tilde{\rho}_S(t_2)\otimes\sigma_R) \\ +\mathbb{HC}\}\end{aligned} \tag{B.22}$$

We now introduce the stationary correlation functions for the reservoir operators:

$$\begin{aligned}G_{\gamma,\gamma'}(t_1,t_2) &= Tr_R\left\{\tilde{X}^\dagger_{\gamma'}(t_1)\tilde{X}_\gamma(t_2)\sigma_R\right\} \\ &= Tr_R\left\{\tilde{X}^\dagger_{\gamma'}(t_1-t_2)\tilde{X}_\gamma(0)\sigma_R\right\} = G_{\gamma,\gamma'}(t_1-t_2)\end{aligned} \tag{B.23}$$

Injecting Eq.B.23 into Eq. B.22 we get:

$$\begin{aligned}\frac{\Delta\tilde{\rho}_S}{\Delta t} = \frac{}{\hbar^2\Delta t}\int_t^{t+\Delta t} dt_1 \int_t^{t_1} dt_2 \sum_{\gamma,\gamma'}\sum_{\Omega,\Omega'} \\ \Big\{e^{i(\Omega'-\Omega)t_1}e^{i\Omega(t_1-t_2)}G_{\gamma,\gamma'}(t_1-t_2)\hat{A}_{\gamma'}(\Omega)\tilde{\rho}_S\hat{A}^\dagger_\gamma(\Omega') \\ -e^{i(\Omega'-\Omega)t_1}e^{i\Omega(t_1-t_2)}G_{\gamma,\gamma'}(t_1-t_2)\hat{A}^\dagger_\gamma(\Omega')\tilde{\rho}_S\hat{A}_{\gamma'}(\Omega)\Big\}\end{aligned} \tag{B.24}$$

Integration variable substitution and discussion on time scales

This far on the discussion we have always integrated over t_2 first then over t_1. This integration paths are represented in Fig.B.1. Now we integrate over the line l_τ of equation $l_\tau : t_2 = t_1 - \tau$ then we integrate over τ, as can be seen in Fig.B.2.

The double integral $\int_t^{t+\Delta t} dt_1 \int_t^{t_1} dt_2$ becomes an integral $\int_0^{\Delta t} d\tau \int_{t+\tau}^{t+\Delta t} dt_1$. We thus write:

$$\begin{aligned}\frac{\Delta\tilde{\rho}_S}{\Delta t} = \frac{1}{\hbar^2\Delta t}\int_0^{\Delta t} d\tau \int_{t+\tau}^{t+\Delta t} dt_1 \sum_{\gamma,\gamma'}\sum_{\Omega,\Omega'} e^{i(\Omega'-\Omega)t_1}e^{i\Omega\tau}G_{\gamma,\gamma'}(\tau)* \\ \Big[\hat{A}_{\gamma'}(\Omega)\tilde{\rho}_S(t_1)\hat{A}^\dagger_\gamma(\Omega') - \hat{A}^\dagger_\gamma(\Omega')\hat{A}_{\gamma'}(\Omega)\tilde{\rho}_S(t_1)\Big] \\ +\,\mathbb{HC}\end{aligned} \tag{B.25}$$

The dependence on τ of Eq.B.25 arises from a term of the form $e^{i\Omega\tau}G_{\gamma,\gamma'}(\tau)$. Since we have assumed $\Delta t \gg \tau_R$ we can send the upper limit of the integration over τ

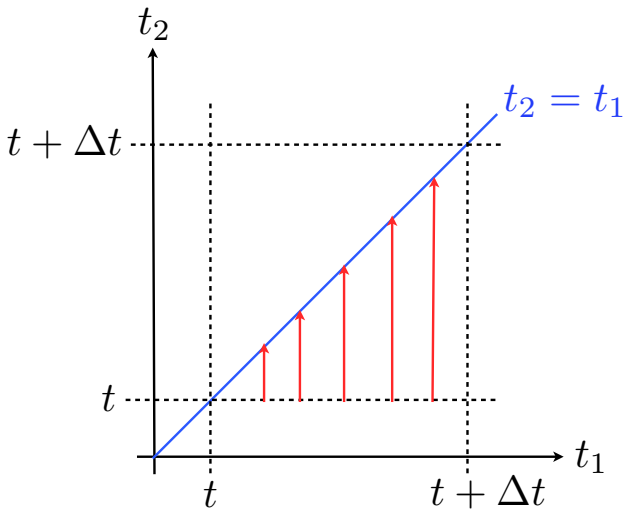

FIGURE B.1: Paths of the double integration over time.

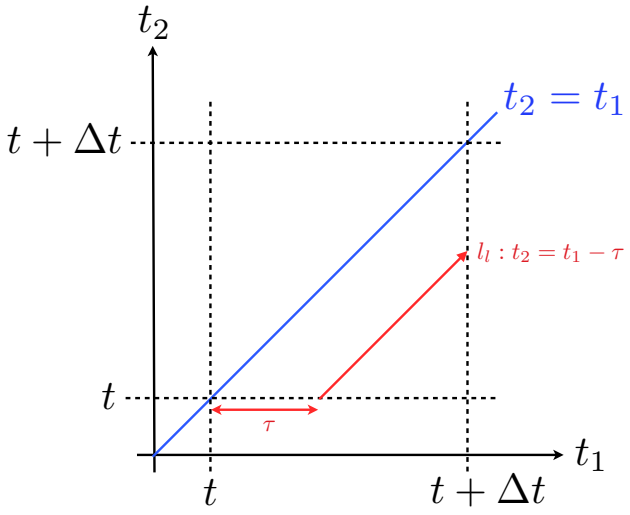

FIGURE B.2: Paths of the double integration after substitution of the time variables.

to infinity. The term under the integral decays rapidly for times bigger than τ. On the other hand, only small valleys of τ are of interest to us. We thus send the lower limit of the integral over t_1 to t (since $\Delta t \gg \tau_{R_a}, \tau_{R_b}$ it is as if we were setting $\tau \mapsto 0$). Finally, we assume that $\Delta t \ll T_S$ where T_S is the typical time scale of the information exchanges between the reservoir and the system. In the

integration over t_1 we thus set $\tilde{\rho}_S(t_1) = \tilde{\rho}_S(t)$, which ultimately leads to:

$$\begin{aligned}\frac{\Delta\tilde{\rho}_S}{\Delta t} = \frac{1}{\hbar^2\Delta t}\sum_{\gamma,\gamma'}\sum_{\Omega,\Omega'}\left[\int_0^\infty e^{i\Omega\tau}G_{\gamma,\gamma'}(\tau)\right]\left[\int_t^{t+\Delta t} dt_1 e^{i(\Omega'-\Omega)t_1}\right] \\ \left[\hat{A}_{\gamma'}(\Omega)\tilde{\rho}_S(t)\hat{A}^\dagger_\gamma(\Omega') - \hat{A}^\dagger_\gamma(\Omega')\hat{A}_{\gamma'}(\Omega)\tilde{\rho}_S(t)\right] \\ + h.c\end{aligned} \tag{B.26}$$

Lindblad master equation

Let us introduce:

$$W_{\gamma,\gamma'}(\Omega) = \int_0^\infty d\tau e^{i\Omega\tau}G_{\gamma,\gamma'}(\tau) \tag{B.27}$$

$$J(\Omega'-\Omega) = \int_t^{t+\Delta t} dt_1 e^{i(\Omega'-\Omega)t_1}\frac{1}{\Delta t} \tag{B.28}$$

Injecting these variables into Eq.B.26 we get:

$$\begin{aligned}\frac{\Delta\tilde{\rho}_S}{\Delta t} = \frac{1}{\hbar^2}\sum_{\gamma,\gamma'}\sum_{\Omega,\Omega'}J(\Omega'-\Omega)W_{\gamma,\gamma'}(\Omega)\left[\hat{A}_{\gamma'}(\Omega)\tilde{\rho}_S(t)\hat{A}^\dagger_\gamma(\Omega')\right. \\ \left.-\hat{A}^\dagger_\gamma(\Omega')\hat{A}_{\gamma'}(\Omega)\tilde{\rho}_s(t)\right] \\ + h.c\end{aligned} \tag{B.29}$$

Given that $\Delta t \ll T_S$ we replace the left hand side of the previous equality by an usual time derivative of the density matrix:

$$\begin{aligned}\frac{d\hat{\rho}_S}{dt} = -\frac{i}{\hbar}\left[\hat{H}_S,\hat{\rho}_S\right] + \frac{1}{\hbar^2}\sum_{\gamma,\gamma'}\sum_{\Omega,\Omega'}J(\Omega'-\Omega)W_{\gamma,\gamma'}(\Omega)e^{i(\Omega'-\Omega)t} \\ \left[\hat{A}_{\gamma'}(\Omega)\hat{\rho}_S(t)\hat{A}^\dagger_\gamma(\Omega') - \hat{A}^\dagger_\gamma(\Omega')\hat{A}_{\gamma'}(\Omega)\hat{\rho}_s(t)\right] \\ + \mathbb{HC}\end{aligned} \tag{B.30}$$

We have $J(x) \propto sin(\frac{x\Delta t}{2})/\frac{x\Delta t}{2}$. Since $\Delta t \mapsto 0$ we will replace every appearance of $J(\Omega'-\Omega)$ by a Kroenecker delta $\delta(\Omega'-\Omega)$. We also define $\Gamma_{\gamma,\gamma'}(\Omega) = W_{\gamma,\gamma'}(\Omega) + W^*_{\gamma',\gamma}(\Omega)$ and $\Delta_{\gamma,\gamma'}(\Omega) = \frac{1}{2i}(W_{\gamma,\gamma'}(\Omega) + W^*_{\gamma',\gamma}(\Omega))$. We obtain then the "standard"

form of the master equation:

$$\frac{d\hat{\rho}}{dt} = -\frac{i}{\hbar}\left[\hat{H}_S, \hat{\rho}_S(t)\right] - \frac{i}{\hbar^2}\sum_{\Omega}\sum_{\gamma,\gamma'}\Delta_{\gamma,\gamma'}(\Omega)\left[\hat{A}^\dagger_\gamma(\Omega)\hat{A}_{\gamma'}(\Omega), \hat{\rho}_S(t)\right] + \frac{1}{\hbar^2}\sum_{\Omega}\sum_{\gamma,\gamma'}\Gamma_{\gamma,\gamma'}(\Omega)\left\{\hat{A}_{\gamma'}(\Omega)\hat{\rho}_S(t)\hat{A}^\dagger_\gamma(\Omega) - \frac{1}{2}\left[\hat{A}^\dagger_\gamma(\Omega)\hat{A}_{\gamma'}(\Omega), \hat{\rho}_S(t)\right]_+\right\} \tag{B.31}$$

where $[.,.]_+$ corresponds to an operator anticommutator. The term $\propto \Delta_{\gamma,\gamma'}$ renormalizes the energies of the system and is absorbed into the definition of $\hat{H}_S$.

Let us note that $\Gamma_{\gamma,\gamma'}(\Omega)$ can be rewritten as:

$$\Gamma_{\gamma,\gamma'} = \int_{-\infty}^{\infty} d\tau e^{i\Omega\tau} G_{\gamma,\gamma'}(\tau). \tag{B.32}$$

With this final modifications we get to the Lindblad master equation for the density matrix:

$$\frac{d\hat{\rho}}{dt} = -\frac{i}{\hbar}\left[\hat{H}_S, \hat{\rho}_S(t)\right] + \frac{1}{\hbar^2}\sum_{\Omega}\sum_{\gamma,\gamma'}\Gamma_{\gamma,\gamma'}(\Omega)\left\{\hat{A}_{\gamma'}(\Omega)\hat{\rho}_S(t)\hat{A}^\dagger_\gamma(\Omega) - \frac{1}{2}\left[\hat{A}^\dagger_\gamma(\Omega)\hat{A}_{\gamma'}(\Omega), \hat{\rho}_S(t)\right]_+\right\} \tag{B.33}$$

In order to obtain the final density matrix of the system we only have to calculate the correlations by taking into account the coupling and the statistics of the reservoirs under consideration.

Dissipative constants

We have $\Gamma_{\gamma,\gamma'}(\Omega) = \int_{-\infty}^{\infty} d\tau\ e^{i\Omega\tau} G_{\gamma,\gamma'}(\tau)$, where

$$G_{\gamma,\gamma'}(\tau) = Tr_R\left\{\tilde{X}^\dagger_\gamma(\tau)\hat{X}_{\gamma'}\hat{\sigma}_R\right\}, \text{ and} \tag{B.34}$$

$$\tilde{X}^\dagger_\gamma(\tau) = e^{iH_0\tau/\hbar}\hat{X}^\dagger_\gamma e^{-iH_0\tau/\hbar}. \tag{B.35}$$

In the case under consideration the reservoir operators are given by:

$$\hat{X}_{\beta} = -i\hbar \int dk\ \kappa_k^* \hat{\beta}_q^\dagger \tag{B.36}$$

$$\hat{X}_{\beta^*} = i\hbar \int dk\ \kappa_k \hat{\beta}_k \tag{B.37}$$

$$\tag{B.38}$$

We assume the reservoir is at equilibrium at temperature T, we thus have:

$$\hat{\sigma}_R = e^{-\hat{H}_R/kT}. \tag{B.39}$$

Since $\hat{H}_R = \int dk\ \hbar\omega_k \hat{\beta}_k^\dagger \hat{\beta}_k$ the reservoir density matrix can be rewritten as a tensor product of the density matrices of each mode:

$$\hat{\sigma}_R = \bigotimes_k e^{-H_{R,k}/kT} = \bigotimes_q \hat{\sigma}_{R,k}, \text{ where} \tag{B.40}$$

$$\hat{\sigma}_{R,k} = \frac{1}{Z_k} e^{-\hbar\omega_k(\hat{\beta}_k^\dagger \hat{\beta}_k + 1/2)/k_b T}. \tag{B.41}$$

After calculation of the partition functions we get:

$$\hat{\sigma}_R = \bigotimes_k \left(1 - e^{-\hbar\omega_k/kT}\right) e^{-\hbar\omega_k \hat{\beta}_k^\dagger \hat{\beta}_k/k_b T} \tag{B.42}$$

We have to calculate correlation functions of the form:

$$G_{\gamma,\gamma'}(\tau) = Tr_R \left(\tilde{X}_\gamma^\dagger(\tau) \hat{X}_{\gamma'} \hat{\sigma}_R \right), \tag{B.43}$$

where the time dependent operators are given by:

$$\begin{aligned} \tilde{\beta}_k(\tau) &= e^{-i\omega_k \tau} \hat{\beta}_k \\ \tilde{\beta}_k^\dagger(\tau) &= e^{i\omega_k \tau} \hat{\beta}_k^\dagger. \end{aligned} \tag{B.44}$$

Since the reservoir is at equilibrium at temperature T the density matrices are diagonal in each associated Fock basis. The only non-zero terms are those coming from terms of the form $\hat{\beta}^\dagger \hat{\beta}$ or $\hat{\beta}\hat{\beta}^\dagger$. We just have to calculate $G_{\beta,\beta}$ and G_{β^*,β^*}.

They are given by:

$$\begin{aligned} G_{\beta,\beta}(\tau) &= Tr_R \left\{ \hbar^2 \int\int dk_1 dk_2 \ \kappa_{k_1}\kappa^*_{k_2} \hat{\beta}_{k_1}\hat{\beta}^\dagger_{k_2} e^{-i\omega_{k_1}\tau} \bigotimes_q \hat{\sigma}_{R,k} \right\} \\ &= \hbar^2 \int dk \ |\kappa_k|^2 e^{-i\omega_k\tau} Tr \left\{ \hat{\beta}_k \hat{\beta}^\dagger_k \hat{\sigma}_{R,k} \right\}, \end{aligned} \tag{B.45}$$

and

$$G_{\beta^*,\beta^*}(\tau) = \hbar^2 \int dk \ |\kappa_k|^2 e^{+i\omega_k\tau} Tr \left\{ \hat{\beta}^\dagger_k \hat{\beta}_k \hat{\sigma}_{R,k} \right\}. \tag{B.46}$$

After calculations this autocorrelations functions are given by:

$$\begin{aligned} G_{\beta,\beta}(\tau) &= \hbar^2 \int dk \ |\kappa_k|^2 \left(n_{th}(\omega_k)+1\right) e^{-i\omega_k\tau} \\ G_{\beta,\beta}(\tau) &= \hbar^2 \int dk \ |\kappa_k|^2 n_{th}(\omega_k) e^{+i\omega_k\tau}, \end{aligned} \tag{B.47}$$

where $n_{th}(\omega)$ is the number of excitations given by the Bose-Einstein distribution at frequency ω.

We now assume a white noise spectrum for the bath so as to have $\forall k,\ \kappa_k = \sqrt{\gamma_m}$. The coefficients in the dissipative terms of the master equation are then:

$$\begin{aligned} \Gamma_{\beta,\beta} &= \hbar^2 |\kappa_k|^2 \left(n_{th}(\omega_m)+1\right) \\ \Gamma_{\beta^*,\beta^*} &= \hbar^2 |\kappa_k|^2 n_{th}(\omega_m). \end{aligned} \tag{B.48}$$

Finally, the Lindblad master equation for a mechanical resonator weakly and linearly coupled to a reservoir at equilibrium at temperature T is:

$$\begin{aligned} \frac{d\hat{\rho}}{dt} = &-\frac{i}{\hbar}\omega_m \left[\hat{b}^\dagger\hat{b}, \hat{\rho}\right] + (n_{th}+1)\left(\gamma_m \hat{b}\hat{\rho}\hat{b}^\dagger - \frac{\gamma_m}{2}\left(\hat{b}^\dagger\hat{b}\hat{\rho} + \hat{\rho}\hat{b}^\dagger\hat{b}\right)\right) \\ &+ n_{th}\left(\gamma_m \hat{b}^\dagger\hat{\rho}\hat{b} - \frac{\gamma_m}{2}\left(\hat{b}\hat{b}^\dagger\hat{\rho} + \hat{\rho}\hat{b}\hat{b}^\dagger\right)\right). \end{aligned} \tag{B.49}$$

Appendix C

Partial derivative equation for the s-ordered quasi-probability distribution

In this appendix we give the correspondences between the different terms in the master equation of the system and the corresponding terms in the partial derivative equation on the s-ordered quasi-probability distribution.

We remind the following set of correspondences between the product of an arbitrary operator $\hat{o}$ and some system operator and the corresponding scalar representation:

$$\begin{array}{|rcl|rcl|}
\hline
\hat{a}\hat{o} & \longleftrightarrow & (\alpha - f^{-}\partial_{\alpha^*})\,O(\alpha,\beta;s,u) & \hat{b}\hat{o} & \longleftrightarrow & (\beta - g^{-}\partial_{\beta^*})\,O(\alpha,\beta;s,u) \\
\hat{a}^{\dagger}\hat{o} & \longleftrightarrow & (\alpha^* - f^{+}\partial_{\alpha})\,O(\alpha,\beta;s,u) & \hat{b}^{\dagger}\hat{o} & \longleftrightarrow & (\beta^* - g^{+}\partial_{\beta})\,O(\alpha,\beta;s,u) \\
\hline
\hat{o}\hat{a} & \longleftrightarrow & (\alpha - f^{+}\partial_{\alpha^*})\,O(\alpha,\beta;s,u) & \hat{o}\hat{b} & \longleftrightarrow & (\beta - g^{+}\partial_{\beta^*})\,O(\alpha,\beta;s,u) \\
\hat{o}\hat{a}^{\dagger} & \longleftrightarrow & (\alpha^* - f^{-}\partial_{\alpha})\,O(\alpha,\beta;s,u) & \hat{o}\hat{b}^{\dagger} & \longleftrightarrow & (\beta^* - g^{-}\partial_{\beta})\,O(\alpha,\beta;s,u) \\
\hline
\end{array} \tag{C.1}$$

And we remind the master equation considered during this thesis:

$$\begin{aligned}\frac{d\hat{\rho}}{dt} =& -i\left[\omega_c\hat{a}^\dagger\hat{a} + \omega_m\hat{b}^\dagger\hat{b} - g_{cm}\hat{a}^\dagger\hat{a} + iF_p(e^{-i\omega_p t}\hat{a} - e^{i\omega_p t}\hat{a}^\dagger), \hat{\rho}\right] \\ &+ \gamma_c\left(\hat{a}\hat{\rho}\hat{a}^\dagger - \frac{1}{2}(\hat{a}^\dagger\hat{a}\hat{\rho} + \hat{\rho}\hat{a}^\dagger\hat{a})\right) \\ &+ \gamma_m(n_{th}+1)\left(\hat{b}\hat{\rho}\hat{b}^\dagger - \frac{1}{2}(\hat{b}^\dagger\hat{b}\hat{\rho} + \hat{\rho}\hat{b}^\dagger\hat{b})\right) \\ &+ \gamma_m n_{th}\left(\hat{b}^\dagger\hat{\rho}\hat{b} - \frac{1}{2}(\hat{b}\hat{b}^\dagger\hat{\rho} + \hat{\rho}\hat{b}\hat{b}^\dagger)\right).\end{aligned} \tag{C.2}$$

Here we give the correspondences for the different terms for any given ordering parameters s, u ($f^\pm = s \pm 1/2$ and $g^\pm = u \pm 1/2$):

$\underline{\hat{a}^\dagger\hat{a}}$ Photon number operator:

$$\left[\hat{a}^\dagger\hat{a}, \hat{\rho}\right] \;\leftrightarrow\; \left\{(f^- - f^+)\partial_\alpha\alpha - (f^- - f^+)\partial_{\alpha^*}\alpha^*\right\}W \tag{C.3}$$

$\underline{\hat{b}^\dagger\hat{b}}$ Phonon number operator:

$$\left[\hat{b}^\dagger\hat{b}, \hat{\rho}\right] \;\leftrightarrow\; \left\{(g^- - g^+)\partial_\beta\beta - (g^- - g^+)\partial_{\beta^*}\beta^*\right\}W \tag{C.4}$$

$\underline{\hat{a}^\dagger\hat{a}(\hat{b}^\dagger + \hat{b})}$ radiation-pressure optomechanical coupling:

$$\begin{aligned}\left[\hat{a}^\dagger\hat{a}(\hat{b}^\dagger + \hat{b}), \hat{\rho}\right] \;\leftrightarrow\; \Big\{ & (f^- - f^+)\partial_\alpha\alpha\,(\beta + \beta^*) - (f^- - f^+)\partial_{\alpha^*}\alpha^*\,(\beta + \beta^*) \\ & + (g^- - g^+)\left(\partial_\beta|\alpha|^2 + f^-\partial_\beta\right) - (g^- - g^+)\left(\partial_{\beta^*}|\alpha|^2 + f^-\partial_{\beta^*}\right) \\ & + (f^+g^+ - f^-g^-)\partial^2_{\beta,\alpha}\alpha + (f^-g^+ - f^+g^-)\partial^2_{\beta,\alpha^*}\alpha^* \\ & - (f^-g^+ - f^+g^-)\partial^2_{\beta^*,\alpha}\alpha - (f^+g^+ - f^-g^-)\partial^2_{\beta^*,\alpha^*}\alpha^* \\ & + f^+f^-(g^- - g^+)\partial^3_{\beta,\alpha^*,\alpha} - f^+f^-(g^- - g^+)\partial^3_{\beta^*,\alpha^*,\alpha} \\ & \Big\}W\end{aligned} \tag{C.5}$$

$\hat{a}^\dagger\hat{b}$ **and** $\hat{a}\hat{b}^\dagger$**:** Linear resonant coupling between modes:

$$\begin{aligned}\left[\hat{a}^\dagger\hat{b},\hat{\rho}\right] &\leftrightarrow \left\{(f^- - f^+)\partial_\alpha\beta - (g^- - g^+)\partial_{\beta^*}\alpha^* + (f^+g^- - f^-g^+)\partial^2_{\alpha,\beta^*}\right\}W \\ \left[\hat{a}\hat{b}^\dagger,\hat{\rho}\right] &\leftrightarrow \left\{(g^- - g^+)\partial_\beta\alpha - (f^- - f^+)\partial_{\alpha^*}\beta^* + (f^-g^+ - f^+g^-)\partial^2_{\alpha^*,\beta}\right\}W\end{aligned} \tag{C.6}$$

Photon dissipative processes

$$\hat{a}\hat{\rho}\hat{a}^\dagger \leftrightarrow \left\{|\alpha|^2 + f^- - f^-\partial_\alpha\alpha - f^-\partial_{\alpha^*}\alpha^* + f^-f^-\partial^2_{\alpha^*,\alpha}\right\}W \tag{C.7}$$

$$\begin{aligned}\hat{a}^\dagger\hat{a}\hat{\rho} + \hat{\rho}\hat{a}^\dagger\hat{a} \leftrightarrow \Big\{&2|\alpha|^2 + 2f^- - (f^- + f^+)\partial_\alpha\alpha - (f^- + f^+)\partial_{\alpha^*}\alpha^* \\ &+ 2f^+f^-\partial^2_{\alpha^*,\alpha}\Big\}W\end{aligned} \tag{C.8}$$

Phonon dissipative processes

$$\hat{b}\hat{\rho}\hat{b}^\dagger \leftrightarrow \left\{|\beta|^2 + g^- - g^-\partial_\beta\beta - g^-\partial_{\beta^*}\beta^* + g^-g^-\partial^2_{\beta^*,\beta}\right\}W \tag{C.9}$$

$$\begin{aligned}\hat{b}^\dagger\hat{b}\hat{\rho} + \hat{\rho}\hat{b}^\dagger\hat{b} \leftrightarrow \Big\{&2|\beta|^2 + 2g^- - (g^- + g^+)\partial_\beta\beta - (g^- + g^+)\partial_{\beta^*}\beta^* \\ &+ 2g^+g^-\partial^2_{\beta^*,\beta}\Big\}W\end{aligned} \tag{C.10}$$

$$\hat{b}^\dagger\hat{\rho}\hat{b} \leftrightarrow \left\{|\beta|^2 + g^+ - g^+\partial_\beta\beta - g^+\partial_{\beta^*}\beta^* + g^+g^+\partial^2_{\beta^*,\beta}\right\}W \tag{C.11}$$

$$\begin{aligned}\hat{b}\hat{b}^\dagger\hat{\rho} + \hat{\rho}\hat{b}\hat{b}^\dagger \leftrightarrow \Big\{&2|\beta|^2 + 2g^+ - (g^+ + g^-)\partial_\beta\beta - (g^+ + g^-)\partial_{\beta^*}\beta^* \\ &+ 2g^+g^-\partial^2_{\beta^*,\beta}\Big\}W\end{aligned} \tag{C.12}$$

Appendix D

One-atom laser approach to single polariton optomechanics. Finite temperature and differential incoherent pumping

In this appendix we present the generalization of the calculations presented in the final section of chapter IV. We include here a finite temperature mechanical reservoir as well as a differential incoherent pumping of the two 1-polariton states.

The master equation under consideration is:

$$\begin{aligned}\frac{d\hat{\rho}(t)}{dt} =& -i[\hat{H}_{tot}+,\hat{\rho}] \\ &+\gamma_{ac}L[\hat{c}_-]\hat{\rho}+\gamma_{ac}L[\hat{c}_+]\hat{\rho} \\ &+\gamma_{inc}^{-}L[\hat{c}_-^{\dagger}]\hat{\rho}+\gamma_{inc}^{+}L[\hat{c}_+^{\dagger}]\hat{\rho} \\ &+n_{th}\gamma_m L[\hat{b}^{\dagger}]\hat{\rho}+(n_{th}+1)\gamma_m L[\hat{b}]\hat{\rho},\end{aligned} \tag{D.1}$$

where the state $|-^{(1)}\rangle$ ($|+^{(1)}\rangle$) is incoherently pumped from the ground state $|G\rangle$ at a rate $\gamma_{inc}^{-}(\gamma_{inc}^{+})$.

As we did in chapter IV we introduce the following set of correlators:

$$\begin{aligned}\forall m \in \mathbb{N}: \quad & N_b[m] = \langle \hat{b}^{\dagger m} \hat{b}^m \rangle, \\ & N_+[m] = \langle \hat{b}^{\dagger m-1} \hat{b}^{m-1} \hat{\sigma}_+^{(1)} \hat{\sigma}_-^{(1)} \rangle, \\ & N_-[m] = \langle \hat{b}^{\dagger m-1} \hat{b}^{m-1} \hat{\sigma}_-^{(1)} \hat{\sigma}_+^{(1)} \rangle, \\ & N_G[k] = \langle \hat{b}^{\dagger m-1} \hat{b}^{m-1} |G\rangle\langle G| \rangle, \\ & N_{b\sigma}[m] = \langle \hat{b}^{\dagger m} \hat{b}^{m-1} \hat{\sigma}_-^{(1)} \rangle, \\ & N_{b^\dagger \sigma_+}[m] = \langle \hat{b}^{\dagger m-1} \hat{b}^m \hat{\sigma}_+^{(1)} \rangle.\end{aligned} \tag{D.2}$$

We remind the reader that $\hat{N}_-[m] = \hat{N}_b[m-1] - \hat{N}_+[m] - \hat{N}_g[m]$. Let us consider the real and imaginary parts of the cross-correlators $N_{b\sigma}[m]$ and $N_{b^\dagger\sigma_+}[m]$ defined as follows:

$$\begin{aligned} N_{b\sigma}[m] &= N^r_{b\sigma}[m] + iN^i_{b\sigma}[m] \\ N_{b^\dagger\sigma_+}[m] &= N^r_{b\sigma}[m] - iN^i_{b\sigma}[m]. \end{aligned} \tag{D.3}$$

The set of differential equations we consider is:

$$\begin{aligned}\forall m \in \mathbb{N}: \quad \dot{N}_b[m] &= -2mg_{cm}N^i_{b\sigma}[m] - m\gamma_m N_b[m] + m^2 n_{th}\gamma_m N_b[m-1], \\ \dot{N}_+[m] &= 2g_{cm}N^i_{b\sigma}[m] + \gamma^+_{inc}N_G[m] - \gamma_{ac}N_+[m] \\ &\quad -(m-1)\gamma_m N_+[m] + (m-1)^2 n_{th}\gamma_m N_+[m-1], \\ \dot{N}_G[m] &= \gamma_{ac}N_b[m-1] - \left(\gamma^-_{inc} + \gamma^+_{inc} + \gamma_{ac} + (m-1)\gamma_m\right) N_G[m] \\ &\quad +(m-1)^2 n_{th}\gamma_m N_G[m-1] \\ \dot{N}^r_{b\sigma}[m] &= -(\omega_m - \Omega^{(1)})N^i_{b\sigma}[m] - (\gamma_{ac} + (m-1/2)\gamma_m)\, N^r_{b\sigma}[m] \\ &\quad +m(m-1)n_{th}\gamma_m N^r_{b\sigma}[m-1] \\ \dot{N}^i_{b\sigma}[m] &= (\omega_m - \Omega^{(1)})N^r_{b\sigma}[m] - (\gamma_{ac} + (m-1/2)\gamma_m)N^i_{b\sigma}[m] \\ &\quad -g_{cm}\left(2N_+[m+1] + mN_+[m] + N_G[m+1] - N_b[m]\right) \\ &\quad +m(m-1)n_{th}\gamma_m N^i_{b\sigma}[m-1]\end{aligned} \tag{D.4}$$

In chapter IV all the correlators in the stationary state were rewritten in terms of $N_b[m]$. Here, because of the possibility to thermally excite phonons, it is no longer possible. For example $N_G[m]$ is determined by the following recurrence relation:

$$N_G[m] = \frac{\gamma_{ac}N_b[m-1] + (m-1)^2 n_{th}\gamma_m N_G[m-1]}{\gamma_{ac} + \gamma^+_{inc} + \gamma^-_{inc} + (m-1)\gamma_m}. \tag{D.5}$$

It is nevertheless still possible to obtain a recurrence relation for the stationary value of $N_b[m]$ as follows:

$$A_T(m)N_b[m-1] + B_T(m)N_b[m] + C_T(m)N_b[m+1] = 0. \tag{D.6}$$

The temperature dependent coefficients of this recurrence relation are given by:

$$\begin{aligned}
A(m) &= \Big(m\tfrac{n_{th}\gamma_m}{g_{cm}}\left((2m-1)(n_{th}-1)\gamma_m-2\gamma_{ac}\right)\\
&\quad+\tfrac{4g_{cm}\gamma_{ac}\gamma^+_{inc}}{((m-1)(n_{th}-1)\gamma_m-\gamma_{ac})\left(\gamma_{ac}+\gamma^+_{inc}+\gamma^-_{inc}-(n_{th}-1)(m-1)\gamma_m\right)}\\
&\quad+4m\tfrac{n_{th}\gamma_m}{g_{cm}}\tfrac{(\omega_m-\Omega^{(1)})^2}{(2m-1)(n_{th}-1)\gamma_m-2\gamma_{ac}},\\
B(m) &= (mn_{th}-1)\tfrac{\gamma_m}{4g_{cm}}\left((2m-1)(n_{th}-1)\gamma_m-2\gamma_{ac}\right)\\
&\quad+g\left(1+\tfrac{m\gamma_m}{(m-1)(n_{th}-1)\gamma_m+\gamma_{ac}}+\tfrac{\gamma_{ac}\left(\gamma_{ac}+2\gamma^+_{inc}-m(n_{th}-1)\gamma_m\right)}{(m(n_{th}-1)\gamma_m-\gamma_{ac})(\gamma_{ac}+\gamma^+_{inc}+\gamma^-_{inc}-m(n_{th}-1)\gamma_m}\right)\\
&\quad+(mn_{th}-1)\tfrac{\gamma_m}{g_{cm}}\tfrac{(\omega_m-\Omega^{(1)})^2}{(2m-1)(n_{th}-1)\gamma_m-2\gamma_{ac}},\\
C(m) &= \tfrac{2g_{cm}\gamma_m}{\gamma_{ac}-m(n_{th}-1)\gamma_m}.
\end{aligned} \tag{D.7}$$

Bibliography

[1] Juan Restrepo, Julien Gabelli, Cristiano Ciuti, and Ivan Favero. Classical and quantum theory of photothermal cavity cooling of a mechanical oscillator. *Comptes Rendus Physique*, 12(9):860–870, 2011.

[2] Michel Devoret, Benjamin Huard, Robert Schoelkopf, and Leticia F. Cugliandolo. *Quantum Machines: Measurement Control of Engineered Quantum Systems: Lecture Notes of the Les Houches Summer School: Volume 96, July 2011.* Oxford University Press, August 2014.

[3] Juan Restrepo, Cristiano Ciuti, and Ivan Favero. Single-polariton optomechanics. *Physical Review Letters*, 112(1):013601, 2014.

[4] Marcus Woo. Device couples light to atom and quantum motion. *Physics*, 7:1, Jan 2014.

[5] Vladimir B. Braginsky and Farid Ya Khalili. *Quantum measurement.* Cambridge University Press, 1995.

[6] Florian Marquardt, Jack Harris, and Steven M. Girvin. Dynamical multistability induced by radiation pressure in high-finesse micromechanical optical cavities. *Physical Review Letters*, 96(10):103901, 2006.

[7] Johannes Kepler, Andrea Apergeri, and Sebastian Muller. *De cometis libelli tres.* A. Apergeri, 1963.

[8] Peter Lebedew. Untersuchungen über die druckkräfte des lichtes. *Annalen der Physik*, 311(11):433–458, 1901.

[9] Ernest Fox Nichols and Gordon Ferrie Hull. The pressure due to radiation. In *Proceedings of the American Academy of Arts and Sciences*, pages 559–599. JSTOR, 1903.

[10] Aashish. A. Clerk, Michel. H. Devoret, Steven M. Girvin, Florian Marquardt, and Rob. J. Schoelkopf. Introduction to quantum noise, measurement, and amplification. *Review of Modern Physics*, 82(2):1155–1208, April 2010.

[11] European gravitational observatory.
http://www.ego-gw.it/public/about/whatis.aspx/.

[12] Laser interferometer gravitational-wave observatory.
http://www.ligo.caltech.edu/.

[13] Vladimir B. Braginsky, Anatoli B. Manukin, and M Yu Tikhonov. Investigation of dissipative ponderomotive effects of electromagnetic radiation. *Soviet Journal of Experimental and Theoretical Physics*, 31:829, 1970.

[14] Florian Marquardt and Steven M. Girvin. Optomechanics. *Physics*, 2:40, May 2009.

[15] Markus Aspelmeyer, Simon Gröblacher, Klemens Hammerer, and Nikolai Kiesel. Quantum optomechanics, throwing a glance [invited]. *Journal of the Optical Society of America B*, 27(6):A189–A197, 2010.

[16] Pierre Meystre. A short walk through quantum optomechanics. *Ann. Phys.*, 525:215–233, 2013.

[17] Markus Aspelmeyer, Tobias J. Kippenberg, and Florian Marquardt. Cavity optomechanics. *RMP*, arXiv:1303.0733, 2013.

[18] Vladimir B. Braginskii and Anatoli Borisovich Manukin. Measurement of weak forces in physics experiments. *Chicago, University of Chicago Press, 1977. 161 p. Translation.*, 1, 1977.

[19] A Dorsel, John D. McCullen, Pierre Meystre, E Vignes, and H Walther. Optical bistability and mirror confinement induced by radiation pressure. *Physical Review Letters*, 51(17):1550–1553, 1983.

[20] JMW Milatz, JJ Van Zolingen, and BB Van Iperen. The reduction in the brownian motion of electrometers. *Physica*, 19(1):195–202, 1953.

[21] Stefano Mancini, David Vitali, and Paolo Tombesi. Optomechanical cooling of a macroscopic oscillator by homodyne feedback. *Physical Review Letters*, 80(4):688, 1998.

[22] Pierre-François Cohadon, Antoine Heidmann, and Michel Pinard. Cooling of a mirror by radiation pressure. *Physical Review Letters*, 83(16):3174, 1999.

[23] Constanze Höhberger Metzger and Khaled Karrai. Cavity cooling of a microlever. *Nature*, 432(7020):1002–1005, 2004.

[24] Olivier Arcizet, Pierre-Fran¸cois Cohadon, Tristan Briant, Michel Pinard, and Antoine Heidmann. Radiation-pressure cooling and optomechanical instability of a micromirror. *Nature*, 444(7115):71–74, 2006.

[25] Sylvain Gigan, Hannes Böhm, Mauro Paternostro, Florian Blaser, G Langer, Jared Hertzberg, Keith Schwab, Dieter Bäuerle, Markus Aspelmeyer, and Anton Zeilinger. Self-cooling of a micromirror by radiation pressure. *Nature*, 444(7115):67–70, 2006.

[26] Albert Schliesser, Pascal DelHaye, Nima Nooshi, Kerry Vahala, and Tobias Kippenberg. Radiation pressure cooling of a micromechanical oscillator using dynamical backaction. *Physical Review Letters*, 97(24):243905, 2006.

[27] Thomas Corbitt, Christopher Wipf, Timothy Bodiya, David Ottaway, Daniel Sigg, Nicolas Smith, Stanley Whitcomb, and Nergis Mavalvala. Optical dilution and feedback cooling of a gram-scale oscillator to 6.9 mk. *Physical Review Letters*, 99(16):160801, 2007.

[28] Ignacio Wilson-Rae, Nima Nooshi, W. Zwerger, and Tobias. Kippenberg. Theory of ground state cooling of a mechanical oscillator using dynamical backaction. *Physical Review Letters*, 99(9):093901, August 2007.

[29] Florian Marquardt, Joe P. Chen, Aashish. A. Clerk, and Steven M. Girvin. Quantum theory of cavity-assisted sideband cooling of mechanical motion. *Physical Review Letters*, 99(9):093902, August 2007.

[30] Aurelien Dantan, Claudiu Genes, David Vitali, and Michel Pinard. Self-cooling of a movable mirror to the ground state using radiation pressure. *Physical Review A*, 77(1):011804, 2008.

[31] Claudiu Genes, David Vitali, Paolo Tombesi, Sylvain Gigan, and Markus Aspelmeyer. Ground-state cooling of a micromechanical oscillator: Comparing cold damping and cavity-assisted cooling schemes. *Physical Review A*, 77(3):033804, 2008.

[32] Aaron D O Connell, M Hofheinz, M Ansmann, Radoslaw C Bialczak, M Lenander, Erik Lucero, M Neeley, D Sank, H Wang, M Weides, et al. Quantum ground state and single-phonon control of a mechanical resonator. *Nature*, 464(7289):697–703, 2010.

[33] Jasper Chan, TP Mayer Alegre, Amir H Safavi-Naeini, Jeff T Hill, Alex Krause, Simon Gröblacher, Markus Aspelmeyer, and Oskar Painter. Laser cooling of a nanomechanical oscillator into its quantum ground state. *Nature*, 478(7367):89–92, 2011.

[34] John Teufel, Tobias Donner, Dale Li, Jennifer Harlow, Michael Allman, Katarina Cicak, Adam Sirois, Jed D. Whittaker, Konrad Lehnert, and Raymond W. Simmonds. Sideband cooling of micromechanical motion to the quantum ground state. *Nature*, 475(7356):359–363, 2011.

[35] Tom P. Purdy, Robert W. Peterson, and Cindy Regal. Observation of radiation pressure shot noise on a macroscopic object. *Science*, 339(6121):801–804, 2013.

[36] Vladimir B. Braginsky, Yuri I Vorontsov, and Kip S. Thorne. Quantum nondemolition measurements. *Science*, 209(4456):547–557, 1980.

[37] Claude Fabre, Michel Pinard, Sophie Bourzeix, Antoine Heidmann, Elisabeth Giacobino, and Serge Reynaud. Quantum-noise reduction using a cavity with a movable mirror. *Physical Review A*, 49(2):1337, 1994.

[38] Stefano Mancini and Paolo Tombesi. Quantum noise reduction by radiation pressure. *Physical Review A*, 49(5):4055, 1994.

[39] Pierre Verlot, Alexandros Tavernarakis, Chiara Molinelli, Aurélien Kuhn, Thomas Antoni, Slawomir Gras, Tristan Briant, Pierre-François Cohadon, Antoine Heidmann, Laurent Pinard, et al. Towards the experimental demonstration of quantum radiation pressure noise. *Comptes Rendus Physique*, 12(9):826–836, 2011.

[40] Sougato Bose, Kurt Jacobs, and Peter L. Knight. Scheme to probe the decoherence of a macroscopic object. *Physical Review A*, 59(5):3204, 1999.

[41] Mauro Paternostro, David Vitali, Sylvain Gigan, MS Kim, Caslav Brukner, Jens Eisert, and Markus Aspelmeyer. Creating and probing multipartite macroscopic entanglement with light. *Physical Review Letters*, 99(25):250401, 2007.

[42] David Vitali, Sylvain Gigan, Anderson Ferreira, HR Böhm, Paolo Tombesi, Ariel Guerreiro, Vlatko Vedral, Anton Zeilinger, and Markus Aspelmeyer. Optomechanical entanglement between a movable mirror and a cavity field. *Physical Review Letters*, 98(3):030405, 2007.

[43] Klemens Hammerer, Claudiu Genes, David Vitali, Paolo Tombesi, Gerard Milburn, Christoph Simon, and Dirk Bouwmeester. Nonclassical states of light and mechanics. *arXiv preprint arXiv:1211.2594*, 2012.

[44] Jing Zhang, Kunchi Peng, and Samuel L. Braunstein. Quantum-state transfer from light to macroscopic oscillators. *Physical Review A*, 68:013808, Jul 2003.

[45] Lu Ding, Christophe Baker, Pascale Senellart, Aristide Lemaitre, Sara Ducci, Giuseppe Leo, and Ivan Favero. Wavelength-sized gaas optomechanical resonators with gigahertz frequency. *Applied Physics Letters*, 98(11):113108, 2011.

[46] Max Ludwig, Björn Kubala, and Florian Marquardt. The optomechanical instability in the quantum regime. *New Journal of Physics*, 10(9):095013, 2008.

[47] Andreas Nunnenkamp, Kjetil Børkje, and Steven M. Girvin. Single-photon optomechanics. *Physical Review Letters*, 107(6):063602, 2011.

[48] Peter Rabl. Photon blockade effect in optomechanical systems. *Physical Review Letters*, 107:063601, Aug 2011.

[49] Klemens Hammerer, Anders S. Sørensen, and Eugene S. Polzik. Quantum interface between light and atomic ensembles. *Review of Modern Physics*, 82:1041–1093, Apr 2010.

[50] Dan M Stamper-Kurn. Cavity optomechanics with cold atoms. *arXiv preprint arXiv:1204.4351*, 2012.

[51] Sydney Schreppler, Nicolas Spethmann, Nathan Brahms, Thierry Botter, Maryrose Barrios, and Dan M. Stamper-Kurn. Optically measuring force near the standard quantum limit. *Science*, 344(6191):1486–1489, 2014.

[52] G Rozas, AE Bruchhausen, A Fainstein, B Jusserand, and A Lemaître. Cavity polariton optomechanics: Polariton path to fully resonant dispersive coupling in optomechanical resonators. *arXiv preprint arXiv:1405.0886*, 2014.

[53] Aurelien Dantan, Bhagya Nair, Guido Pupillo, and Claudiu Genes. Hybrid cavity mechanics with doped systems. *arXiv preprint arXiv:1406.7100*, 2014.

[54] Alexander Carmele, Berit Vogell, Kai Stannigel, and Peter Zoller. Optonanomechanics strongly coupled to a rydberg superatom: coherent versus incoherent dynamics. *New Journal of Physics*, 16(6):063042, 2014.

[55] Jing Zhang, Tiancai Zhang, André Xuereb, David Vitali, and Jie Li. Mechanical non-classicality and atom-light-mirror nonlocality. *arXiv preprint arXiv:1402.3872*, 2014.

[56] Chung K. Law. Interaction between a moving mirror and radiation pressure: A hamiltonian formulation. *Physical Review A*, 51:2537–2541, Mar 1995.

[57] Gunter Plunien, Berndt Muller, and Walter Greiner. The casimir effect. *Physics Reports*, 134(2):87–193, 1986.

[58] Claude Cohen-Tannoudji, Bernard Diu, and Franck Laloë. *Mécanique quantique Tome 1.* Hermann, 1977.

[59] V Weisskopf and EP Wigner. Calculation of the natural brightness of spectral lines on the basis of dirac ś theory. *Zeitschrift fur Physik*, 63:54, 1930.

[60] Albert Einstein. Über die von der molekularkinetischen theorie der wärme geforderte bewegung von in ruhenden flüssigkeiten suspendierten teilchen. *Annalen der physik*, 322(8):549–560, 1905.

[61] Crispin Gardiner and Peter Zoller. *Quantum noise: a handbook of Markovian and non-Markovian quantum stochastic methods with applications to quantum optics*, volume 56. Springer, 2004.

[62] George W. Ford, John T. Lewis, and Robert F. O Connell. Quantum langevin equation. *Physical Review A*, 37(11):4419, 1988.

[63] Cristiano Ciuti and Iacopo Carusotto. Input-output theory of cavities in the ultrastrong coupling regime: The case of time-independent cavity parameters. *Physical Review A*, 74:033811, Sep 2006.

[64] Edmund X. DeJesus and Charles Kaufman. Routh-hurwitz criterion in the examination of eigenvalues of a system of nonlinear ordinary differential equations. *Physical Review A*, 35(12):5288–5290, June 1987.

[65] Mani Hossein-Zadeh and Kerry J Vahala. Observation of optical spring effect in a microtoroidal optomechanical resonator. *Optics letters*, 32(12):1611–1613, 2007.

[66] Claude Cohen-Tannoudji, Bernard Diu, and Franck Laloë. *Mécanique quantique Tome 2.* Hermann, 1977.

[67] Jiang Qian, AA Clerk, K Hammerer, and Florian Marquardt. Quantum signatures of the optomechanical instability. *Physical Review Letters*, 109(25):253601, 2012.

[68] Niels Lörch, Jiang Qian, Aashish Clerk, Florian Marquardt, and Klemens Hammerer. Laser theory for optomechanics: Limit cycles in the quantum regime. *Physical Review X*, 4(1):011015, 2014.

[69] Jean-Michel Raimond and Serge Haroche. *Exploring the quantum*. Oxford University Press, Oxford, 2006.

[70] Richard B Lehoucq, Danny C Sorensen, and Chao Yang. *ARPACK users' guide: solution of large-scale eigenvalue problems with implicitly restarted Arnoldi methods*, volume 6. Siam, 1998.

[71] Ryuichi Ashino, Michihiro Nagase, and Rémi Vaillancourt. Behind and beyond the matlab ode suite. *Computers & Mathematics with Applications*, 40(4):491–512, 2000.

[72] Eugene Wigner. On the quantum correction for thermodynamic equilibrium. *Physical Review*, 40(5):749–759, June 1932.

[73] Wolfgang P Schleich. *Quantum optics in phase space*. John Wiley & Sons, 2011.

[74] Kevin E. Cahill and Roy J. Glauber. Ordered expansions in boson amplitude operators. *Physical Review*, 177(5):1857–1881, January 1969.

[75] Kevin E. Cahill and Roy J. Glauber. Density operators and quasiprobability distributions. *Physical Review*, 177(5):1882–1902, January 1969.

[76] K Vogel and H Risken. Quasiprobability distributions in dispersive optical bistability. *Physical Review A*, 39(9):4675, 1989.

[77] Denzil A. Rodrigues and Andrew D. Armour. Amplitude noise suppression in cavity-driven oscillations of a mechanical resonator. *Physical Review Letters*, 104(5):053601, 2010.

[78] Arnaud Verger, Iacopo Carusotto, and Cristiano Ciuti. Quantum monte carlo study of ring-shaped polariton parametric luminescence in a semiconductor microcavity. *Physical Review B*, 76(11):115324, 2007.

[79] Alberto Amo, Jérôme Lefrère, Simon Pigeon, Claire Adrados, Cristiano Ciuti, Iacopo Carusotto, Romuald Houdré, Elisabeth Giacobino, and Alberto Bramati. Superfluidity of polaritons in semiconductor microcavities. *Nature Physics*, 5(11):805–810, 2009.

[80] Simon Pigeon. *Fluides quantiques et dispositifs à polaritons*. PhD thesis, Université Paris-Diderot-Paris VII, 2011.

[81] Iacopo Carusotto and Cristiano Ciuti. Quantum fluids of light. *Reviews of Modern Physics*, 85(1):299, 2013.

[82] Max Ludwig and Florian Marquardt. Quantum many-body dynamics in optomechanical arrays. *Physical Review Letters*, 111(7):073603, 2013.

[83] Ivan Favero, Constanze Metzger, Stephan Camerer, D König, H Lorenz, Jorg P. Kotthaus, and Khaled Karrai. Optical cooling of a micromirror of wavelength size. *Applied Physics Letters*, 90(10):104101, 2007.

[84] Jack Harris, Benjamin M. Zwickl, and Andrew Jayich. Stable, mode-matched, medium-finesse optical cavity incorporating a microcantilever mirror: Optical characterization and laser cooling. *Review of scientific instruments*, 78(1):013107, 2007.

[85] Constanze Metzger, Ivan Favero, Alexander Ortlieb, and Khaled Karrai. Optical self cooling of a deformable fabry-perot cavity in the classical limit. *Physical Review B*, 78(3):035309, July 2008.

[86] Koji Usami, A Naesby, Tolga Bagci, B Melholt Nielsen, Jin Liu, S Stobbe, Peter Lodahl, and Eugene Simon Polzik. Optical cavity cooling of mechanical modes of a semiconductor nanomembrane. *Nature Physics*, 8(2):168–172, 2012.

[87] Utku Kemiktarak, Mathieu Durand, Michael Metcalfe, and John Lawall. Cavity optomechanics with sub-wavelength grating mirrors. *New Journal of Physics*, 14(12):125010, 2012.

[88] Daniel Ramos, Eduardo Gil-Santos, Valerio Pini, Jose M Llorens, Marta Fernández-Regúlez, Álvaro San Paulo, Montserrat Calleja, and Javier Tamayo. Optomechanics with silicon nanowires by harnessing confined electromagnetic modes. *Nano letters*, 12(2):932–937, 2012.

[89] Robert A Barton, Isaac R. Storch, Vivekananda P. Adiga, Reyu Sakakibara, Benjamin R. Cipriany, B Ilic, Si Ping Wang, Peijie Ong, Paul L. McEuen, Jeevak M. Parpia, and Harold G. Craighead. Photothermal self-oscillation and laser cooling of graphene optomechanical systems. *Nano letters*, 12(9):4681–4686, 2012.

[90] Yuk Tung Liu and Kip S Thorne. Thermoelastic noise and homogeneous thermal noise in finite sized gravitational-wave test masses. *Physical Review D*, 62(12):122002, 2000.

[91] Massimo Cerdonio, Livia Conti, Antoine Heidmann, and Michel Pinard. Thermoelastic effects at low temperatures and quantum limits in displacement measurements. *Physical Review D*, 63(8):082003, 2001.

[92] Michel Pinard and Aurélien Dantan. Quantum limits of photothermal and radiation pressure cooling of a movable mirror. *New Journal of Physics*, 10(9):095012, 2008.

[93] Simone De Liberato, Neill Lambert, and Franco Nori. Quantum noise in photothermal cooling. *Physical Review A*, 83(3):033809, 2011.

[94] André Xuereb, Koji Usami, Andreas Naesby, Eugene S Polzik, and Klemens Hammerer. Exciton-mediated photothermal cooling in gaas membranes. *New Journal of Physics*, 14(8):085024, 2012.

[95] Constanze Metzger, Max Ludwig, Clemens Neuenhahn, Alexander Ortlieb, Ivan Favero, Khaled Karrai, and Florian Marquardt. Self-induced oscillations in an optomechanical system driven by bolometric backaction. *Physical Review Letters*, 101:133903, Sep 2008.

[96] Georg Heinrich, Max Ludwig, Jiang Qian, Björn Kubala, and Florian Marquardt. Collective dynamics in optomechanical arrays. *Physical Review Letters*, 107(4):043603, 2011.

[97] Michael Schmidt, Vittorio Peano, and Florian Marquardt. Optomechanical metamaterials: Dirac polaritons, gauge fields, and instabilities. *arXiv preprint arXiv:1311.7095*, 2013.

[98] Daniel WC Brooks, Thierry Botter, Sydney Schreppler, Thomas P. Purdy, Nathan Brahms, and Dan M. Stamper-Kurn. Non-classical light generated by quantum-noise-driven cavity optomechanics. *Nature*, 488(7412):476–480, 2012.

[99] William Marshall, Christoph Simon, Roger Penrose, and Dik Bouwmeester. Towards quantum superpositions of a mirror. *Physical Review Letters*, 91(13):130401, 2003.

[100] Uzma Akram, Nikolai Kiesel, Markus Aspelmeyer, and Gerard J. Milburn. Single-photon optomechanics in the strong coupling regime. *New Journal of Physics*, 12:083030, August 2010.

[101] Andreas. Nunnenkamp, Kjetil Børkje, and Steven M. Girvin. Cooling in the single-photon strong-coupling regime of cavity optomechanics. *Physical Review A*, 85:051803, May 2012.

[102] André Xuereb, Claudiu Genes, and Aurélien Dantan. Strong coupling and long-range collective interactions in optomechanical arrays. *Physical Review Letters*, 109(22):223601, 2012.

[103] Tom P. Purdy, Daniel. W. C. Brooks, T. Botter, Nathan Brahms, Z.-Y. Ma, and Dan M. Stamper-Kurn. Tunable cavity optomechanics with ultracold atoms. *Physical Review Letters*, 105:133602, Sep 2010.

[104] Francesco Bariani, Johannes Otterbach, Huatang Tan, and Pierre Meystre. Single-atom quantum control of macroscopic mechanical oscillators. *Physical Review A*, 89(1):011801, 2014.

[105] Klemens Hammerer, Margareta Wallquist, Claudiu Genes, Max Ludwig, Florian Marquardt, Philipp Treutlein, Peter Zoller, Jinwu Ye, and H. Jeff Kimble. Strong coupling of a mechanical oscillator and a single atom. *Physical Review Letters*, 103(6):063005, August 2009.

[106] H. Jeff Kimble. Strong interactions of single atoms and photons in cavity qed. *Physica Scripta*, 1998(T76):127, 1998.

[107] Emmanuelle Peter, Pascale Senellart, David Martrou, Aristide Lemaître, J Hours, JM Gérard, and J Bloch. Exciton-photon strong-coupling regime for a single quantum dot embedded in a microcavity. *Physical Review Letters*, 95(6):067401, 2005.

[108] Olivier Gazzano. *Sources brillantes de photons uniques indiscernables et démonstration d'une porte logique quantique*. PhD thesis, Paris 7, 2013.

[109] Andreas Wallraff, David I Schuster, Alexandre Blais, L Frunzio, R-S Huang, J Majer, S Kumar, Steven M Girvin, and Robert J Schoelkopf. Strong coupling of a single photon to a superconducting qubit using circuit quantum electrodynamics. *Nature*, 431(7005):162–167, 2004.

[110] Alexandre Blais, Ren-Shou Huang, Andreas Wallraff, S. M. Girvin, and R. J. Schoelkopf. Cavity quantum electrodynamics for superconducting electrical circuits: An architecture for quantum computation. *Physical Review A*, 69:062320, Jun 2004.

[111] Ivan Favero and Khaled Karrai. Cavity cooling of a nanomechanical resonator by light scattering. *New Journal of Physics*, 10(9):095006, 2008.

[112] Claudiu Genes, Helmut Ritsch, and Ddavid Vitali. Micromechanical oscillator ground-state cooling via resonant intracavity optical gain or absorption. *Physical Review A*, 80(6):061803, 2009.

[113] Lu Ding, Christophe Baker, Pascale Senellart, Aristide Lemaitre, Sara Ducci, Giuseppe Leo, and Ivan Favero. High frequency gaas nano-optomechanical disk resonator. *Physical Review Letters*, 105(26):263903, December 2010.

[114] Alejandro Fainstein, N. Daniel Lanzillotti-Kimura, Bernard Jusserand, and B Perrin. Strong optical-mechanical coupling in a vertical gaas/alas microcavity for subterahertz phonons and near-infrared light. *Physical Review Letters*, 110(3):037403, 2013.

[115] Claude Cohen-Tannoudji, Jacques Dupont-Roc, and Gilbert Grynberg. *Processus d'interaction entre photons et atomes*. Edp Sciences, 2012.

[116] Edwin T Jaynes and Frederick W Cummings. Comparison of quantum and semiclassical radiation theories with application to the beam maser. *Proceedings of the IEEE*, 51(1):89–109, 1963.

[117] Daniel Braak. Integrability of the rabi model. *Physical Review Letters*, 107(10):100401, 2011.

[118] WL Smith. Approximate formulae for the overlap integral of two harmonic oscillator wave functions. *Journal of molecular spectroscopy*, 225(1):39–42, 2004.

[119] Howard Carmichael. *Statistical Methods in Quantum Optics 1: Master Equations and Fokker-Planck Equations*, volume 1. Springer, 2002.

[120] Atac Imamoglu, Helmut Schmidt, Gareth Woods, and Moshe Deutsch. Strongly interacting photons in a nonlinear cavity. *Physical Review Letters*, 79(8):1467, 1997.

[121] Maximilian J. Werner and Atac Imamoglu. Photon-photon interactions in cavity electromagnetically induced transparency. *Physical Review A*, 61(1):011801, 1999.

[122] Philippe Grangier, Daniel F Walls, and Klaus M Gheri. Comment on "strongly interacting photons in a nonlinear cavity". *Physical Review Letters*, 81(13):2833, 1998.

[123] Elena Del Valle and Fabrice P. Laussy. Regimes of strong light-matter coupling under incoherent excitation. *Physical Review A*, 84(4):043816, 2011.